Application of Artificial Intelligence Techniques to Chemical Engineering Problems

A THESIS SUBMITTED FOR THE DEGREE OF

DOCTOR OF PHILOSOPHY

IN CHEMICAL ENGINEERING

IN THE FACULTY OF ENGINEERING AND TECHNOLOGY

NAGPUR UNIVERSITY

BY

IMRAN RAHMAN

CHEMICAL ENGINEERING DIVISION

NATIONAL CHEMICAL LABORATORY

PUNE – 411 008, INDIA

APRIL 2005

Application of Artificial Intelligence Techniques to Chemical Engineering Problems

A THESIS

SUBMITTED FOR THE DEGREE OF

DOCTOR OF PHILOSOPHY

IN

CHEMICAL ENGINEERING

IN THE FACULTY OF ENGINEERING AND TECHNOLOGY

NAGPUR UNIVERSITY

BY

IMRANUR RAHMAN

CHEMICAL ENGINEERING DIVISION

NATIONAL CHEMICAL LABORATORY

PUNE – 411 008, INDIA

APRIL 2005

CERTIFICATE

This thesis "Application of Artificial Intelligence Techniques to Chemical Engineering Problems" is a bonafide work done by Mr. Imranur Rahman, at Chemical Engineering Division, National Chemical Laboratory (NCL), Pune. It has been completed under my guidance and supervision. The work forms the requirement for award of the degree of Doctor of Philosophy in the Faculty of Engineering and Technology, Nagpur University, Nagpur.

This research work fulfills the requirements relating to the nature and standard of work for the award of the degree. The work embodied in this thesis has not been submitted to any other University or Institute for the award of any other Degree or Diploma.

Dr. B. D. Kulkarni
Research Supervisor

DECLARATION

I hereby declare that the work presented in this thesis entitled “Application of Artificial Intelligence Techniques to Chemical Engineering Problems” has been carried out by me under the guidance and supervision of Dr. B.D. Kulkarni, at Chemical Engineering Division, National Chemical Laboratory (NCL), Pune. No part of this thesis has been submitted elsewhere for the award of any Degree or Diploma.

Imranur Rahman

ACKNOWLEDGEMENTS

I remain deeply indebted to my research advisor Dr. B. D. Kulkarni for introducing me to a fascinating and challenging frontier of artificial intelligence that has given me a new outlook. I record my deep sense of gratitude for his cogent advice, personal care, encouragement and enthusiastic support throughout the work.

My heartful thanks are due to Dr. S.S. Tambe for his helpful suggestions during this research work. The donation of time, material and knowledge by him is greatly appreciated. I would also like to express my deep sense of appreciation to Dr. D. D. Ravetkar who kindly responded to my request whenever I needed. I highly appreciate the help rendered by lab colleagues during the course of this work.

It is pleasure to thank Dr. B. K. Sinha, Ex-Director, CMERI, Durgapur for having inspired me throughout this research work.

Finally, I would like to thank my wife Nishat and our children Ramsha and Adnan for putting up with me during the period of this work.

(*IMRAN RAHMAN*)

Abstract

Modeling of chemical processes by conventional methods is difficult due to the inherent complexity and quite often the inadequate information about them. Thus, Its recourse to alternative methods is necessary to analyze complex chemical processes and to develop empirical models which can properly represent the behavior of the system concerned. The optimization problems in chemical engineering have been tackled using various nonlinear programming (NLP) and mixed integer nonlinear programming (MINLP) techniques. However these techniques involve gradient based sequential search to converge into arbitrary local optima instead of global optima. The proposed artificial intelligence (AI) tools may prove advantageous in such instances.

Most processes in industry have nonlinear characteristics, the control algorithms are based on linear versions of the processes and, in many instances, such controllers do an adequate job. In some process situations, however, the use of the full nonlinear nature of a process may provide operational advantages and, hence, it may be desirable to derive nonlinear control laws. Nonlinear continuous processes or batch processes spanning a wide range of dynamic behavior are typical of such examples, where use of the nonlinear controllers would be appropriate.

In the last decade AI tools, such artificial neural networks (ANN), fuzzy logic (FL), genetic algorithms (GA) etc. have found numerous applications in almost all scientific, engineering, and technology discipline. The AI techniques have also been used to solve chemical engineering problems involving nonlinear process control, process identification, and process optimization.

Neural networks involve many interconnected processing elements which demonstrate the ability to learn and generalize from training patters. They can learn complex interrelationships between two sets of data representing independent and dependent variables, respectively. ANNs have found numerous applications in modeling, classification, data compression, noise filtering etc.

Fuzzy logic is a powerful tool for modeling human thinking and perception. It is an attempt at formalizing the reasoning that characterizes human decision making when coping with

uncertainty and approximation. Fuzzy logic control is suitable for complex, ill-defined, nonlinear processes where human experience can aid mathematical models.

The genetic algorithms are based on mimicking the mechanisms of natural selection and genetics, which play a dominant role in the Darwinian evolution of biological organisms. The GAs are known to be efficient in searching noisy, discontinuous and non-convex solution spaces. Genetic algorithms provides robust stochastic optimization tool which converges to global optima and can be readily applied to optimizations problems. The GA-based optimization has several attractive features such as: (i) convergence to a global rather than to a local minimum, (ii) the objective function need not satisfy smoothness, differentiability, and continuity conditions, and (iii) robustness.

In this thesis, the AI tools such as fuzzy logic, genetic algorithms and B-spline neural networks have been explored for optimization, control and identification of chemical processes. The thesis consists of nine chapters. Chapter one deals with a general introduction of modeling and optimization along with the brief introduction to ANN, FL, and GA methodologies.

In chapter 2, genetic algorithm (GA) is applied to batch distillation column to determine the optimal reflux policy for obtaining distillate of the desired purity. A new scheme is introduced for calculating the reflux ratio of a cut. It is seen that the reflux ratio calculated by this method is lower than the one calculated by simple method for desired purity. Two industrially relevant binary mixtures (acetone-water and para/ortho nitrochlorobenzene) have been studied.

Chapter 3 describes usage of genetic algorithms (GAs) for the optimization of continuous distillation columns. Both simple and azeotropic systems are considered in the analysis. In particular, for a specified degree of separation the problem of finding the optimal values of: (i) number of stages, (ii) reflux ratio (entrainer quantity in the case of azeotropic distillation), and (iii) feed location(s), has been addressed. Feasibility of utilizing the GA technique has been demonstrated by considering separation of two binary and one azeotropic systems of industrial relevance.

Genetic algorithms have been applied for optimization of reactive and catalytic distillation columns in chapter 4. For a specified degree of production and separation by reactive

distillation, the optimal values of number of trays, boil up fraction, liquid hold up and feed flow rate on trays are found out, whereas in the case of catalytic distillation column, reflux ratio, column pressure and bottom flow rate are optimized. Non-ideal vapor-liquid equilibrium is considered. The present study demonstrates the utility of GA technique for optimization of reactive distillation and catalytic distillation systems.

In chapter 5, a fuzzy logic control(FLC) strategy has been introduced for controlling chaotic dynamics exactly at the unstable steady-state responsible for the chaotic motion. The effectiveness of the proposed strategy is demonstrated on two chemical reaction/reactor systems exhibiting a chaotic behavior.

Chapter 6 describes, a novel strategy for FLC-design is developed wherein control rules and membership functions (MFs) are optimized using genetic algorithms (GA). This is the most difficult part of fuzzy logic controllers (FLC), which are being increasingly recommended for chemical processes is designing fuzzy control rules and tuning of membership functions thereof. Efficacy of the proposed FLC has been demonstrated for the servo and regulatory control of a non-isothermal continuous stirred tank reactor (CSTR) and nonlinear pH control.

Chapter 7 deals with an adaptive fuzzy logic controller (FLC), that tunes the output membership function online by recursive least square (RLS) algorithm. Proper design of control rules and membership functions (MFs) is important in the successful application of a fuzzy logic controller. Efficacy of the proposed FLC has been demonstrated by considering the control of two non-linear chemical systems namely: (i) continuous fermentation process, and (ii) non-isothermal CSTR.

Chapter 8 describes a nonlinear model-predictive control scheme based on the B-spline neurofuzzy model. It is applied to isothermal free-radical polymerization of methyl methacrylate using azobisisobutyronitrile (AIBN) as initiator and toluene as solvent in CSTR. The neurofuzzy network approximates the dynamic relationship between the manipulated variable (initiator flow rate) and the control variable (number-average molecular weight). Specifically, the neurofuzzy network model predicts the one step ahead value of the control variable and this is used in the framework of Newton-Raphson method to determine the control action. The objective of

nonlinear model predictive control is to control the number-average molecular weight of the polymer.

Finally, chapter 9 provides summary and future prospects of research.

Table of Contents

Chapter 4

Chapter 5

Chapter 6

Chapter 7

Chapter 8

Chapter 9

Chapter 1

General Introduction and Overview

1.1 Background

The pressure on the process industries to improve yield, reduce wastage, eliminate toxins and above all increase profits makes it essential to increase the efficiency of process operations. One of the possible approaches for achieving this is through the improvement of existing process monitoring and control systems and optimization of processes.

Many process monitoring and control schemes are based upon a representation of dynamic relationship between cause and effect variables. In such schemes this representation is typically approximated using conventional methods such as ARX, ARMAX etc. which are some form of linear dynamic models. Most optimization problems in chemical engineering are nonlinear in either the objective function or constraints, resulting in nonlinear programming (NLP) models, which often converge to a local optima instead of global optima.

Modeling of chemical processes by conventional methods is difficult due to the inherent complexity of chemical systems and inadequate information about them. Thus, it is important to develop and use alternative methods that can be applied to systems with inadequate information. The optimization problems in chemical engineering have been tackled using various NLP and mixed integer nonlinear programming (MINLP) techniques. However these technique involve gradient based sequential search and quite often converge into arbitrary local optima instead of global optima computations at some stage in their optimization simulation.

Artificial intelligence (AI) techniques are now being used by the practicing engineers to solve a whole range of hitherto intractable problems. AI technologies include artificial neural networks (ANNs), fuzzy logic (FL), genetic algorithms (GAs), and others. Their underlying methods differ from conventional computing and include concepts that simulate the way human beings solve problems or how processes work in nature. For example, ANNs learn by training, and FL works with uncertainty and partial information.

Artificial intelligence is a technology concerned with devising computer programs to achieve machine intelligence. Alternatively, AI techniques are focused on

developing computational approaches to intelligent behavior. These computer programs usually deal with processes involving complexity, uncertainty and ambiguity.

1.1 Artificial Intelligence Techniques

In the last decade AI tools, such artificial neural networks (ANN), fuzzy logic (FL), genetic algorithms (GA) have found numerous applications in almost all scientific, engineering, and technology disciplines.

1.2.1 Artificial Neural Networks (ANNs)

ANNs are inspired by the very basic properties possessed by the brain's neural network consisting of billions of interconnected neurons. ANNs are based on the concept that a highly interconnected system of simple processing elements can learn complex interrelationships between two sets of data representing independent and dependent variables, respectively. The main benefits of neural networks are that they are well structured for adaptive learning and have the capability of parallel processing and generalization. ANNs have found numerous applications in modeling, classification, data compression, noise filtering etc.

1.2.2 Fuzzy Logic (FL)

Fuzzy logic tends to mimic human thinking in the instances when the information is fuzzy in nature. It, unlike the Boolean or crisp logic, deals with problems that have vagueness, uncertainty, or imprecision and uses membership functions with values ranging between 0 and 1. Fuzzy systems involve the procedures of fuzzification with membership functions, reasoning with a fuzzy rule using a proper inference method and a defuzzifcation process.

The advantages of fuzzy logic is in its logical approach and transparency, where it is easy to incorporate *a priori* knowledge about the system into an explicit fuzzy rule base. It is especially suitable for complex, ill-defined, nonlinear processes where human experience has the edge over mathematical models (Rhinehart and Murugan, 1996). Fuzzy systems have found significant applications in fuzzy controller, pattern recognition and information processing.

.

1.2.3 Neurofuzzy Network

Neurofuzzy systems have emerged in recent years as researchers (Brown and Harris, 1994) have tried to combine the natural linguistic/symbolic transparency of fuzzy systems with provable learning and representation capability of linear in the weights of artificial neural networks (ANN). This combination brings the learning abilities of neural networks to the fuzzy decision system. The advantages of both approaches are thus merged. Different kinds of network structures and learning algorithms for neurofuzzy system have been proposed by several researchers (Kaur and Lin, 1998)

Non-linear system dynamical modeling using neural networks including a B-spline neuro-fuzzy network has been widely studied in recent years (Brown and Harris, 1994). As for the membership functions, the B-spline basis function is a very good choice, due to its desirable numerical properties such as local compact support, easy numerical computation and partition of unity (Hong *et al.*, 1998)

1.2.4 Genetic Algorithms(GA)

Genetic algorithms are the stochastic search methods based on the principle of natural evolution observed in the biological world. The process of natural evolution is characterized by (i) the competition among species for the existence and, (ii) the "survival-of-the-fittest' rule. The GAs simulate these processes on a computer to accomplish complex computational tasks. Specifically, GAs have found applications in function optimization, scheduling and sequencing.

1.3 AI Applications in Chemical Engineering

The above described AI techniques are generic in nature and possess tremendous potential for applications in chemical engineering. The AI techniques are developed and used in this thesis to solve chemical engineering problems involving nonlinear process control, process identification, and process optimization.

1.3.1 Process Control

Most processes in industry have nonlinear characteristics although the control algorithms are based on linearised versions of the processes and, in many instances, such controllers do an adequate job. In some process situations, however, the use of the full nonlinear nature of a process may provide operational advantage and, hence, it may be desirable to derive nonlinear control laws. Nonlinear continuous processes or batch processes spanning a wide range of dynamic behavior are typical of such examples, where use of the nonlinear controllers would be appropriate.

Instead of deriving a controller via modeling the controlled process quantitatively and mathematically, the fuzzy control methodology tries to establish the controller directly from domain experts or operators who are controlling the process manually and successfully, Clearly, this is a typical characteristic of an expert system where primary attention is paid to the human behavior and experience, rather than to the process being controlled. It is this distinctive feature that makes fuzzy control applicable and attractive for dealing with those problems where the process is so complex and ill-defined that it is either impossible or too expensive to derive a mathematical model which is accurate and simple enough to be used by traditional methods, but the process may be controlled satisfactorily by human operator.

In recent years, model-based control strategies have found wide-spread acceptance due to their robustness. These control strategies require process model for their implementation. Due to the complex nature of the modern-day plants and nonlinear nature of the involved chemical processes, development of process model becomes tedious, time-consuming and costly affair. In such situations, ANN and FL based models can be developed. These models can be constructed from plant input-output data without putting too much emphasis on the knowledge of involved physico-chemical phenomena.

1.3.2 Process Identification

Process models developed from the knowledge of fundamental principles, such as conservation laws of mass, energy, and momentum often turn out to be complex since most chemical processes exhibit nonlinear characteristics and, thus require simplifying

assumptions for their solution. A lack of sufficient understanding of the involved physical phenomena compounds the problem further. Owing to such difficulties, process identification techniques are used to develop non-parametric (e.g. autoregressive moving average) models which are constructed exclusively from the experimental process input-output data. The drawback of such techniques, however, is that the model structure must be specified a priori- a difficult task since it involves selecting by trial and error a reasonable model from numerous alternatives. The drawbacks alluded to above can be overcome by using ANNs, GAs and GP methodologies.

1.3.3 Process Optimization

Most optimization problems in chemical engineering are nonlinear in either the objective function or constraints, resulting in nonlinear programming (NLP) models. In addition, problems in plant design and scheduling often involve both continuous and discrete variables, resulting in mixed-integer linear/non-linear programming (MILP/MINLP) problems. Due to nonlinearity of problem, only local convergence can be guaranteed and the obtained result may represent a local optima. Moreover, MINLP methods are complex, computationally intensive and many simplifications become necessary to make them affordable.

In a number of papers, stochastic methods are proposed for the solution of certain optimization problems in chemical plant design for global optima. The stochastic optimization algorithms although computationally intensive, are finding wide-spread acceptance in the chemical engineering applications owing to their affordability and the speed of the modern computing technology. Genetic algorithm is one such robust stochastic optimization tool which converges to global optima and can be readily applied to optimizations problems.

1.4 Overview of AI Techniques

1.4.1 Overview of Fuzzy Logic Controller

Unlike in the crisp set theory where the membership of an element in a crisp set is either zero or one, the fuzzy set theory (Zadeh, 1965) allows an element to belong to a fuzzy set with a degree that can vary between zero and one. In fuzzy set theory, the range

of values that a variable can assume forms its universe of discourse (UOD). A UOD is partitioned into a number of fuzzy sets, each characterized by a linguistic variable and defined by a membership function (MF). An MF is a curve defining how different points in the UOD are mapped to a degree of membership that varies between zero and one. For example, if the set-point error (hereafter simply referred to as 'error') is a fuzzy variable, its UOD may be decomposed into a number of fuzzy sets using linguistic variables such as NEGATIVE-LARGE(*NL*), NEGATIVE-SMALL(*NS*), ZERO(*ZE*), POSITIVE SMALL(*PS*), AND POSITIVE LARGE(*PL*) errors, and the shape of the membership functions of the respective fuzzy sets can be selected from among a number of alternatives namely, triangular, gaussian, sigmoid etc.

The fuzzy logic controller (FLC) consists of four elements : (i) a fuzzifier, (ii) a rule-base, (iii) an inference engine, and (iv) a defuzzifier. An FLC essentially maps the crisp inputs(*e*) defining the process states into crisp outputs(*u*) signifying the control action. For achieving this the inputs are first mapped into fuzzy sets which is performed by the fuzzifier. The rule base defines control rules which are derived from the heuristic knowledge of a skilled process operator and/or process engineer. A rule establishes relationship between the linguistic terms associated with the fuzzy input-output variables, such as:

If error *e* is *PS* and change in error *ce* is *PL* then *u* is *PL*,

Depending upon which control rule(s) is satisfied (fired), the inference engine computes the corresponding fuzzy output. Finally, the defuzzifier converts the fuzzy output from the inference engine to its crisp value for implementation on the process.

Many defuzzifIcation techniques have been proposed in the literature such as centroid defuzzifier, height defuzzfier and modified height defuzzifer etc

1.4.2 Overview of B-spline Neurofuzzy Network (BNN)

Neurofuzzy systems result from the fusion of neural networks and fuzzy logic. Neural networks provide a highly sophisticated capability for non-linear function approximation and the B-spline neurofuzzy network has desirable properties such as compact support, a partition of unity, locality, logicality and transparency (Hong *et al.*,

1998). In the following section the input-output relation of the fuzzy system, with functional rule base and B-spline basis functions as membership functions is explained.

A neurofuzzy network using B-spline function as the membership function. A general one-dimensional B-spline model is formed as linear combination of L B-spline basis functions as

$$f(x) = \sum_{j=1}^{L} \omega_j B_m^j(x) \tag{1.1}$$

The coefficient ω_j's represent the set of adjustable parameters associated with the set of basis functions. The set of basis functions $B_m^j(x)$'s in the model is a polynomial of a given degree m and is uniquely defined by an ordered sequence of real values denoted as a knot vector $\tau = \{\tau_1, \tau_2, ..., \tau_{L+m+1}\}$. The known sequence forms a partitioning of the input domain into ($L+m$) disjoint intervals. The definition of basis functions set can be expressed as a recursion (Dierckx, 1995).

$$B_m^j = \frac{x - \tau_j}{\tau_{j+m} - \tau_j} B_{m-1}^j(x) + \frac{\tau_{j+m+1} - x}{\tau_{j+m+1} - \tau_{j+1}} B_{m-1}^j(x) \tag{1.2}$$

with

$$B_0^j(x) = \begin{cases} 1 & \tau_j < x < \tau_{j+1} \\ 0 & otherwise \end{cases}$$

The multidimensional B-spline basis functions are formed by a direct multiplication of one dimensional basis functions

$$N_j(\mathbf{x}) = \prod_{i=1}^{n} B_{i,m}^{k_i}(x_i) \tag{1.3}$$

for $j = 1, ..., p$, where $p = \prod_{i=1}^{n} L_i$, $\mathbf{x} = [x_1, x_2, ..., x_n]^T \in R^n$. $k_i = 1, ..., L_i$, L_i is the number of B-spline basis functions defined in x , the ith component of x. The multidimensional B-spline basis function models are constructed as a tensor product of one-dimensional models using $p = \prod_{i=1}^{n} L_i$ basis functions as

$$f(x) = \sum_{j=1}^{p} N_j(\mathbf{x})\omega_j = \sum_{k=1}^{p} \omega_j \prod_{i=1}^{n} B_i^{k_i}(x_i) \tag{1.4}$$

1.4.3 Overview of Genetic Algorithms

The genetic algorithms (Goldberg, 1989) are based on the mechanisms of natural selection and genetics, which play a dominant role in the Darwinian evolution of biological organisms. GAs are stochastic optimization formalisms and known to be efficient in searching noisy, discontinuous and nonconvex solution spaces (Venkatasubramanian and Sundaram, 1998) and their characteristic features are:

- They are ‘’zeroth’’ order search techniques implying that they need only the scalar values of the objective function being optimized.
- GAs perform a global search and hence they mostly converge to (or in the vicinity of) the global optimum of the objective function.
- The search procedure of GA’s is stochastic hence they can be utilized without invoking ad-hoc assumptions, such as smoothness, differentiability, and continuity, pertaining to the form of the objective function. Owing to this feature, GAs can solve optimization problems that cannot be conveniently solved using the classical gradient-based algorithms, which require the objective function to simultaneously satisfy the above-stated three criteria.
- The GA procedure can be effectively parallelized, which helps in efficiently searching a large multi-dimensional solution space.

For comprehending the working principles of GAs, consider a generic version of the optimization problem defined in equation (1.5) :

$$\text{Minimize } f(\mathbf{x}),\quad x_k^L \le x_k \le x_k^U;\ k = 1,2,...,K \tag{1.5}$$

where x_k denotes the kth decision variable and $f(\mathbf{x})$ represents the nonlinear objective function. For obtaining a GA-based solution to the minimization problem, first a population of probable (candidate) solutions is randomly generated. Each solution is coded as a binary string (also termed “chromosome”) that is subdivided into as many segments as the number (K) of decision variables. How good a candidate solution performs at fulfilling the optimization task is ascertained by evaluating its fitness value (score). GAs in essence search solutions possessing high fitness. The fitness value of a solution is obtained by evaluating a prespecified fitness function, $\xi(\mathbf{x})$. Depending upon

whether the optimization task involves function maximization or minimization, the corresponding fitness function is defined by suitably transforming the objective function. More specifically, for problems involving function maximization (minimization) the fitness value should increase (decrease) with increasing value of the objective function. Upon evaluating the fitness scores of all candidate solutions in a population, three GA operators namely, *selection*, *crossover* and *mutation* are used sequentially to produce a "new generation" of probable solutions. The significance of three GA operators is described in the following.

- *Selection*: This operator selects strings from the current population with a view to forming a mating pool of parent strings. The parent strings are selected in such a manner that strings with better fitness value (score) get priority for inclusion in the pool.
- *Crossover*: The action of this important GA operator produces offspring strings wherein randomly selected parts of two parent strings are mutually exchanged to form two offspring per pair of parent strings. In essence, the crossover operator helps in improving the combinatorial diversity of the offspring population by utilizing the building blocks of the parent population (Vekatasubramanian and Sundaram, 1998).
- *Mutation*: This operator flips (mutates) the randomly selected bits of the offspring strings from zero to one and vice versa. Such an operation introduces characteristics hitherto absent in the offspring population thereby conducting a local search around the point solutions represented by the unmutated offspring strings.

The solutions represented by the new-generation chromosomes are usually better (in terms of their fitness values) as compared to those represented by the chromosomes in the current population. Subsequently, the new population is subjected to the actions of the three GA operators and this procedure is iterated over successive populations till convergence is achieved. The essence of the GA-methodology can be stated as: better solutions in the current population are selected for reproduction and their offspring, generated via crossover and mutation operations, replace the sub-optimal (i.e. with low

fitness values) solutions. The solution population, owing to the repetitive actions of the three GA operators, improves itself from one generation to the next. The GA converges eventually and the best chromosome i.e., the one possessing maximum fitness score, represents the solution to the optimization problem.

1.5 Scope of the Thesis

AI techniques are generic in nature and posses tremendous potential for applications in chemical engineering. In this thesis, the AI tools such as fuzzy logic, genetic algorithms and B-spline neural network have been explored for optimization, control and identification of chemical processes.

In chapter 2, genetic algorithm is applied to batch distillation column to determine the optimal reflux policy for obtaining distillate of the desired purity. The constant reflux ratio to be used during each cut is calculated on purity specification of a particular cut. A new scheme is introduced wherein the reflux ratios are calculated assuming an infinitesimally small change in composition covering the range of composition within each cut. These reflux ratios of a particular cut, are averaged to give the constant reflux ratio of that cut. It is seen that the reflux ratio calculated by this method is lower than the one calculated by simple method for desired purity. Two industrially relevant binary mixtures (acetone-water and para/ortho nitrochlorobenene) have been studied.

Chapter 3 describes GAs for the optimization of continuous distillation columns. Both simple and azeotropic systems are considered in the analysis. In particular, for a specified degree of separation the problem of finding the optimal values of: (i) number of stages, (ii) reflux ratio (entrainer quantity in the case of azeotropic distillation), and (iii) feed location(s), has been addressed. The GA-based optimization has several attractive features such as: (i) convergence to a global rather than to a local minimum, (ii) the objective function need not satisfy smoothness, differentiability, and continuity conditions, and (iii) robustness. Feasibility of utilizing the GA technique has been demonstrated by considering separation of two binary and one azeotropic systems of industrial relevance.

Genetic algorithms have been applied for optimization of reactive and catalytic distillation columns in chapter 4. For a specified degree of production and separation by reactive distillation, the optimal values of number of trays, boil up fraction, liquid hold up and feed flow rate on trays are found out, whereas in the case of catalytic distillation column, reflux ratio, column pressure and bottom flow rate are optimized. Non-ideal vapor-liquid equilibrium is considered. The present study demonstrates the utility of GA technique for optimization of reactive distillation and catalytic distillation systems.

In chapter 5, a fuzzy logic control (FLC) strategy has been introduced for controlling chaotic dynamics exactly at the unstable steady-state responsible for the chaotic motion. Control of chaotic dynamics continues to be a nontrivial task. The effectiveness of the proposed strategy is demonstrated on two chemical reaction/reactor systems exhibiting a chaotic behavior.

Chapter 6 describes, a novel strategy for FLC-design is developed wherein control rules and membership functions (MFs) are optimized using a powerful stochastic optimization method namely, the genetic algorithms (GA). This is the most difficult part of fuzzy logic controllers (FLC), which are being increasingly recommended for chemical processes is designing fuzzy control rules and tuning of membership functions (MFs) thereof. Efficacy of the proposed FLC has been demonstrated for the servo and regulatory control of a non-isothermal continuous stirred tank reactor (CSTR) and nonlinear pH control.

Chapter 7 deals with an adaptive fuzzy logic controller (FLC), that tunes the output membership function online by recursive least square (RLS) algorithm. Proper design of control rules and membership functions (MFs) is important in the successful application of a fuzzy logic controller. Efficacy of the proposed FLC has been demonstrated by considering the control of two non-linear chemical systems namely : (i) continuous fermentation process, and (ii) non-isothermal continuous stirred tank reactor (CSTR).

Chapter 8 describes a nonlinear model-predictive control scheme based on the B-spline neurofuzzy model. It is applied to isothermal free-radical polymerization of methyl methacrylate using azobisisobutyronitrile (AIBN) as initiator and toluene as solvent in CSTR. The neurofuzzy network approximates the dynamic relationship

between the manipulated variable (initiator flow rate) and the control variable (number-average molecular weight). Specifically, the neurofuzzy network model predicts the one step ahead value of the control variable and this is used in the framework of Newton-Raphson method to determine the control action. The objective of nonlinear model predictive control is to control the number-average molecular weight of the polymer.

Finally, chapter 9 provides summary and future prospects of research.

References

Diwekar, U. M., 1992, Unified approach to solving optimal design control problems in batch distilation, *AIChE J*., 38:1551- 1562.

Venkatasubramanian, V. and Sundaram A., 1998, *Encyclopedia of Computational Chemistry*, pp. 1115-1127, John Wiley, Chichester.

Diwekar, U. M., Malik, R. K., Madhavan, K. P., 1987, Optimal reflux rate policy determination for multicomponent batch distillation columns, *Comput., Chem. Eng*., 1:629-637.

Georgoulaki, A. and Korchinsky, W.J., 1997, Simulation of Heterogeneous Azeotropic distillation: An improved algorithm using modified UNIFAC Thermodynamic predictions and the Napthali-Sandholm matrix method, *Trans I. Chem. E*, 75A: 101-115.

Edgar, T. F. and Himmelblau, D.M., 1989, *Optimization of Chemical Processes*, (McGraw- Hill: Singapore).

Wang, K., Qian Y., Yuan Y. and Yao, P., 1998, Synthesis and optimization of heat integrated distillation systems using an improved genetic algorithm, *Comput. Chem. Eng*., 23: 125-136.

Napthali, L.M. and Sandholm, D. P., 1971, Multicomponent separation calculations by linearization, *AIChE. J*,. 17: 1148.

Cardoso, M.F., Salcedo, R.L., Azevedo, S.F., Barbosa, D., 2000, Optimization of reactive distillation processes with simulated annealing, *Chem. Eng. Sci*., 55: 5059-5078.

Eldarsi, H.S. and Douglas, P.L., 1998, Methyl-tert-butyl ether catalytic distillation column, *Trans. I.Chem. E*., 76(May):517-523.

L.A. Zadeh, Fuzzy Sets(1965), *Informat. Control*, 8: 338-353

J. Mendel, 1995, Fuzzy Logic Systems for Engineering: A Tutorial, *Proceeding of the IEEE*, 83:345-377.

B. Kosko, 1997, *Fuzzy Engineering*, Prentice Hall Internal Inc., New Jersey, USA.

Tambe, S. S., Kulkarni, B. D, Deshpande, P. B.,1996, *Elements of Artificial Neural Networks with Selected Applications in Chemical Engineering, and Chemical and Biological Sciences*, Simulation and Advanced Controls, Louisville, KY.

Goldberg, D. E., 1989,Genetic Algorithms in Search, Optimization and Machine Learning, Addison-Wesley, Reading, MA.

Deb, K., 1995, *Optimization for Engineering Design, Algorithms and Examples*, Prentice-Hall: New Delhi.

Goldberg, D. E.,1989,*Genetic Algorithm in Search Optimization and Machine Learning*, Addison-Wesley, Reading: MA.

Holland, J.,1975, *Adaptation in Natural and Artificial Systems*, University of Michigan Press: Ann Arbor, MI.

Morimoto, T., Suzuki, J., Hashimoto, Y., 1997, Optimization of a fuzzy controller for fruit storage using neural networks and genetic algorithms, *Engg. Appl. Artf. Intl.*, 10: 453-461.

Pham, D.T., Karaboga, D.,1998, Cross breeding in genetic optimization and its application to fuzzy logic controller design, *Artf. Intl. in Engg*., 12:15-20.

Mendel, J. M., Mouzouris, G.C.,1997, Designing fuzzy logic systems, *IEEE Transactions on Circuit and Systems- II: Analog and Digital Signal Processing*, 44(11):885-894.

Lennox, B., Motague, G.A., Frith, A.M., Chris Gent, Bevan V., 2001, Industrial application of neural networks – an investigation, *Journal of Process Control*, 11: 497-507.

Kaur, D. and Lin, B., 1998, On the design of neural-fuzzy control system, International, *Journal of Intelligent Systems*, 13:11-26.

Rhinehart, RR, Murugan, P., 1996, Improve process control using fuzzy logic, *Chemical Eng. Progress*, 11:60-65.

Wu, Z. Q., Harris, C.J., 1997, A neurofuzzy network structure for modelling and state estimation of unknown nonlinear systems, *Internal Journal of System Science*, 28(4): 335-345.

Hong, X., Harris, C.J., Wilson P.A.,1998, *Neurofuzzy network State space identification algorithms using prefiltering for non-linear kalman filtering*, Research Report MANTIS No. 1, University of Southampton, Southampton.

Brown, M. and Harris, C.J., 1994, *Neurofuzzy Adaptive Modeling and Control*, Prentice Hall, Hemel Hempstead.

Dierckx, P., 1995, *Curve and Surface Fitting with Splines*, Monographs on numerical analysis, Clarendon Press, Oxford.

Chapter 2

Optimization of Batch Distillation Processes Using Genetic Algorithms

2.1 Introduction

Batch distillation is one of the most widely used unit operations in chemical processing industry. It is a convenient separation tool due to its inherent flexibility in operation and capability to handle number of components. The design of a batch distillation column is however more complex in comparison to that of a continuous distillation column since it is carried out under unsteady-state conditions involving either variable reflux or constant reflux policy. Constant product composition can be achieved in variable reflux policy, whereas the product composition varies under constant reflux policy.

The composition of the more volatile component in the distillate declines with the progress in distillation. For a desired purity of the distillate it is therefore necessary to cut the fraction collected. It is a common practice to have three to four of such cuts during distillation. The objective function is thus to obtain the position of cut or the amount of distillate collected in each cut subject to minimization of total vapor load. Each cut corresponds to a constant reflux operation and the reflux ratio is determined by the bottom composition of the MVC. For convenience this will be referred to as simple optimal reflux policy.

An optimal reflux policy can be usually determined by solution of one of the following optimization problems.

- Maximum distillate problem – the objective is to maximize the amount of distillate of a specified purity in a given length of time.
- Minimum time problem – to minimize the batch time required for producing a prescribed amount of distillate of a specified purity.
- Maximum profit problem – the objective is to maximize profit for specified concentration of distillate.

Various efforts to address these problems are summarized by Mukherjee *et al.* (2001). The most commonly used techniques and their variants, for batch distillation optimization are Pontryagin's maximum principle and non-linear programming (NLP)

methodology. The maximum principle method necessitates repeated numerical solutions of a two-point boundary value problem. As a result, an instability may develop in computation owing to the boundary conditions at one end or the other. Also, the method cannot handle bounds on the control variables (Murty *et al*., 1980, Diwekar, 1992). The NLP methodology is a gradient based technique requiring derivative information corresponding to the objective function and good initial guesses to assure convergence to global optimum. Additionally objective function should be smooth and continuously differentiable (well-defined slope values). In many real life situation the objective function is often multimodal, noisy, and fraught with discontinuities. Simultaneous fulfillment of these criteria cannot be therefore guaranteed thus leading to suboptimal solutions.

In recent years, "stochastic(random) search algorithms" are becoming popular owing to their capability of performing multi-modal optimization (Venkatasubramanian and Sundaram, 1998, Marti, 1992) and differ from the deterministic counterparts in that they involve a random component at some stage(s) during their implementation. It should however be noted that a randomized search does not necessarily indicate a direction-less search. The stochastic optimization algorithms although computationally intensive, are finding wide-spread acceptance in the chemical engineering applications owing to their affordability and the speed of the modern computing technology. Accordingly, in the present paper a stochastic search technique, namely genetic algorithm (GA) has been successfully explored for the optimization of batch distillation columns.

Earlier, Mukherjee *et al*. (2001) used GA for optimization of batch distillation columns for separation of, (i)methanol-water, (ii) o/p chlorotoluenes and (iii) water-DMF systems. In this chapter we follow a similar procedure but improvise on the method to determine the constant reflux ratio to be used during each cut of fraction collection. The reflux ratios are calculated assuming an infinitesimally small change in composition covering the range of composition within each cut. These reflux ratios of a particular cut, are averaged to give the constant reflux ratio of that cut. It is seen that the reflux ratio

calculated by this method is lower than the one calculated by simple method for desired purity. The total vapor load is also calculated based on average reflux ratio. In the present study, two binary batch distillation processes of industrial relevance namely, acetone-water and para/ortho nitrochlorobenzene have been considered. Comparison of this method is made with the simple method used by Mukherjee *et al*. (2001). The acetone-water and para/ortho nitrochlorobenzene mixtures are widely encountered in pharmaceutical industry. The latter system poses separation difficulties owing to the

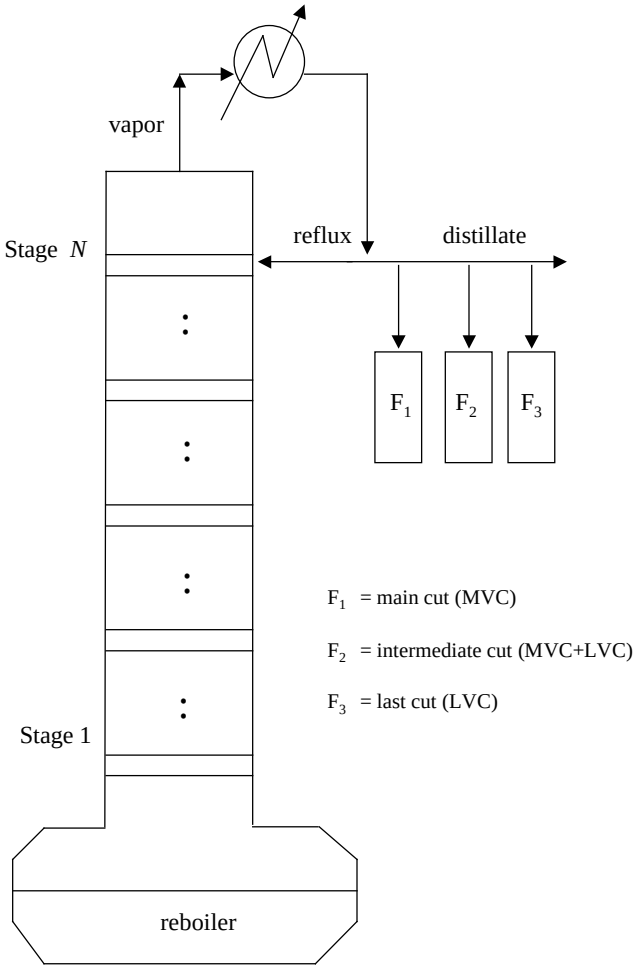

closeness in their boiling points.

Figure 2.1: Schematic of a batch distillation column

2.2 Problem Formulation

In a batch distillation process, the major component of the operating cost is the energy and, therefore, minimization of the total vapor load becomes a worthwhile objective.

$$f(\mathbf{x}) = V = \sum_{k=1}^{Q} (R_k + 1) \times \Delta B_k \tag{2.1}$$

In this equation, V refers to the total vapor load , R_k the reflux ratio for the kth cut, ΔB_k the reduction in moles in the bottom which must be equal to distillate quantity, D_k and Q, refers to the total number of cuts. The bottom compositions of the more volatile component designated as $= [\, x^{m}_{b_1}, x^{m}_{b_2}, \ldots . x^{m}_{b_k}, \ldots . x^{m}_{b_{Q-1}} \,]$ forms the decision variable space. In general, there would be Q -1 values of the bottom compositions of the MVC leading to Q-1 dimensional decision variable vector. The solution to the minimization problem defined in equation (2.1) should satisfy following constraints;

- Inequality constraint

$$x^{m}_{b_i} > x^{m}_{b_1} > x^{m}_{b_2} \ldots . x^{m}_{b_k} > \ldots . x^{m}_{b_{Q-1}} > x^{m}_{b_f} \tag{2.2}$$

where $x^{m}_{b_i}$ and $x^{m}_{b_f}$ represent the specified initial and the final bottom composition of the MVC.

In the present work we use the Fenske-Underwood-Gilliland (FUG) method for batch distillation. It has been shown by Diwekar *et al*. (1987) that the FUG-method, though simple, compares quite favorably with the rigorous tray-by-tray approach. The solution procedure is briefly explained in Appendix A.1.

2.3 Genetic Algorithm Formalism

Solutions to the vapor load minimization problem defined in equation (2.1) have been obtained using the GA formalism. The genetic algorithms (Holland, 1975, Goldberg,1989) are based on the 'survival-of-the-fittest' mechanism of natural selection and propagation of genetic characteristics. GAs utilize these principles for efficient search of noisy, discontinuous and nonconvex solution spaces in arriving at an optimal solution. The characteristic features of GAs are: (i) they can deal with function without any condition on its smoothness, differentiability, and continuity, (ii) they do not need information as regards the derivatives of the objective function, and (iii) they use a stochastic (random) search to converge to (or in the vicinity of) the global optimum of the objective function. Owing to the above-stated attractive features, GAs in recent years are being increasingly used for solving diverse optimization problems (see e.g. Cartwright and Long, 1993, Wang *et al.*, 1996, Manolas *et al.*, 1996, Hanagandi *et al.*, 1996 and Garcia and Scott, 1998).

2.4 Results and Discussion

The performance of GA technique for optimizing the batch distillation columns is evaluated by considering the separation of two binary mixture namely (i) acetone-water and (ii) para/ortho nitrochlorobenzene.

In the GA-based function minimization procedure, the fitness function value should scale inversely with decreasing objective function value. The choice of an appropriate fitness function fulfilling this criterion is critical for obtaining good solutions. Accordingly, the following fitness function is written as;

$$\xi_i = \left(\frac{w_1}{V} \right) \tag{2.3}$$

where w_1 is the weight factor. Weight factors are used for: (i) avoiding the computational errors, such as, numerical overflow, division by zero, etc. during the evaluation of the objective function (ii) expressing the relative importance of cost components, and (iii) making the fitness values more (or less) sensitive to the objective

function values. In the GA procedure, a check for the constraint satisfaction is made before evaluating the fitness value of a candidate solution. If any of the equality or purity constraints are violated then corresponding candidate solution is penalized by assigning a zero fitness score (Goldberg, 1989). This way it is ensured that the constraint violating solution does not compete in the subsequent generations. A more rigorous penalty function approach (Deb, 1995) could also be used as an alternative to the above stated simple approach for constraint handling.

The values of the GA-specific parameters used in the optimization simulations are: decision variable, K = 2; population size, N_{pop}= 20; probability of crossover, P_{cr} = 0.95; probability of mutation, P_{mut} = 0.01. The values of K, N_{pop} and l_{chr} are chosen such that : (i) the GA simulations do not take long CPU times to converge and (ii) the GA-searched solutions possess adequate precision. It may be noted that as the N_{pop} value (representing the size of solution population) decreases, the CPU time required to manipulate the candidate solutions also goes down proportionately. On the other hand, it is essential that N_{pop} should be sufficiently large to explore the solution-space as widely as possible. The values of K = 2 and chromosome length, l_{chr} =20 for the three cut suggest that in a binary-coded solution string, each decision variable is represented with a 10 (=l_{chr}/K) bit precision. This precision can be lowered (enhanced) by appropriately reducing (increasing) the l_{chr}/K ratio.

Table 2.1 presents the operational data for the two binary systems considered here.

Table 2.1: Parameters corresponding to the two binary systems

Parameters	Acetone-water	Para-ortho nitrochloro benzene
Weight (%) of discharge of MVC	99	99
Initial weight (%) at still of MVC	60	35
Final weight (%) at still of MVC	5	5
Quantity (kg) of feed	100	100
Molecular weight of MVC	58	157.50

Molecular weight of LVC	18	157.50

All the simulations were carried out assuming that a maximum of three cuts can be drawn. Also the actual number of stages (N) were restricted to lie between $1.25\times N_m$ and $1.75\times N_m$, where N_m refers to the minimum number of stages. Optimal values of the distillate (D_k^*) and reflux ratios (R_k^*) for $N/N_m = 1.25, 1.5, 1.75$ that minimized the total vapor load for acetone-water and para/ortho nitrochlorobenzene systems are tabulated in Table 2.2.

Table 2.2: Optimum reflux policy for three cuts (*n* =3)

System	N/N_m	*cut no.* (k)	**Present Method**			**Simple Method**		
			D_k^* (kg)	R_k^*	V^*	D_k^* (kg)	R_k^*	V^*
Acetone -water	1.25	1	35.06	2.80	246.14	35.06	2.81	299.45
		2	51.21	2.95		51.21	3.32	
		3	58.21	6.00		58.21	12.72	
	1.50	1	34.68	1.38	154.79	34.68	1.39	195.73
		2	49.70	1.45		49.70	1.64	
		3	58.20	3.15		58.20	7.60	
	1.75	1	38.28	0.93	125.11	38.28	0.95	151.61
		2	51.15	1.04		51.15	1.19	
		3	58.17	2.55		58.17	5.96	
Para/ ortho nitro chloro benzene	1.25	1	18.91	113.0	5596.5	18.91	151.05	7870.0
		2	27.05	193.6		27.05	271.10	
		3	31.72	396.4		31.72	588.71	
	1.50	1	18.81	72.1	3680.6	18.81	98.21	5161.3
		2	27.07	130.9		27.07	177.43	
		3	31.73	259.6		31.73	385.70	
	1.75	1	18.84	59.41	3040.3	18.84	80.95	4251.6
		2	27.94	112.8		27.94	160.84	
		3	31.80	225.5		31.80	318.40	

The corresponding results obtained using the simple method are also listed in the Table 2.2 and plotted in Figures 2.2 and 2.3. It is seen from the results that : (i) for a fixed value of the N / N_m ratio, the optimal reflux ratio, R_k^*, increases continuously with increasing k and, (ii) the optimal total vapor load (V^*) decreases with increasing N / N_m ratio. For the same quantity and purity of distillate the present methodology provides much better optimal solution in that the values of the reflux ratios are much lower as also the total vapor load.

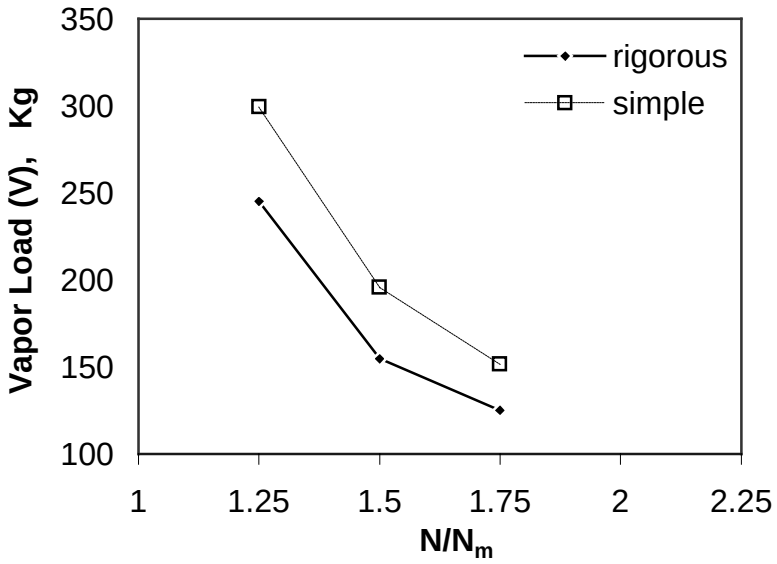

Figure 2.2: Effect of the N/N_m ratio on the total vapor load(V) for acetone-water system

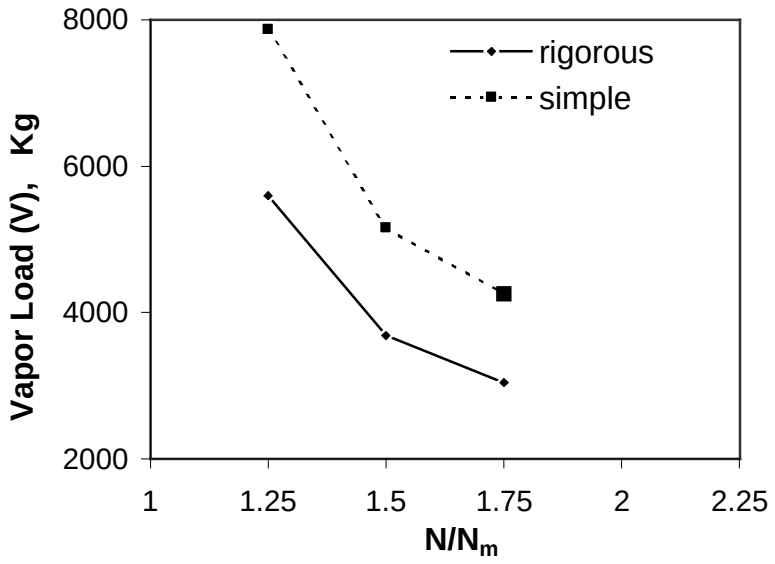

Figure 2.3: Effect of the N/N_m on the total vapor load(V) for para/ortho nitrochlorobenzene system

2.5 Conclusions

This study presents a stochastic formalism, namely genetic algorithm for optimizing batch distillation processes. The commonly used techniques have a number of shortcomings extensively reported in literature. Genetic algorithm technique was successfully employed for optimizing two industrially relevant binary batch distillation systems using a method based on average reflux ratio. The results clearly shows superiority of the present method over the conventional method.

References

Mukherjee, S., Dahule, R.K., Tambe, S.S., Ravetkar, D.D., Kulkarni, B.D., 2001, Consider genetic algorithms to optimize batch distillation, *Hydrocarbon Processing*, Sept.:59-66.

Murty, B. S. N., Gangiah, K., Husain, A., 1980, Performance of various methods in computing optimal control policies, *Chem. Eng. J.*, 19:201-208.

Diwekar, U. M., 1992, Unified approach to solving optimal design control problems in batch distillation, *AIChE J.*, 38:1551- 1562.

Venkatasubramanian, V. and Sundaram, A., 1998, *Encyclopedia of Computational Chemistry*, pp. 1115-1127, John Wiley, Chichester.

Marti, K., 1992, *Stochastic Optimization, Numerical Methods and Technical Applications*, Springer-Verlag, New York.

Diwekar, U. M., Malik, R. K., Madhavan, K. P., 1987, Optimal reflux rate policy determination for multicomponent batch distillation columns, *Comput. Chem. Eng.*, 11:629-637.

Holland, J., 1975, *Adaptation in Natural and Artificial Systems*, University of Michigan Press, Ann Arbor, MI.

Goldberg, 1989, D. E., *Genetic Algorithm in Search, Optimization, and Machine Learning*, Addison-Wesley, Reading, MA.

Cartwright, H., Long, R., 1993, Simultaneous optimization of chemical flowshop sequencing and topology using genetic algorithms, *Ind. Eng. Chem. Res.*, 32: 2706-2713.

Wang, C., Quan, H., Xu, X.,1996, Optimal design of multiproduct batch chemical process using genetic algorithms, *Ind. Eng. Chem. Res.*, 35:3560-3566.

Manolas, D., Gialamas, T., Frangopoulos, C., Tsahalis, P., 1996, A genetic algorithm for optimization of an industrial cogeneration system., *Comput. Chem. Eng.*, 20: S1107-S1112.

Hanagandi, V., Ploehn, H., Nikolaou, M., 1996, Solution of the self-consistent field model for polymer adsorption by genetic algorithms, *Chem. Eng. Sci.*, 51:1071-1078.

Garcia, S., Scott, E., 1998, Use of genetic algorithms in thermal property estimation : Part I-Experimental design optimization, *Numer. Heat Trans.,* 33A:135-148.

Ramanathan, S.P., Mukherjee, S., Dahule, R.K., Ghosh, S., Rahman, I., Tambe, S.S., Ravetkar, D.D., Kulkarni, B.D., 2001, Optimization of continuous distillation columns using stochastic optimization approaches, *Trans. I.Chem. E.*, Part A, 79: 310-322.

Deb, K., 1995, Optimization for Engineering Design, Algorithms and Examples, Prentice- Hall, New Delhi.

Chapter 3

Optimization of Continuous Distillation Columns Using Genetic Algorithms

3.1 Introduction

Continuous distillation is one of the most widely used separation techniques in chemical process industry and exhaustive scientific and practical knowledge of this process has been gained over the last few decades. Being an energy intensive process, optimum operation of continuous distillation columns assumes considerable economic importance. In a typical continuous distillation column operation (see Figure 3.1), the feed enters at any in-between stage and vapors are produced in the reboiler located at column's bottom. The vapors while moving upwards inside the column, get progressively enriched in the more volatile component (MVC) and are condensed in the condenser. A portion of the condensate is then collected as the product while the rest is fed back to the column as reflux; the reflux as it travels down the column gets enriched in the less volatile component (LVC).

Often, chemical mixtures comprise components forming azeotropes that are difficult to separate using simple distillation. In azeotropic distillation, a third component called "entrainer" is added to facilitate the separation of components to the desired purity. For instance, azeotropic distillation is widely used for separating alcohol and water. Its typical schematic consisting of two inlet streams is shown in Figure 3.2. The principal stream (F) is composed of the feed approaching the alcohol-water azeotrope and the other stream comprises (L^{I}_{N+1}) entrainer-rich reflux. The ternary mixture that leaves from the column top is fed to a decanter wherein it separates into organic and aqueous layers. While the entrainer-rich organic layer is returned to the column, the aqueous layer is fed to the stripper for the recovery of dissolved entrainer and alcohol. The other distillation product i.e., anhydrous alcohol, is drawn out at the bottom of the column. In this distillation process, a make-up stream of the entrainer is needed to account for the losses caused by its presence in the product as well as vent streams.

In a typical distillation column, choice of operating parameters include fixing of feed location and reflux ratio (entrainer quantity for azeotropic distillation), whereas the number of stages becomes the design variable. At total (minimum) reflux, we have minimum (infinite) number of stages. Thus, it is seen that all distillation columns operate between these extreme limits. In continuous distillation, reboiler and condenser

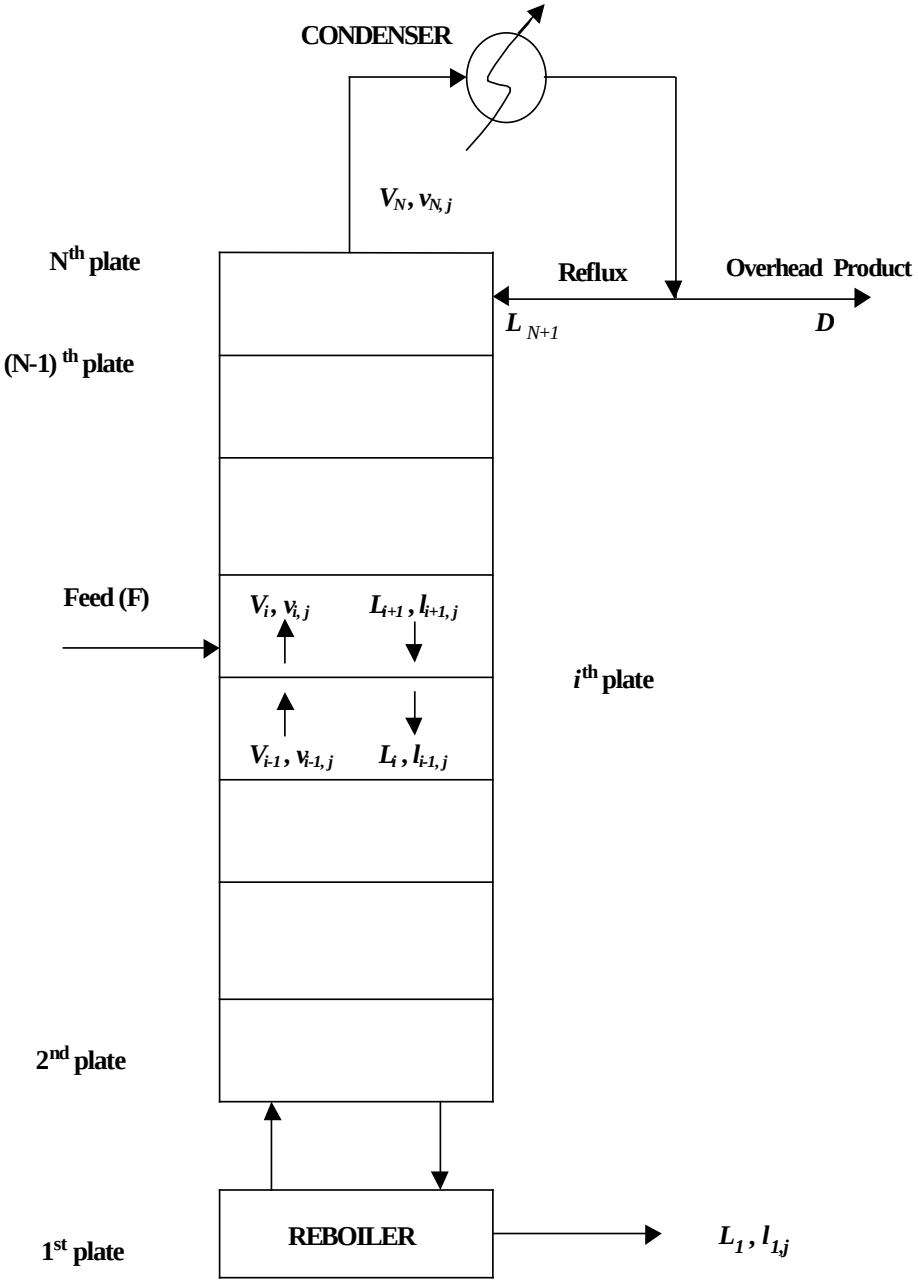

Figure 3.1: Schematic of continuous distillation column

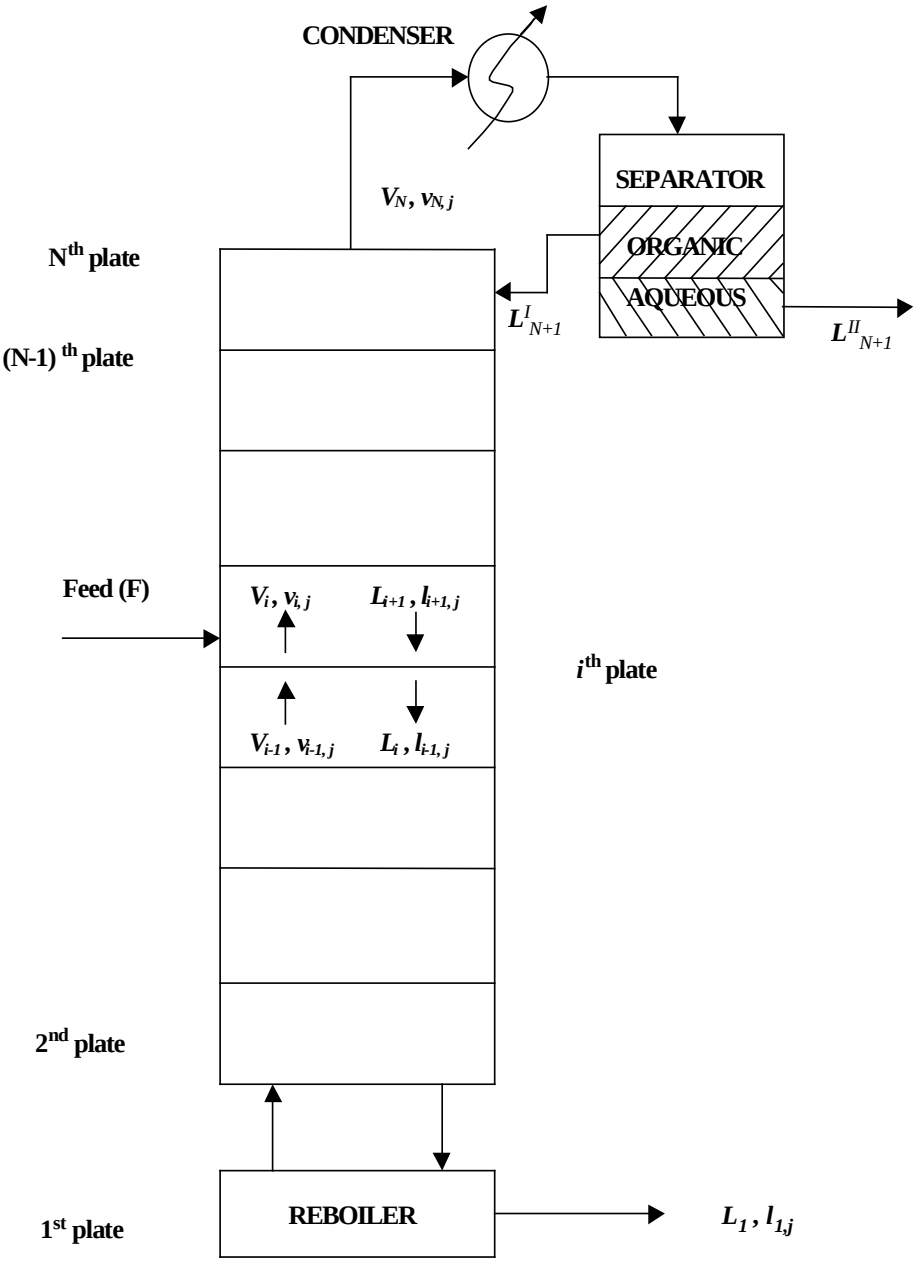

Figure 3.2: Schematic of azeotropic distillation

operations are energy intensive. While an increasing reflux ratio increases both the energy consumption and the tower diameter, it decreases the number of distillation stages. This eventually results in a trade-off between the energy and fixed costs necessitating process optimization. The objective of such an optimization is determination of the optimal operating and design parameters for achieving the desired degree of separation at the lowest total cost. The total cost of a distillation operation is made up of two major components. In the first component, the annual running cost of utilities i.e., the heating media to produce vapors, and cooling media for vapor condensation, are accounted for. The second cost component refers to the annual fixed charges that take into account interest and depreciation on the installation cost of the column, condenser, and reboiler; this component also includes maintenance of the installed equipment.

Several optimization studies dealing with various design aspects of continuous distillations are reported in the literature (e.g., Prokapakis and Sieder,1982, Ryan and Doherty, 1989, Skovborg and Michelson,1992, Viswanathan and Grossman, 1993, Luyben and Floudasi,1994 and Kingsley and Lucia,1988). A comprehensive list of pre-1989 references on distillation column optimization can also be found in Edgar and Himmelblau(1989).

For optimizing continuous distillation columns, the mixed integer nonlinear programming (MINLP) seems to be an attractive approach (Viswanathan and Grossman, 1993, Luyben and Floudas,1994). A related optimization study (Skovborg and Michelson, 1992) employing the outer loop method around the well-known Napthali-Sandholm procedure has also been performed. Both these techniques involve gradient computation at some stage during optimization. It is known that the MINLP formalism can get entrapped into a locally optimum solution instead of the desired globally optimum one. Moreover, MINLP methods are complex, computationally intensive and many simplifications become necessary to make them affordable (Wang *et al.*,1998).

For optimizing continuous azeotropic distillation, Prokapakis and Seider(1983) used Powell's algorithm together with material and energy balances, and equilibrium relations. Powell's algorithm is a direct optimization methodology and simple to

execute. The drawback of the direct methods, however, is that they are not as efficient and robust as the indirect methods, such as the gradient-based Newton's (quadratic) approximation techniques (Edgar and Himmelblau, 1989). Kingsley and Lucia(1988) studied the relationship between two-phase and three-phase solutions to heterogeneous distillation simulation and optimization problems. Here, the problem necessitating a global optimization methodology was addressed using the tunneling algorithm. This algorithm is again gradient-based and, therefore, involves derivative computations.

It is noticed from the above discussion that a majority of studies on continuous distillation optimization include applications of deterministic optimization methods (MINLP, Powell's method, tunneling method, etc.). These formalisms are mostly calculus-based involving direct computation of the gradient. The gradient-based techniques invariably require the objective function to be smooth, continuous and differentiable (well-defined slope values). When the objective function is multimodal, noisy, and fraught with discontinuities, simultaneous fulfillment of these criteria cannot be guaranteed thus leading to suboptimal solutions. For instance, if the search space includes mixed integer (e.g., the number of distillation stages) and continuous (e.g., reflux ratio) variables, then the objective function could be non-monotonic and possess multiple local minima. In recent years, the other class of optimization formalisms, known as "stochastic (random) search algorithms" are becoming popular owing to their capability of performing multi-modal optimization. The stochastic methods differ from the deterministic ones in that they involve a random component at some stage(s) during their implementation. It should however be noted that a randomized search does not necessarily indicate a direction-less search. The stochastic optimization algorithms although computationally intensive, are finding wide-spread acceptance in chemical engineering applications owing to their affordability and speed of the modern computing technology. Accordingly, a stochastic search technique, namely genetic algorithms (GAs) has been successfully explored for the optimization of continuous distillation columns.

3.2 Problem Formulation

3.2.1 Continuous Simple Distillation

The objective function used in this study is representative of the total annual cost (C_T) that is made-up of two components namely, the operating cost (C_1) and fixed cost (C_2). While C_1 accounts for the energy cost pertaining to the reflux ratio and reboiler duty, the cost component C_2 accounts for the number of stages. The overall optimization objective is expressed as:

$$\text{Minimize } C_T(\mathbf{x}) ; \qquad x_k^l \le x_k \le x_k^u \tag{3.1}$$

where C_T (\$) is a function of a K-dimensional decision variable vector, $\mathbf{x}$ ($=[x_1, x_2, ..., x_k, ..., x_K]^T$) and x_k^L and x_k^U respectively refer to the lower and upper bounds on x_k. The three decision variables (K =3) considered for optimization are: (i) the total number of stages (N), which is a function of real-valued x_1, (ii) reflux ratio (x_2), and (iii) the feed location f_l (a function of x_3 and x_1). The evaluation procedure for the cost components C_1 and C_2 is discussed in Appendix D.1. The solution to the minimization problem defined in equation (3.1) should satisfy following constraints:

- Purity constraints

$$x_d^{spec} - x_d^{simu} \le 0$$

$$x_b^{spec} - x_b^{simu} \le 0 \tag{3.2}$$

  where x_d^{spec} and x_b^{spec} respectively represent the desired top and bottom concentrations (mole %) of the MVC, and x_d^{simu} and x_b^{simu} refer to the optimized (simulated) values of the top and bottom concentrations of the MVC, respectively.

- Equality constraints

  As defined by the material balance, equilibrium, summation of mole fraction and heat balance (MESH) equations (see Appendix A.2).

In the present work, the matrix method developed by Napthali and Sandholm[9] has been utilized for the simulation of simple multicomponent distillation to solve the steady-state MESH equations for each plate. The Napthali and Sandholm (NS) method uses the Newton-Raphson technique to simultaneously solve for all the variables in the MESH

equations. For simulation purposes, the full NS matrix method for continuous distillation simulation is combined with the UNIQUAC method for predicting the vapor-liquid equilibrium (VLE).

3.2.2 Continuous Azeotropic Distillation

Optimization objective for the azeotropic distillation also involves minimization of the total cost, C_T, with the associated bounds on the three decision variables (see equation 3.1). The decision variable, $x_{2,}$ in the present case signifies entrainer quantity. For a *C*-component azeotropic system, the optimized solution should satisfy following purity constraints.

$$x_{bj}^{spec} - x_{bj}^{simu} \leq 0; \qquad j = 1,2,...,C \tag{3.3}$$

where x_{bj}^{spec} and x_{bj}^{simu} respectively refer to the desired and optimized bottom concentrations of the *j*th component of azeotropic mixture.

By assuming constant molar overflow (Magnussen *et al.*,1979), it is possible to simplify the equality constraints defined by the MESH equations. Under this assumption, the energy balance can be ignored and only the total stage mass balance and component balance equations, which are coupled with the equilibrium equations, need to be solved. The equality constraints in respect of the MES (mass balance, equilibrium and summation) equations are described in Appendix A.3.

In the case of heterogeneous azeotropic distillation, two phases are formed following condensation of vapors on the top plate. Thus, additional computations taking into account the liquid-liquid equilibrium are necessary for determining the composition and amount of reflux. For simulating an azeotropic distillation column, the above–described simplified NS method considering material balance on each plate, is coupled with the phase separation calculations for the condenser; the prediction of the vapor-liquid and liquid-liquid equilibria has been made using UNIQUAC method.

3. 3 Genetic Algorithms

Solutions to the cost minimization problem defined in equation (3.1) were obtained using GA stochastic optimization formalisms.

Owing to the above-stated attractive features, GAs have been utilized in diverse chemical engineering optimization applications (see e.g. Cartwright and Long,1993, Wang *et al*., 1996, Manholas *et al*., 1996, Hanagandi *et al*.,1996, Onnen *et al*.,1997, Wrate and Wozniak, 1997 and Garcia and Scott 1998a and 1998b). In the earlier studies on GA-based optimization of distillation processes, Fraga and Matias(1996) optimized a reduced optimization problem wherein a preselected sequence of distillation units and associated heat exchanger network (HEN) was considered for the separation of ternary azeotropic mixtures. The objective function evaluation used by Fraga and Matias(1996) is a design procedure in itself determining the unit design parameters (reflux rate and number of stages) and the HEN along with the full annualized operating cost. For this objective, they used a parallel version of the GA that was implemented using a distributed memory multicomputer in the form of a network of workstations. In the other study, Wang *et al.* (1998) utilized an improved GA (IGA) for synthesizing an optimal distillation sequence and its HEN, with the objective of minimizing the total annual cost. The specific problems considered for validating the IGA methodology were separation of five- and four-component (non-azeotropic) feed streams. As can be seen, the GA-based studies alluded to above analyzed the HEN-augmented distillation columns. In small and medium-scale industries, distillation columns are often operated in a stand-alone mode i.e., without HEN-augmentation. This happens particularly when hot and cold streams are not readily available. In the present paper, therefore, the basic continuous and azeotropic distillation optimization problem involving a single distillation column has been addressed.

3.4 Results and Discussion

3.4.1 Continuous Distillation Optimization

For evaluating the performance of GA technique for optimizing the steady-state staged continuous distillation columns, we have considered separation of two industrially important binary mixtures: (i) methanol-water, and (ii) ethanol-water. Many times a distillation column is operated with multiple feeds and therefore the methanol-water system with two feed streams has also been examined. The

procedural details of the above-stated optimization case studies and the results obtained thereby are described in the following.

Since the number of stages (N) can assume only discrete values, the related decision variable (x_1) is converted into its integer equivalent. Also, for the procedural convenience, the values of the feed location variable (x_3) are normalized. Accordingly, following expressions have been used for computing the value of N and the discrete value (f_l) of the feed location variable, x_3.

$$N = \text{int}(x_1)$$

$$f_l = \text{int}[1 + x_3 (N-2)]; \quad 0 \le x_3 \le 1; \quad x_1\text{-}1 > f_l > 1 \tag{3.4}$$

where int(.) refers to the integer function. In equation (3.4), the reboiler and condenser respectively represent the first and the last distillation stages.

In the GA-based function minimization procedure, the fitness function value should scale inversely with decreasing objective function value. The choice of an appropriate fitness function fulfilling this criterion is critical for obtaining good solutions. Accordingly, a number of fitness function forms were tested and the one given below, which in addition to the total cost also accounts for the purity constraints, yielded consistently good solutions;

$$\xi(\mathbf{x}) = R_1 + R_2 \tag{3.5}$$

where,

$$R_1 = \left[w_1 \times \left(1 - \frac{1}{1+\exp^{-C_T \times w_2}} \right) \right], \tag{3.6}$$

and

$$R_2 = \left[w_3 \times \left(\frac{1}{1 + abs(x_d^{spec} - x_d^{simu}) + abs(x_b^{spec} - x_b^{simu})} \right) \right] \tag{3.7}$$

In the above, the term defined by R_1 takes into account the total distillation cost, while R_2 accounts for the purity constraints; w_1, w_2 and, w_3 are the weight factors used for scaling. In the GA procedure, a check for the constraint satisfaction is made before evaluating the fitness value of a candidate solution. If any of the equality or purity constraints are violated then corresponding candidate solution is penalized by assigning it

a zero fitness score (Goldberg,1989). This way it is ensured that the constraint violating solution does not compete in the subsequent generations. A more rigorous penalty function approach (Deb,1995) could also be used as an alternative to the above-stated simple approach for constraint handing.

With these preliminaries, the results of the GA-based optimization corresponding to the three case studies are described below.

The values of GA parameters used in the optimization simulations are: N_{pop}= 30; P_{cr} = 0.95; P_{mut} = 0.01 and l_{chr} = 120. In Table 3.1, the parameter values corresponding to the three binary systems, are listed. The GA-optimized values of the three process decision variables namely: (i) number of stages (N), (ii) reflux ratio, R (= x_2), and feed location (f_l) along with the respective purity values (for bottom and top composition) and the corresponding minimized value of the total cost, are listed in Table 3.2. For illustration purposes, the composition and temperature profiles as a function of the stage number, pertaining to the GA-based solution for the ethanol-water system, are shown in Figures 3.3 and 3.4, respectively.

Table 3.1: System parameters used for simulating simple continuous distillation simulation

Binary system parameter	methanol – water (single feed)	methanol-water (two feeds)	ethanol-water
Number of feeds	1	2	1
Feed composition of MVC (mole %)	50	60, 40	60
Feed Flow rate (kmol/hr)	60	30, 30	60
Top composition of MVC, x_d^{spec} (mole %)	99	99	95
Bottom composition of MVC, x_b^{spec} (mole %)	5	5	1

Table 3.2: GA-based optimized solutions for continuous distillation*

System	N	R	f_l	x_d^{simu}	x_b^{simu}	C_T ($/year)	C_{PROD} [#] ($/kg)
Methanol-water (single feed)	28	0.9763	12	0.990	0.050	151117	0.0208
Methanol-water (double feed)	25	0.933	9, 7	0.990	0.050	145906	0.0200
Ethanol-water	47	2.7316	33	0.948	0.009	137548	0.0151

* The desired purity values of the more volatile compound (MVC) in top (x_d^{spec}) and bottom (x_b^{spec}) compositions were: (i) methanol-water system: x_d^{spec} =0.99, x_b^{spec} =0.05, (ii) ethanol-water system: x_d^{spec} =0.95, x_b^{spec} =0.01, and (iii) water-acetic acid system: x_d^{spec} =0.90, x_b^{spec} =0.01.

[#] C_{PROD} is the cost per kg of distillate.

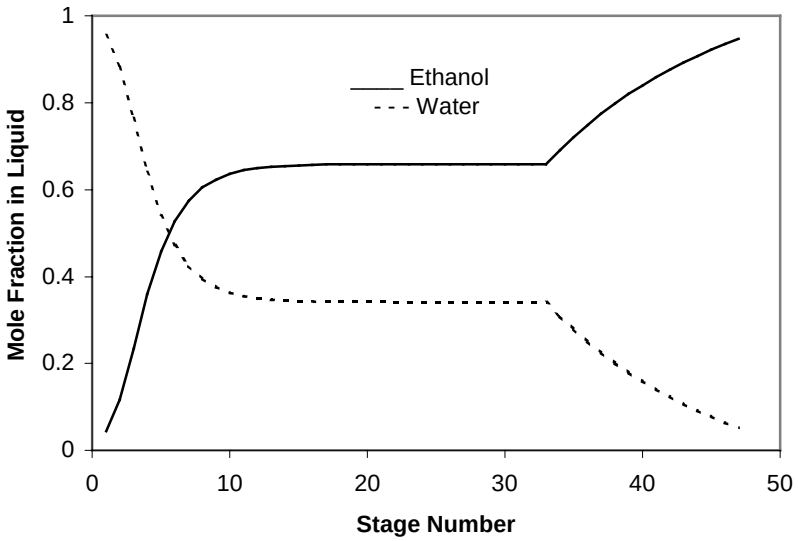

Figure 3.3: Composition profiles corresponding to the GA-based optimal solution for the ethanol-water system

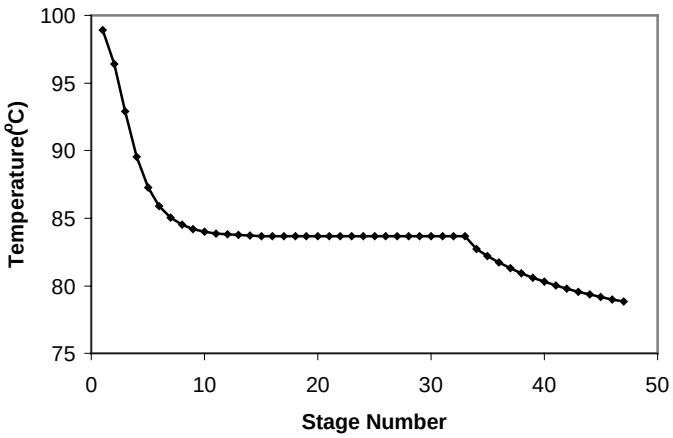

Figure 3.4: Temperature profile corresponding to the GA-based optimal solution for the ethanol-water system

A comparison of the GA-based optimal solutions reveals that the total cost values minimized by both the approaches have nearly same magnitudes (see Tables 3.2), although the optimized values of N, R and f_l show minor differences. It is also observed that the optimal solutions very closely satisfy the purity constraints in respect of the top and bottom compositions of the MVC.

3.4.2 Continuous Azeotropic Distillation Optimization

A industrially important system necessitating azeotropic distillation is ethanol-water where benzene is utilized as an entrainer. The column specifications used in the optimization simulations corresponding to the ethanol-water is given in Table 3.3. In these simulations, a fitness function similar to equation (3.5), but modified to account for the purity constraint with respect to the third component (benzene), has been utilized. In this function, while the term R_1 remains unchanged, the term R_2 is modified as:

$$R_2 = \left[w_3 \times \left(\frac{1}{1 + abs(x_{b1}^{spec} - x_{b1}^{simu}) + abs(x_{b2}^{spec} - x_{b2}^{simu}) + abs(x_{b3}^{spec} - x_{b3}^{simu})} \right) \right] \qquad (3.8)$$

where x_{bj}^{spec} and x_{bj}^{simu} (j =1-3) represent the desired and simulated bottoms concentrations of the ternary system components. The GA-based solutions

corresponding to ethanol-water system is listed in Table 3.4. These simulations were performed using the same values of the GA-parameters as in the earlier case studies. They are in good agreement with those obtained using GAs. The equilibrium composition and temperature profiles as a function of stage number in respect of the GA-based optimal solution for the ethanol-water-benzene system are depicted in Figures 3.5 and 3.6, respectively. The trends of profiles shown in the figures are in good agreement with those obtained by Georgoulaki and Korchinsky(1997).

Table 3.3: Column specifications* for continuous azeotropic distillation of ethanol-water-benzene systems

Feed	Component flows (kmol/hr)		
	Benzene	Ethanol	Water
• First feed	2	55.6	79.4
• Second feed at N_{st}	$x_2^{\#}$	0.5	0.5

* Column pressure: 1.1 atm,
\# to be optimized

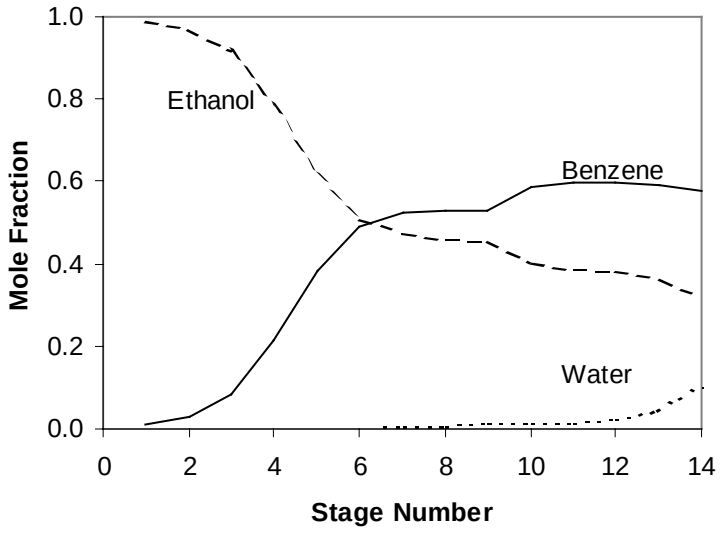

Figure 3.5: Composition profiles (GA-based) for ethanol-water-benzene system

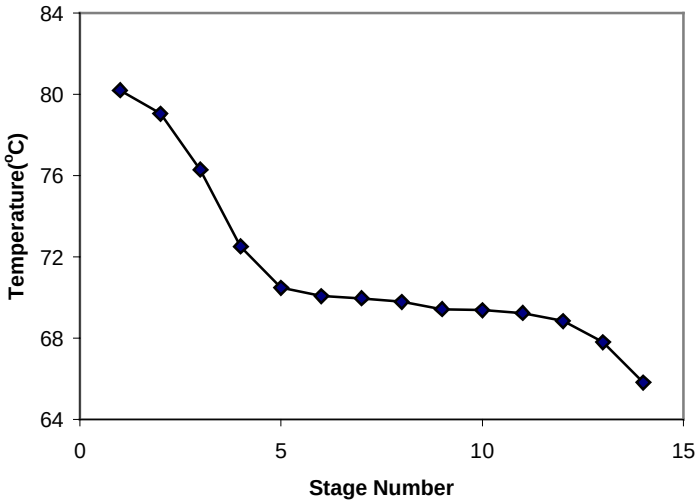

Figure 3.6: Temperature profile corresponding to the GA-based optimal solution for the ethanol-water-benzene system

Table 3.4: GA-based optimized results for continuous azeotropic distillation*

System	x_{b1}^{simu}	x_{b2}^{simu}	x_{b3}^{simu}	N	L_{N+1}^{I} kmol/hr	f_l	C_T ; ($/year)	C_{PROD} [#] ; ($/ kg)
Ethanol-water-benzene	0.9862	0.0003	0.0135	14	25.92	9	1975109	0.0726

* The desired purity values of the bottom product for both the systems were: x_{b1}^{spec} =0.99, x_{b2}^{spec} =0.005, x_{b3}^{spec} =0.005 .

[#] C_{PROD} refers to cost per kg of bottom product.

3.4.3 Issues Related to GA-based Optimization

For nonlinear objective functions, the decision surface may consist of multiple local minima of various shapes and sizes. In the case of problems involving function minimization, locating the deepest local or the global minimum assumes great importance. The stochastic nature of the GA search method to an extent assists in achieving this objective. Notwithstanding this observation, a special care was taken during GA implementation that the search space gets thoroughly explored. Specifically, for a fixed set of GA-specific parameter values, multiple optimization simulations were performed using each time a different random number sequence. Usage of different random number sequences changes the initial candidate solution population in the GA-based optimization. In this way, a different search sub-space is explored each time thereby giving the optimization algorithm a fair chance of locating the deepest local or the global minimum on the objective function surface. Since multiple optimization simulations are necessary to obtain an overall optimal solution, it becomes necessary to examine the CPU times requirements of the GA methodology. It is seen from the CPU time values that GA method is not computationally costly, even if multiple optimization runs need to performed. Thus it can be inferred that the GA formalism is more robust.

Table 3.5: CPU time consumed by GA-based optimization simulations*

System	GA	
	N_{gen}	CPU time(sec)
(i) Methanol-water (single feed)	5	34
(ii) Methanol-water (double feed)	52	153
(iii) Ethanol-water	100	293
(iv) Ethanol-water- benzene	142	509

* evaluated on 366MHz Pentium Celeron PC

3.5 Conclusions

To summarize, this paper presents a stochastic formalisms, namely GA for the optimization of continuous simple and continuous azeotropic distillation columns. These optimization paradigms possess positive characteristics, such as: (i) only objective function measurements and not the measurements (or direct calculation) of the objective function derivatives, are needed in their optimization procedures, (ii) simplicity of the algorithms, and (iii) tolerance to noisy objective functions. A particularly significant advantage of the GA methodology is that unlike most commonly used gradient-descent optimization methods, it does not require the objective function to be smooth, differentiable and continuous, simultaneously. The efficacy of GA formalisms for the optimization objective involving minimization of the total distillation cost, has been demonstrated by considering two binary (non-azotropic) and one tertiary (azeotropic) systems of industrial importance; the column parameters optimized are the number of stages, reflux ratio (entrainer quantity for azeotropic distillation) and feed location. The optimization results obtained thereby suggest that the GA methodology can be gainfully employed for optimizing continuous distillation columns.

Nomenclature

C	number of components
C_T	total annualized cost ($)
C_1	energy cost ($)
C_2	fixed cost ($)
C_{PROD}	product cost ($/kg)
E	discrepancy function for energy balance
f_l	integer-valued feed location
F	feed flow (kmol/hr)
h	enthalpy of liquid (kcal/mol)
H	enthalpy of vapor (kcal/mol)
k	number of decision variables
l	liquid flow of component. (kmol/hr)
L	total liquid flow (kmol/hr)
l_{chr}	chromosome length
m	equilibrium constant
M	discrepancy function for component mass balance
n	string index
N	total number of stages including condenser and reboiler
N_{gen}	number of generations
N_{pop}	population size
P_o	system pressure, atm
P_1	bottom pressure, atm
p	vapor pressure, atm
Δp	pressure drop in each plate.
P_{cr}	probability of crossover
P_{mut}	probability of mutation
Q	discrepancy function for equilibrium relationship
Q_{mut}	variable probability of mutation

Q_r reboiler duty (kcal/hr)

R reflux ratio

S vapor side-stream

s liquid side-stream

T_1 reboiler temperature, °C

T_N condenser temperature, °C

V total vapor flow

v vapor component flow

x_{dj}^{spec} desired concentration of jth distillate component

x_{bj}^{spec} desired concentration of jth bottom component

x_{dj}^{simu} optimized concentration of jth distillate component

x_{bj}^{simu} optimized concentration of jth bottom component

$\mathbf{x}$ decision variable vector

x_1 real-valued decision variable representing number of stages

x_2 reflux ratio; in the case of azeotropic distillation entrainer quantity

x_3 normalized feed location

Z_n probability of selecting nth string

Greek symbols

ξ_n fitness value of nth chromosome

γ activity coefficient

β decay rate

η Murphree's stage efficiency

φ stripping factor

λ_{steam} latent heat of steam vaporization

Superscripts

I organic liquid phase

II aqueous liquid phase

References

Prokapakis, G. J. and Seider, W. D., 1983, Feasible specification in azeotropic distillation, *AIChE. J.*, 29(1): 49-60.

Ryan, P.J. and Doherty, M. F., 1989, Design/optimization of ternary heterogeneous azeotropic distillation sequences, *AIChE. J.*, 35(10):1592-1601.

Skovborg, P. and Michelsen, M. L.,1992, A flexible algorithm for simulation and optimization of continuous distillation, *Comput. Chem. Eng.*, 16: S255-S262.

Viswanathan, J. and Grossmann, I. E., 1993, Optimal feed locations and number of trays for distillation columns with multiple feeds, *Ind. Eng. Chem. Res.*, 32: 2943-2949.

Luyben, M. L. and Floudas, C. A., 1994, Analyzing the interaction of design and control-1, A multiobjective framework and application to binary distillation synthesis, *Comput. Chem. Eng.*, 18: 933-969.

Kingsley, J. P. and Lucia, A., 1988, Simulation and optimization of three-phase distillation processes, *Ind. Eng. Chem. Res.*, 27(10):1900-1910.

Edgar, T. F. and Himmelblau, D.M., 1989, *Optimization of Chemical Process*, (McGraw-Hill: Singapore).

Wang, K., Qian Y., Yuan, Y. and Yao, P., 1998, Synthesis and optimization of heat integrated distillation systems using an improved genetic algorithm, *Comput. Chem. Eng.*, 23: 125-136.

Napthali, L.M. and Sandholm, D. P., 1971, Multicomponent separation calculations by linearization, *AIChE. J.*, 17: 1148.

Magnussen, T., Michelsen, M. L. and Fredenslund, Aa, 1979, Azeotropic distillation using UNIFAC, *I. Chem. E. Symp. Ser.*, 56: 4.2,1.

Holland, J., 1975, *Adaptation in Natural and Artificial Systems*, (University of Michigan Press: Ann Arbor, MI)

Goldberg, D. E., 1989, Genet*ic Algorithm in Search, Optimization, and Machine* Learning,Addison-Wesley, Reading: MA.

Venkatasubramanian, V. and Sundaram, A., 1998, *Encyclopedia of Computational Chemistry*, pp. 1115-1127 (John Wiley, Chichester).

Cartwright, H. and Long, R., 1993, Simultaneous optimization of chemical flow-shop sequencing and topology using genetic algorithms, *Ind. Eng. Chem. Res.*, 32: 2706-2713.

Wang, C., Quan, H. and Xu., X., 1996, Optimal Design of multiproduct batch chemical process using genetic algorithms, *Ind. Eng. Chem. Res.*, 35: 3560-3566.

Manolas, D., Gialamas, T., Frangopoulos, C. and Tsahalis, P.A, 1996, Genetic algorithm for optimization of an industrial cogeneration system, *Comput. Chem. Eng.*, 20: S1107-S1112.

Hanagandi, V., Ploehn, H. and Nikolaou, M., 1996, Solution of the self-consistent field model for polymer adsorption by genetic algorithms, *Chem. Eng. Sci.*, 51: 1071-1078.

Onnen, C., Babuska, R., Kaymak, U., Sousa, J., Verbruggen, H. and Isermann, R., 1997, Genetic algorithms for optimization in predictive Control, *Control Eng. Practice*, 5: 1363-1372.

Wrate, C. and Wozniak, L., 1997, Hydrogenerator system identification using a simple genetic algorithm, *IEEE Trans. Energy Convers.*, 12: 60.

Garcia, S. and Scott, E.,1998, Use of genetic algorithms in thermal property Estimation: Part I- Experimental design optimization, *Numer. Heat Trans.*, 33A: 135-148.

Garcia, S., Guynn, J. and Scott, E., 1998, Use of genetic algorithms in thermal property estimation: Part II- Experimental design optimization, *Numer. Heat Trans.*, 33A: 149.

Fraga, E. S. and Matias, T. S., 1996, Synthesis and optimization of a nonideal distillation system using a parallel genetic algorithm, *Comput. Chem. Eng.*, 20: S79-S84.

Pham, D. T., and Karoboga, D., 1997, Genetic algorithms with variable mutation rates: application to fuzzy logic controller design, *Proc. Instn. Mech. Engrs*, 211, Part-I: 157-167.

Deb, K., 1995, *Optimization for Engineering Design, Algorithms and Examples*, Prentice-Hall: New Delhi.

Georgoulaki, A. and Korchinsky, W.J., 1997, Simulation of Heterogeneous Azeotropic Distillation: An improved algorithm using modified UNIFAC Thermodynamic predictions and the Napthali-Sandholm matrix method", *Trans I. Chem. E*, 75A:101-115.

Fredenslund, A., Gmehling J., Rasmussen P.,1977, *Vapor-liquid Equilibria Using UNIFAC*, Elsevier Scientific Publishing Co., Amsterdam.

Chapter 4

Optimization of Reactive Distillation Using Genetic Algorithms

4.1 Introduction

Reactive/catalytic distillation have potential advantage over the more conventional distillation. Both have demonstrated the potential to lower costs and reduced energy consumption, waste production and utilization of the heat of reaction. There are three main cases in the chemical industry, in which combined distillation and chemical reaction occur (Alejski K. *et al.*,1996) :

(1) use of a distillation column as a chemical reactor in order to increase conversion of reactants,

(2) improvement of separation in distillation column by using a chemical reaction in order to change unfavorable relations between component volatilities,

(3) course of parasitic reactions during distillation, decreasing yield of process.

Most of the studies in reactive distillation are simulation studies, which covers composition/temperature profiles, column pressure, reflux ratio or boil-up fraction, total number of trays, feed plate location and liquid-phase volumes on each tray (Cardoso *et al.*,2000). While Ciric and Gu (1994), Cardoso *et al.* (2000) and Eldarsi *et al.* (1998) focused on the optimization of reactive distillation column.

Ciric and Gu (1994) studied optimization of reactive distillation column for more than one chemical reaction by mixed integer non-linear programming (MINLP) technique. The solution of this problem yields optimum number of trays, the optimal feed tray location(s) and composition(s), and the composition profiles within the column. Later, Cardoso *et al.* (2000) used simulated annealing based MINLP algorithm and an adaptive random search MINLP algorithm developed to solve the above problem yielding better results.

Eldarsi and Douglas (1998) optimized an MTBE catalytic distillation column using Aspen Plus. The AspenPlus's complex optimization algorithm together with the model was used for optimization. The decision variables selected were pressure, reflux ratio and bottom flow rate.

It is known that the MINLP formalism can get entrapped into a locally optimum solution instead of desired globally optimum one. Moreover, MINLP methods are

complex, computationally intensive and many simplifications become necessary to make them affordable(Wang, 1998).

In the recent year, genetic algorithms are becoming increasingly popular due to its capability of finding a global optima. GAs work according to the principles of natural genetic and perform stochastic search. It has been proved to be robust optimization technique for finding global optima. GAs, although are computationally intensive, are finding wide-spread acceptance in the chemical engineering applications due to their affordability and day by day increasing speed of computers.

In this chapter, GAs have been successfully explored for optimization of reactive and catalytic distillation columns by adopting the column model of Ciric and Gu(1994). The column simulation model is based on an extension of conventional distillation columns (Cardoso *et al*., 2000).

4.2 Problem Formulation

The objective function is the minimization of the total annualized cost (C_T)which is composed of two basic terms: annualized operating cost and annualized installed cost(investment). The optimization problem for design of reactive distillation column is (Cardoso *et al*., 2000)

$$C_T = \min\left\{\sum_{i=1}^{c} c_i \sum_{k=1}^{N} F_{ik} + c_H Q_B + c_w Q_c + C_{cs} + C_{ci} + C_r + C_c \right\} \qquad (4.1)$$

where c_i is the raw material i, F_{ik} is the flow rate of component i onto tray k, c_H is cost of steam, c_W cost of cooling water and Q_B, Q_c correspond to reboiler and condenser duties. C_{cs}, C_{ci}, C_r, C_c are annualized installed costs of the column shell, trays, reboiler, condenser respectively.

To evaluate the C_T, the operating conditions determined by column simulation for each decision vector have to be known. These decision vectors are used to calculate column cost calculation (Appendix D.2).

In this study, a procedure for the simulation of reactive distillation columns (Appendix A.4) based on the method developed by Bastos (1987) for conventional distillation column as well as one described by Cardoso *et al.* (2000) for the chemical

reaction is used. The simulation of reactive distillation processes involves the simultaneous solution of material and energy balances and stoichiometric relationships, and this corresponds to the solution of considerable large set of non-linear equations.

The Newton-Raphson algorithm is used to compute the composition profile by solving the material balance. The use of the Newton-Raphson method requires a proper starting guess for the composition profile, which is always available from the previous studies.

The simulation stops with a feasible distillation column when the global material balance of all components is obeyed. The global material balance is assumed to be all right when

$$\sqrt{\sum_{i=1}^{C}\left[\sum_{k=1}^{N}(F_{ik}+\sum_{j=1}^{R}\nu_{ij}\varepsilon_{jk})-P_i\right]^2}<\varsigma_c \qquad (4.2)$$

where F_{ik} is the flow rate of component i onto tray k, P_i is the production rate of component i. ν_{ij} is stoichiometric coefficient of component i in the reaction j, ε_{jk} is the extent of reaction j (j =1,R) on tray k and ς_c is appropriate value. The algorithm ends up when global material balance to the column is verified. A non-plausible column is obtained when Newton-Raphson method exceeds a pre-specified maximum number of iterations failing to satisfy the global material balance. This situation leads to infeasible column and objective function value is simply penalized with a large constant value. The simulation algorithm is shown in Figure 4.1.

4.3 Genetic Algorithms

Genetic algorithms (GAs) are based on the mechanisms of natural genetics such as reproduction, crossover, and mutation. As GAs are based on the population of points and the probabilistic transition rules, not deterministic rules, they offer higher probability of finding the global optimum compared with other deterministic optimization methods (Goldberg, 1989). GAs are efficient in searching of noisy, discontinuous and nonconvex solution spaces and arriving at an optimal solution. Apart from this, GAs do not need derivatives of the objective function being minimized, they require only scalar values.

Due to above advantage, GAs have been used for solving diverse optimization problems (see e.g. Cartwright and Long(1993), Wang *et al.* (1996), Manolas *et al.* (1996), Hanagandi *et al.* (1996). And recently, Ramanathan *et al.* (2001) showed feasibility of GAs to continuous distillation for minimization of cost of column.

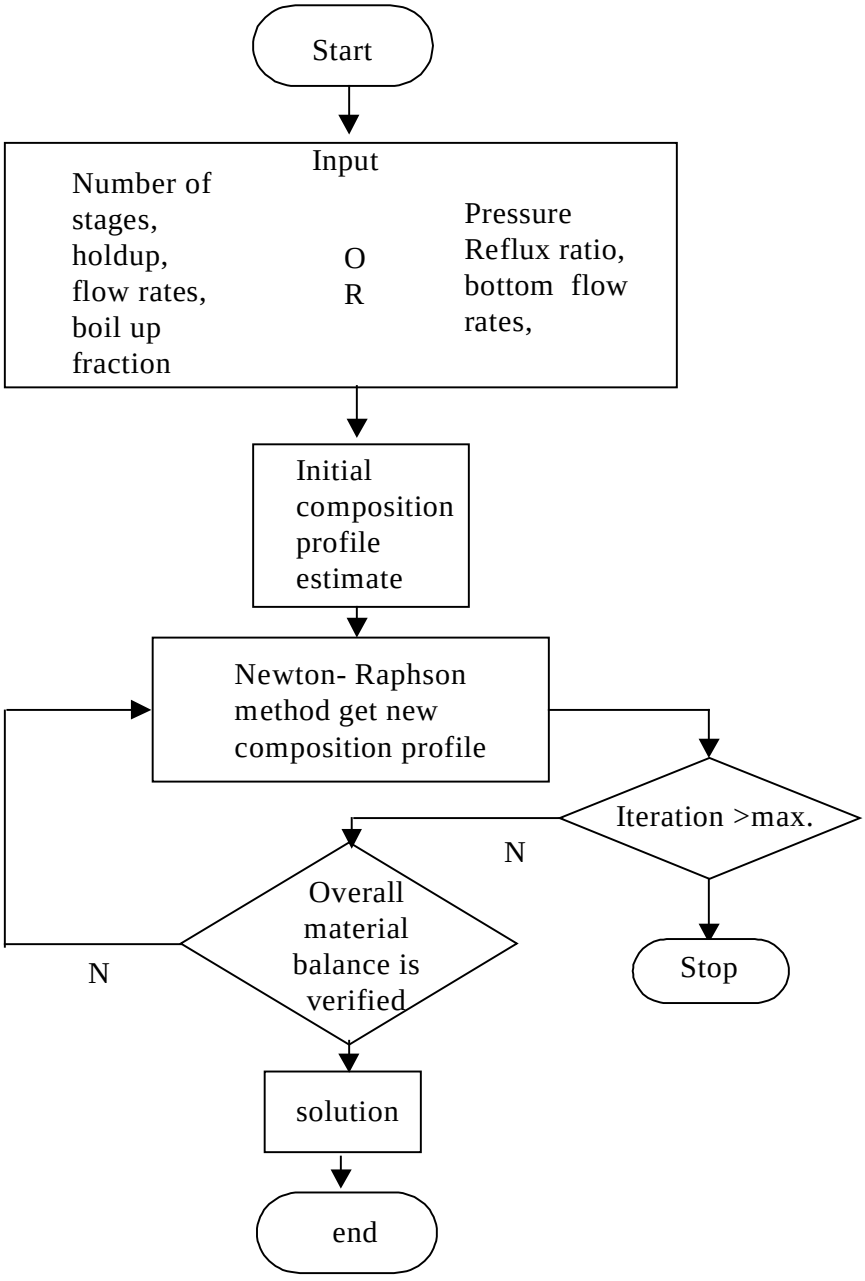

Figure 4.1: Simulation algorithm

4.4 Results and Discussion

For evaluating the performance of the GA techniques for optimizing the steady-state continuous reactive distillation columns, we have considered production of ethylene glycol and MTBE.

In the GA-based function minimization procedure, the fitness function value should scale inversely with decreasing value of the objective function. The choice of an appropriate fitness function fulfilling this criterion is critical for obtaining good solutions. Accordingly, a number of fitness function forms were tested and the one given below, which in addition to the total cost also accounts for the purity constraints, yielded consistently good solutions.

$$Z = \left(1 - \frac{1}{1 + \exp(-C_T \times w_1)}\right) \tag{4.3}$$

In the above, the term defined by Z takes into account the total distillation cost. w_1 is the weight factor used for making the fitness function values more(or less) sensitive to the objective function values. In the GA before evaluating the fitness value a check for the constraint satisfaction is made before evaluating the fitness value of a candidate solution. If any of the constrains are violated then corresponding candidate solution is penalized by assigning it a zero fitness score. This one of the way for ensuring that constraint violation solution does not compete for a place in the mating pool. A more rigorous penalty function approach could also be used as an alternative to the above-stated simple approach for the constraint handling.

In case of ethylene glycol production, one of the variable for optimization is number of trays. As the number of trays changes, the number of variables concerning holdup and flow rate on trays also change. The problem of optimization is defined based on maximum number of variables to be optimized; however, for a column less than the maximum trays, problem is solved for required variable while the other variables simply ignored.

4.4.1 Case Studies

4.4.1.1 Ethylene glycol

Ethylene glycol is typically obtained from the reaction of ethylene oxide and water

$$C_2H_4O + H_2O \rightarrow C_2H_6O_2 \tag{4.4}$$

The unwanted byproduct diethylene glycol (DEG) is also produced from the reaction of ethylene glycol and ethylene oxide. Both the reactions are highly exothermic.

$$C_2H_4O + C_2H_6O_2 \rightarrow C_4H_{10}O_3 \tag{4.5}$$

Ciric and Gu (1994) described two good reasons for producing ethylene glycol via reactive distillation. First, the large volatility difference between ethylene oxide and ethylene glycol will lead to rapid separation of oxide from glycol in the column, improving the overall selectivity. Secondly, reactive distillation can directly absorb the heat of reaction into the heat required for separation, achieving a natural heat integration that may reduce operating costs.

Figure 4.2 shows a schematic diagram of the reactive distillation process. A production rate of 6.6 mol/s of ethylene glycol and ethylene oxide feed of 7.3 mol/s and water feed of 7.5 mol/s are assumed. The enthalpy of vaporization of the mixture is assumed to be constant all over the column with the value of 40.0×10^3 kJmol^{-1} (Ciric & Gu, 1994). Cost data for this problem can be found Appendix E.

The three decision variable considered for optimization of ethylene glycol reactive distillation column are (i) the total number of trays, (ii) liquid holdup on each trays (iii) boil up fraction and (iv) feed flow rates of ethylene oxide and water. Liquid holdup on all trays are considered. Four trays from bottom are assigned as distillation zone and remaining trays are used as reactive zone, therefore feed of ethylene oxide restricted to reactive zone and water to top two trays. Earlier Cardoso *et al.* (2000) concluded that optimum columns may be designed by fixing number of trays anywhere between 5 and 17.

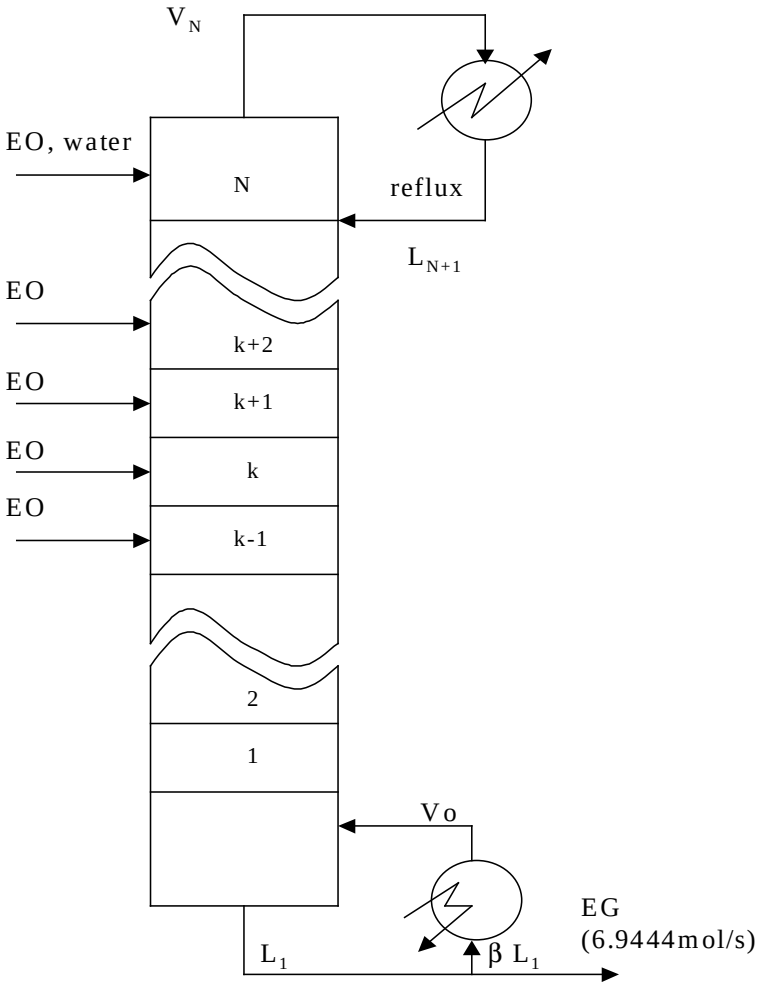

Figure 4.2: Schematic of a reactive distillation column

Optimization were performed with both ideal and non-ideal VLE, for trays between 5 and 17 at atmospheric pressure. Table 4.1 shows the column specification and temperature profiles. The objective function for ideal VLE, the best solution obtained by Cardoso *et al.*(2000) was 15.03×10^{6} US\$yr^{-1} with 7 trays. While the GA-based optimization results (Table 4.3) shows 15.0111×10^{6} US\$yr^{-1} for the same number of trays. The composition profile shown in Figure 4.3 matches with earlier studies.

Table 4.1: Column specification and temperature profiles for the best solution obtained ideal VLE

Tray	Feed, mol s^{-1}		Liquid holdup, m^3	Temp. K	Molar flow rate, mol s^{-1}	
	Ethylene oxide	Water			Liquid	Vapor
1	.000	.000	.000	470.00	463.32	456.29
2	.000	.000	.000	459.76	463.41	456.29
3	.000	.000	.000	404.02	463.41	456.29
4	.000	.000	.000	374.53	463.41	456.29
5	2.000	.000	1.290	373.48	463.41	459.56
6	.129	.839	.193	373.35	466.41	460.35
7	5.171	6.311	.193	372.96	466.64	470.55

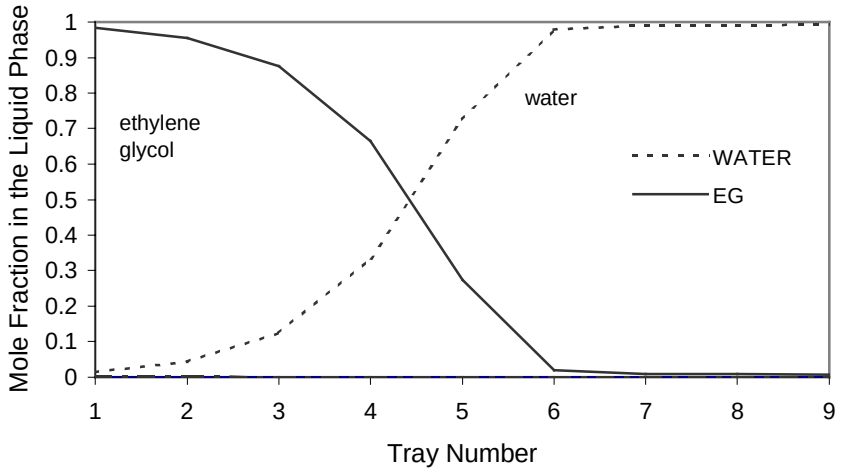

Figure 4.3: Composition profiles for the best solution obtained (ethylene glycol, ideal VLE)

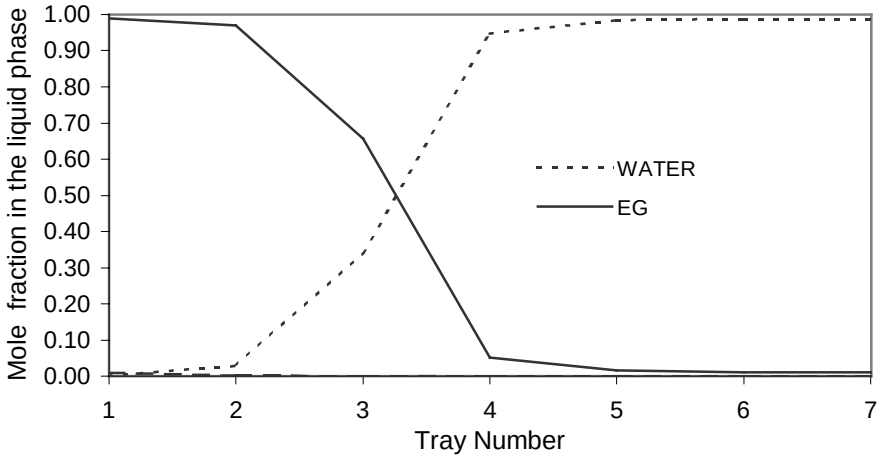

Figure 4.4: Composition profiles for the best solution obtained (ethylene glycol, non-ideal VLE)

Optimization was also performed for non-ideal case at atmospheric pressure. Okasinki and Doherty (1998) have shown that the ideal equilibrium model used by Ciric and Gu(1994) is unrealistic, and proposed that the Wilson model be used instead, since this gives vapor-liquid equilibrium curves much closer to those observed (Gmehling & Onken, 1977).

The column specifications and temperature profiles for best solution obtained, with 9 trays are shown in Table 4.2. The objective function calculated by GA is 15.01272×10^{6} US$yr^{-1} which is better than 15.10×10^{6} US$yr^{-1} reported by Cardoso *et al.* (2000) for nonideal case with 10 trays. The composition profile is also shown in Figure 4.4 which is in line with Cardoso *et al*. (2000). The results obtained by GA optimization is shown in Table 4.3.

Table 4.2: Column specification and temperature profiles for the best solution obtained non-ideal VLE

Tray	Feed, mol s^{-1}		Liquid holdup m^3	Temperature K	Molar flow rate, mol s^{-1}	
	Ethylene oxide	Water			Liquid	Vapor
1	.000	.000	.000	469.52	741.60	734.54
2	.000	.000	.000	467.53	741.63	734.54
3	.000	.000	.000	461.68	741.63	734.54
4	.000	.000	.000	444.64	741.63	734.54
5	0.129	.000	1.742	406.71	741.63	734.69
6	1.742	.000	1.290	374.67	741.81	735.58
7	1.355	.000	1.613	373.55	741.44	737.12
8	0.677	.387	1.226	373.47	742.42	738.38
9	3.397	6.763	1.226	372.84	743.27	748.81

Table 4.3: GA-optimized results for ethylene glycol production

	Ideal case	Non-ideal case
Column diameter	2.21 m	2.805 m
Column height	7.70 m	9.634 m
β	0.985	0.9904
Q_B	18.25 MW	29.3817 MW
Q_C	18.82 MW	29.95 MW
Cost	1.501115E+07 US$/yr	1.501272E+07 US$/yr

The optimization results shows that the variation of objective function is not much. The reason is reactant costs (EO and water) alone accounts for more than 90% of

total cost. In this case it is concluded that column dimension have little effect on objective function. And it is still beneficial to go for column optimization since a designer can end up with cost up to 40×10^{6} US$yr^{-1} for a feasible design.

4.4.1.2 MTBE

MTBE is produced from reaction of methanol and isobutylene catalyzed by a strong acid ion exchange resin. This reaction is reversible.

$$CH_3OH + (CH_3)_3C \Leftrightarrow CH_2 = (CH)_3C - O - CH_3 \qquad (4.6)$$

Typically, the isobutylene is mixed with other C_4 species that are inert under the process conditions.

By converting isobutylene to MTBE, higher purity of the inerts (e.g. 1-butene is obtained at lower cost compared to other chemical processes, Isobutylene (IB) and 1-butene (1B) contained in the butylenes stream are difficult to separate because their relative volatility is close to 1. Therefore it is very expensive to obtain a stream with high purity of 1-butene which has important chemical end uses, Clementi *et al.* (1979). However, MTBE process offers an attractive method for separating isobutylene from 1-butene since isobutylene reacts with methanol to produce MTBE which is separated as a bottoms product, and the 1-butene stream is recovered as an overhead product. (Eldarsi *et al.*, 1998).

Eldarsi *et al.* (1998) found pressure, reflux ratio and bottom flow rate were possible candidates for decision variable for optimization. The optimization function was profit maximization. Simulations were performed using non-ideal VLE data (Appendix B). The binary interaction parameters are available for MTBE, isobutylene, and methanol system, but not for other C_4 components in the hydrocarbon stream. For the purpose of calculating binary interaction parameters, all C_4 hydrocarbons were assumed to be isobutylene. Average value of latent heat of vaporization 20,500 J/mol is considered for calculation of reboiler and condenser duty.

Figure 4.5 shows the schematic diagram of catalytic distillation column consisting of 17 trays including reboiler and condensor. 8000 kg catalyst was distributed over 10 reactive trays, 7 to 16 with 800 kg each. The butylenes feed consist of isobutylene (197

mol/s) and 1-butene (366 mol/s) and its location was fixed at tray 7 (last reactive tray) because of the relatively high volatility, the flow rate of the methanol was maintained at 197 mol/s. Methanol feed was taken on tray 8. These feed location exhibits a higher isobutylene conversion (Eldarsi *et al.* 1998). The possible remaining decision variables therefore are; a) reflux ratio, b) MTBE bottom flow rate and c) operating pressure of the catalytic distillation column.

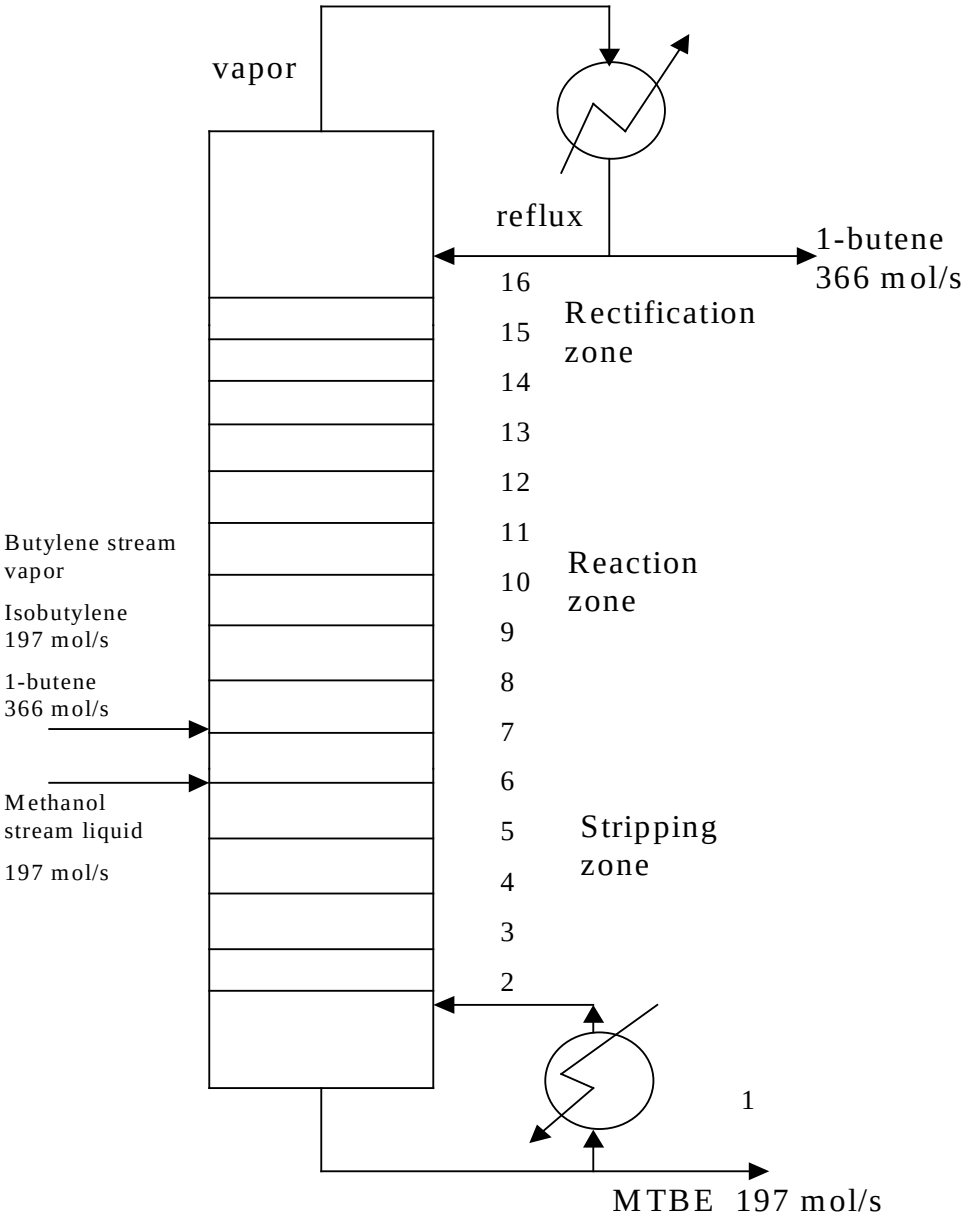

Figure 4.5: Schematic of a catalytic distillation column

The different raw material and utility cost as in first problem were considered and since weight of catalyst is constant, cost of catalyst is not considered while finding the objective function. Assuming non-ideal vapor liquid equilibrium (Tanskanen, 2000), the column specification and temperature profiles for best solution obtained, with 17 trays are shown in Table 4.4. The GA-optimum values of operating pressure, reflux ratio and MTBE bottom flow rate are 9.8676, 7.172 and 197.45 respectively. The composition profile shown in Figure 4.6 is similar to Eldarsi *et al.* (1998) for similar configuration. The GA optimized results are shown in Table 4.5.

Table 4.4: Column specification temperature profiles for the best solution obtained (MTBE)

Tray	Feed, mol s^{-1}			Catalyst weight kg	Molar flow rate, mol s^{-1}		Temp K
	Isobutylene	1-butene	Methanol		Liquid	Vapor	
1	.0	.0	.0	-	197.45	2990.97	419.0
2	.0	.0	.0	-	2822.18	2990.97	416.9
3	.0	.0	.0	-	2822.18	2990.97	413.3
4	.0	.0	.0	-	2822.18	2990.97	406.5
5	.0	.0	.0	-	2822.18	2990.97	394.5
6	.0	.0	.0	-	2822.18	2990.97	379.0
7	197.0	366.0	.0	800	2822.18	2990.97	364.2
8	.0	.0	197.0	800	2678.23	2990.97	357.3
9	.0	.0	.0	800	2514.55	2990.97	355.9
10	.0	.0	.0	800	2534.23	2990.97	355.8
11	.0	.0	.0	800	2549.50	2990.97	355.6
12	.0	.0	.0	800	2562.99	2990.97	355.4
13	.0	.0	.0	800	2575.78	2990.97	355.2
14	.0	0	.0	800	2588.59	2990.97	355.1
15	.0	.0	.0	800	2601.48	2990.97	355.0
16	.0	.0	.0	800	2613.72	2990.97	354.4
17	.0	.0	.0	-	2624.97	366.00	353.7

Table 4.5: GA-optimized results for MTBE production

Column diameter	5.714 m
Column height	12.715 m
Pressure	9.887 atm.
Q_B	53.80 MW
Q_C	61.31 MW
Cost	2.056695E+09 US$/yr

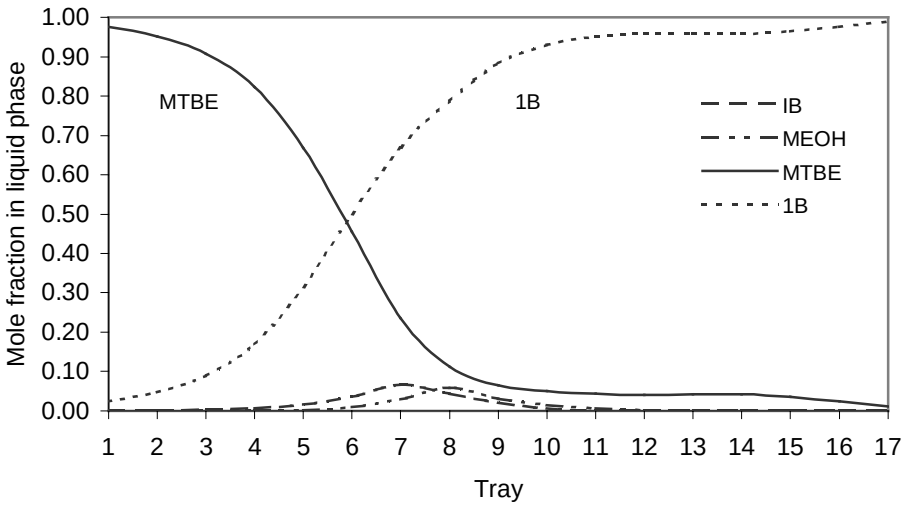

Figure 4.6: Predicted concentration profile for reactants, product (MTBE) and inert (1-butene)

4.5 Conclusions

The efficacy of GAs, a stochastic optimization technique for minimization of total cost of reactive/catalytic distillation column, has been demonstrated by considering production of i) ethylene glycol from ethylene oxide and water by reactive distillation and ii) MTBE from isobutylene and methanol by catalytic distillation. Optimization of reactive distillation column based on Ciric and Gu (1994) formulation of column model and simulation algorithm based on conventional distillation (Bastos, 1987) are carried out. While for catalytic distillation a simple model is used. The column parameters optimized are number of trays, liquid holdup, feed flow rates and boil-up fraction for ethylene glycol production. In case of MTBE production by catalytic distillation the column parameters are pressure, reflux ratio and bottom flow rate. The optimization results obtained suggest that the GA methodologies can be successfully employed for optimizing the reactive and catalytic distillation column.

References

Alejski, K., Dynamic simulation of the multicomponent reactive distillation, 1996, *Chem. Eng. Sci.*, 51(18):4237-4252.

Ciric, A. R. & Gu, D., 1994, Synthesis of nonequilibrium reactive distillation processes by MINLP optimization., *AIChE J.*, 40(9):1479.

Cardoso, M.F., Salcedo, R.L., Azevedo, S.F., Barbosa, D., 2000, Optimization of reactive distillation processes with simulated annealing, *Chem. Eng. Sci.*, 55: 5059-5078.

Eldarsi, H.S. and Douglas, P.L., 1998, Methyl-tert-butyl ether catalytic distillation column, *Trans. I.Chem.E.*, 76(May): 517-523.

Wang, K. Qian Y., Yuan Y. and Yao, P., 1998, Syntheses and optimization of heat integrated distillation systems using an improved genetic algorithms, *Comput. Chem. Eng.*, 23:125-136.

Bastos, J., 1987, *Modeling extractive distillation processes*, Ph.D. thesis, Universidade do Porto (in Portuguese).

Goldberg, D. E., 1989, *Genetic Algorithm in Search, Optimization, and Machine Learning*, Addison-Wesley, Reading, MA.

Cartwright, H., Long, R.,1993, Simultaneous optimization of chemical flow-shop sequencing and topology using genetic algorithms, *Ind. Eng. Chem. Res.*, 32:2706-2713.

Wang, C., Quan, H., Xu, X. ,1996, Optimal design of multiproduct batch chemical process using genetic algorithms, *Ind. Eng. Chem. Res.*, 35: 3560-3566.

Manolas, D., Gialamas, T., Frangopoulos, C., Tsahalis, P., 1996, Genetic algorithm for optimization of an industrial cogeneration system., *Comput. Chem. Eng.*, 20: S1107-S1112.

Hanagandi, V., Ploehn, H., Nikolaou, M., 1996, Solution of the self-constraint field model for polymer adsorption by genetic algorithms, *Chem. Eng. Sci.*, 51:1071-1078.

Ramanathan, S.P., Mukherjee, S., Dahule, R.K., Ghosh, S., Rahman, I., Tambe, S.S., Ravetkar, D.D., Kulkarni, B.D., 2001, Optimization of continuous distillation columns using stochastic optimization approaches, *Trans. I.Chem. E.*, Part A, 79: 310-322.

Okasinki, K.J., & Doherty, M.F., 1998, Design methods for kinetically controlled, tray reactive distillation columns, *Ind. and Eng. Chem. Res.*, 37(7): 2821.

Gmehling, J., & Onken, U., 1977, *Vapor-liquid equilibrium data collection, aqueous-organic systems*. DECHEMA Chem. Data Series, DECHEMA, Frankfurt/Main, Germany.

Eldarsi, H.S. and Douglas, P.L., 1998, Methyl-tert-butyl ether catalytic distillation column, *Trans. I.Chem .E*, Part A, 76(May):509-516.

Deb, K., 1995, *Optimization for Engineering Design, Algorithms and Examples*, Prentice- Hall, New Delhi.

Cleminti, A., Oriani, G., Ancillotti, F. and Pecci, G., 1979, Up-grade C4 with MTBE process, *Hydrocarbon Processing*, December, 109-113.

Tanskanen, J., Pohjola, V.J., 2000, A robust method for predicting state profiles in a reactive distillation, *Compu.Chem, Eng.*, 24:81-88.

Rehfinger, A., Hoffman, U., 1990, Kinetics of methyl tertiary butyl ether liquid phase synthesis catalyzed by ion exchange resin-I, Intrinsic rate expression in liquid phase activities, *Chem. Eng. Sci.*, 45(6):1605-1617.

Chapter 5

Stabilization of Chaotic Dynamics of Complex Chemical Processes Using a Fuzzy Logic Controller

5.1 Introduction

Control of nonlinear dynamical systems has attracted significant attention in recent years. One approach to chaos control, proposed by Ott, Grebori and Yorke (1990), stabilizes the unstable periodic orbits (UPOs) of the system by applying small perturbations in the neighborhood of the desired UPO. Variants of the OGY approach and other methodologies for stabilizing the UPOs can be found in the literature e.g. Shinbrot *et al.*, 1993, Bielawski *et al.*, 1994, Pyragas *et al.*, 1992, Bandyopadhyay *et al.*, 1997. The second approach to controlling the unstable behavior of chaotic systems aims at stabilizing the dynamics exactly at the unstable steady-state (USS) responsible for the chaotic motion. Since an USS repels trajectories in its neighborhood, deriving a control algorithm which ensures that the trajectory stays at the USS is not trivial. Although some model-based techniques are available for fulfilling such an objective, they require a phenomenological or an empirical process model which in most instances is difficult to formulate. The conventional controllers such as the feed-forward or the proportional-integral-derivative (PID) are known for their inefficient handling of processes possessing fast dynamics and having large dead times. Also, they can lead to potential runaway conditions and long dead times for ill-defined or complex-to-predict systems (Huddleston and Flowers, 1998). Since many chaotic systems possess these characteristics, it is desirable to explore alternative strategies for chaos control. Thus, in this study, a fuzzy logic based strategy has been proposed for stabilizing a chaotic trajectory at an USS. Fuzzy logic controllers (FLCs) can smoothly handle control problems involving complex non-linear, partially understood systems and also those involving uncertainties. Moreover, these controllers do not require a mathematical model of the process for implementing a control action.

5.2 Fuzzy Logic Controller

Unlike in the crisp set theory where the membership of an element in a crisp set is either zero or one, the fuzzy set theory (Zadeh, 1965) allows an element to belong to a fuzzy set with a degree that can vary between zero and one. In fuzzy set theory, the range of values that a variable can assume forms its universe of discourse (UOD). A UOD is partitioned into a number of fuzzy sets, each characterized by a linguistic variable and

defined by a membership function (MF). An MF is a curve defining how different points in the UOD are mapped to a degree of membership that varies between zero and one. For example, if the set-point error (hereafter simply referred to as 'error') is a fuzzy variable, its UOD may be decomposed into a number of fuzzy sets using linguistic variables such as LARGE, MEDIUM, SMALL errors, and the shape of the membership functions of the respective fuzzy sets can be selected from among a number of alternatives namely, triangular, gaussian, sigmoid etc

Figure 5.1 shows a block diagram of the proposed fuzzy logic controller used for the chaos control. As can be seen, the FLC consists of four elements : (i) a fuzzifier, (ii) a rule-base, (iii) an inference engine, and (iv) a defuzzifier. An FLC essentially maps the crisp inputs defining the process states into crisp outputs signifying the control action. For achieving, this the inputs are first mapped into fuzzy sets which is performed by the fuzzifier. The rule base defines control rules which are derived from the heuristic knowledge of a skilled process operator and/or process engineer. A rule establishes relationship between the linguistic terms associated with the fuzzy input-output variables. Depending upon which control rule(s) is satisfied (fired), the inference engine computes the corresponding fuzzy output. Finally, the defuzzifier converts the fuzzy output from the inference engine to its crisp value for implementation on the process.

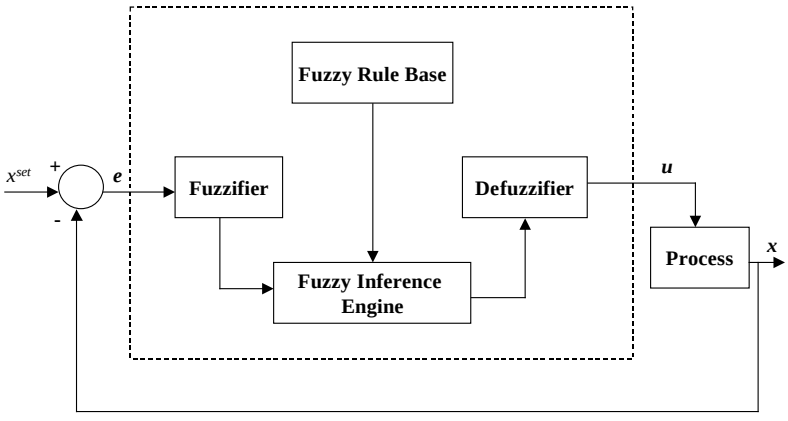

Figure 5.1 : Block diagram of fuzzy logic controller (FLC)

The FLC used for stabilizing the chaotic dynamics comprises a rule-base with only 8 rules. Seven of the rules are of simple proportional-to-error type while the remaining one

also incorporates the integral action. It was found that using the fuzzy form of the derivative-of-error action goes on to increase the complexity of the FLC manifold without improving the control quality significantly. Thus, the derivative term was not considered in the control law. It is well known that the use of integral action though improves steady-state performance and helps remove offsets, it leads to poor transient response. Thus, the scope of the integral action was limited to a narrow range of the input variable (*error*), ensuring excellent transient as well as steady-state performance. In all, seven linguistic terms(CE, PS, PM, etc.) have been used to characterize the FLC input fuzzy set i.e. the set-point error (*e*), and the output namely, the manipulated variable (*u*) (Figures 5.2.1 and 5.2.2). The fuzzy set 'zero' (ZE) in Figure 5.2.3 marks the error band in which the integral action is included. The seven proportional rules and one integral control rule that make up the rule base are:

(A) Proportional control rules :

(1) IF *error* (*e*) is CE (CENTRAL) then *control action* (u_p) is CE,

(2) IF *error* (*e*) is PS (POSITIVE SMALL) then *control action* (u_p) is PS,

(3) IF *error* (*e*) is PM (POSITIVE MEDIUM) then *control action* (u_p) is PM,

(4) IF *error* (*e*) is PL (POSITIVE LARGE) then *control action* (u_p) is PL,

(5) IF *error* (*e*) is NS (NEGATIVE SMALL) then *control action* (u_p) is NS,

(6) IF *error* (*e*) is NM (NEGATIVE MEDIUM) then *control action* (u_p) is NM,

(7) IF *error* (*e*) is NL (NEGATIVE LARGE) then *control action* (u_p) is NL.

(B) Integral control rule

(8) IF *error* (*e*) is ZE then *manipulated variable* (u_i) is $C_I \times \delta E \times \mu$

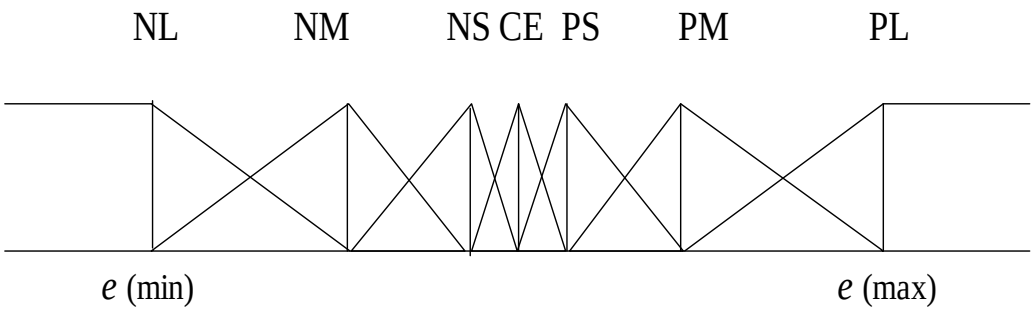

Figure 5.2.1: Fuzzy sets corresponding to the setpoint error, *e*

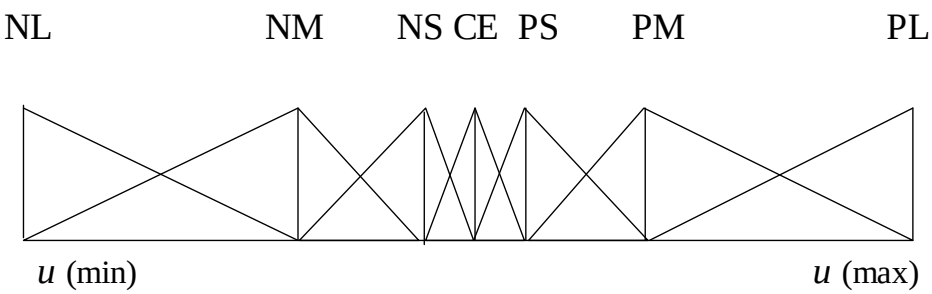

Figure 5.2.2: Fuzzy sets for the control action, *u*

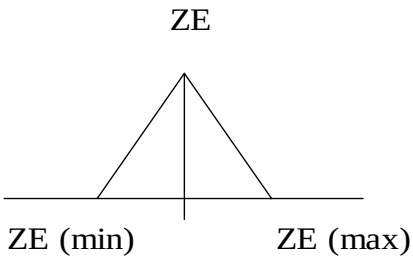

Figure 5.2.3: Fuzzy sets for the integral action

Here u_p and u_i refers to the fuzzy outputs pertaining to proportional-to-error and integral-of-error; δE denotes the sum-of-errors from the instance the error goes into the domain of the fuzzy set, ZE (δE is reset to zero when the error falls out of the ZE set); μ refers to the membership of error in ZE the set and, C_I denotes the constant for the integral action. The following modified form of the height defuzzification formula was used to determine the output from the proportional control rules.

$$u_p = [\sum_{l=1}^{M} \bar{y}^l \mu_{A^l}(\bar{y}^l)/\delta^{l^2}]/[\sum_{l=1}^{M} \mu_{A^l}(\bar{y}^l)/\delta^{l^2}] \quad (5.1)$$

where $\bar{y}^l$ denotes the center of gravity of the fuzzy set A appearing in the consequent part of the *l*th fuzzy proportional rule; M is the number of fuzzy rules in the rule base; $\mu_{A^l}(\bar{y}^l)$ is the product of memberships of the crisp inputs in the sets appearing in the antecedent part of rule *l*, δ^l is a measure of spread of the fuzzy set in the consequent of *l*th rule. When the integral rule (8) gets fired, the corresponding u_i value is added to the crisp output, u_p, corresponding to the proportional control to obtain the final FLC output .The efficacy of the above FLC strategy was tested on two chemical reactor systems exhibiting chaos. The results obtained thereby are described below.

5.3 Case Studies

5.3.1 Non Isothermal CSTR

The model describing the dynamics of an exo-, endothermic reaction, A à B à C, in a jacketed continuous stirred tank reactor (CSTR) is given as (Kahlert, *et al*., 1981, Bandopadhyay, *et al*., 1997):

$$dx_1/dt = 1 - x_1 - Da\ x_1 \exp[x_3/(1+\varepsilon_A x_3)] + d_1 \quad (5.2)$$

$$dx_2/dt = -x_2 + Da\ x_1 \exp[x_3/(1+\varepsilon_A x_3)] - Da\ S\ x_2 \exp[\kappa x_3/(1+\varepsilon_A x_3)] + d_2 \quad (5.3)$$

$$dx_3/dt = -x_3 + B\ Da\ x_1 \exp[x_3/(1+\varepsilon_A x_3)] - Da\ B\alpha\ S\ x_2 \exp[\kappa x_3/(1+\varepsilon_A x_3)] - \beta(x_3 - x_{3c}) + \beta\ ut + d_3 \quad (5.4)$$

The parameter values leading to chaos are *Da* =0.26, *S* = 0.5, ε = 0, κ= 1,α =0.426 and β=7.9999. The corresponding unstable steady-state values are $x_{1s} = 0.0819$, $x_{2s} = 0.1391$

and $x_{3s} = 3.7627$. Here, x_1 and x_2 represent the dimensionless concentrations of species A and B, respectively, x_3 denotes the dimensionless CSTR temperature, and x_{3c} refers to the reactor coolant temperature. The load disturbances in feed compositions and in the temperature are denoted by d_1, d_2 and d_3 respectively. For control purposes, the manipulated variable (u) has been defined as the deviation from the reference value of x_{3c}. The numerical integration of the CSTR system was performed using Gear's routine with the integration step size of .001 dimensionless time units. Figure 5.3.1 shows the phase plane plot of the uncontrolled CSTR dynamics (Equation 5.2-5.4) exhibiting chaotic behavior. For control simulations the set-point error e was evaluated as $e = x_3^{set} - x_3$ where x_3^{set} refers to the set-point. With the system beginning at an arbitrary point in the phase space, the FLC is required to stabilize the chaotic trajectory exactly at the USS defined earlier. Figure 5.3.2 shows the x_3 and u (FLC output) versus time profiles for the controlled CSTR system. In this case the value of manipulated variable was updated at every 30 integration steps. The plots clearly indicate that the FLC has fulfilled the control objective of stabilizing the chaotic motion at the USS without allowing any offset**.** The ability of the FLC to impart the desired control action in the presence of stochastic load disturbances was also tested. For testing, random noise was incorporated at every integration step in the time evolution equation (5.4) for CSTR temperature. Thus the load disturbance term d_3 assumes random values obeying the Gaussian distribution with mean and standard deviation values of 0 and 0.5, respectively. The time profiles of the CSTR temperature, x_3 and the and controller output (5.4) in presence of the random disturbances are shown in Figure 5.3.3. Additionally, the results when a constant (deterministic) disturbance of unit magnitude is added (d_3 =1) are depicted in Figure. 5.3.4. As can be noted from these graphs, the FLC delivers excellent action in the presence of either type of load disturbances.

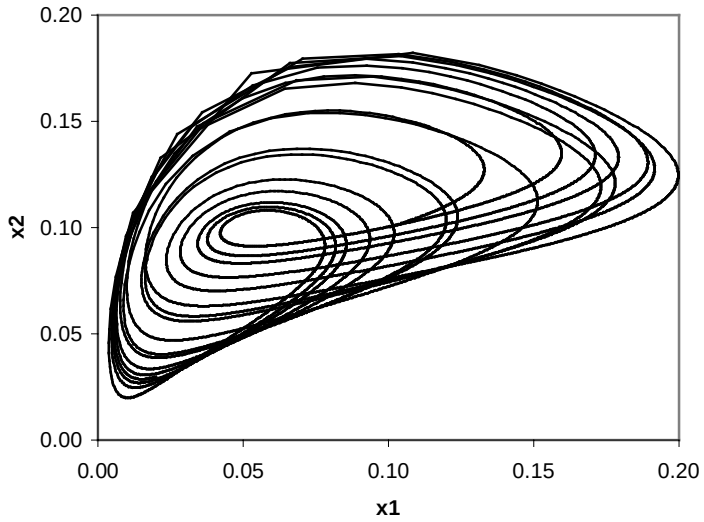

Figure 5.3.1: Phase plane plots showing the chaotic dynamics of the non-isothermal CSTR

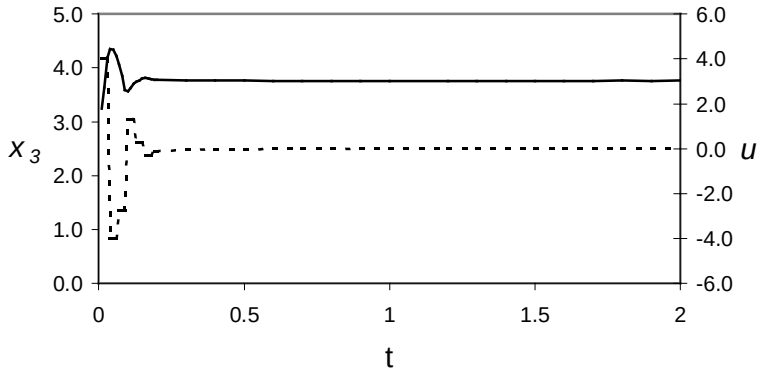

Figure 5.3.2: Plot showing x_3 (—) and u (- - -) versus time (t) for the FLC controlled CSTR system with no load disturbances

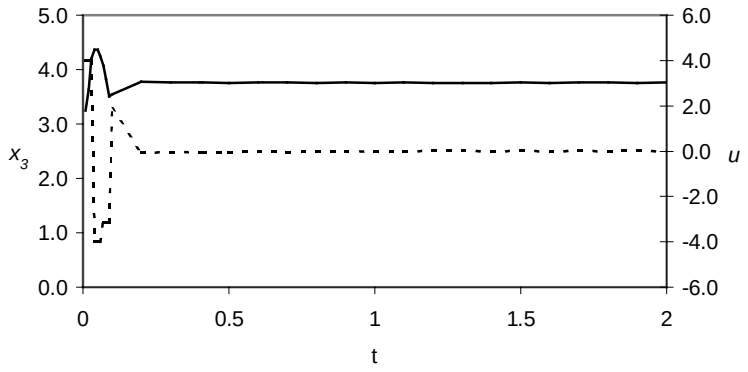

Figure 5.3.3: Plot showing x_3 (—) and u (- - -) versus time(t) for the FLC controlled CSTR system in presence of stochastic disturbances

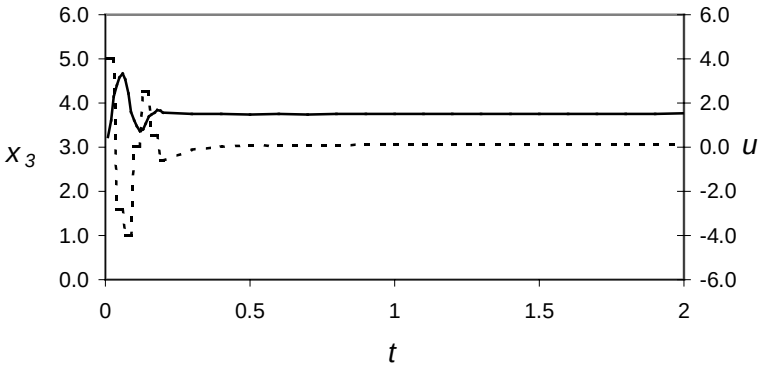

Figure 5.3.4: Plot showing x_3 (—) and u (- - -) versus time(t) for the FLC controlled CSTR system in presence of deterministic load disturbances

5.3.2 Biochemical Chaos Control

Due to enzyme regulation, biochemical systems exhibit a rich variety of dynamic behavior. The following three variable model describing the autocatalytic reaction of substrate x_1 into product x_2, and a reversible deposition of x_1 into an inactive form x_3, has been shown to display chaotic behavior(Peng *et al.*, 1981).

$$dx_1/dt = 1 - Bx_1x_2^2 - Ex_1x_2 + x_3 + d_1 \tag{5.5}$$

$$dx_2/dt = A(x_1x_2^2 - x_2 + (D + ut)) + d_2 \tag{5.6}$$

$$dx_3/dt = F(Ex_1x_2 - x_3) + d_3 \qquad (5.7)$$

The parameter values leading to chaos (Figure 5.4.1) are : A= 4, B=0.35, D =0.1, E=1.4 and F=0.2 and corresponding USS is x_{1S}=1.324, x_{2S}=0.6365, x_{3S}=1.180). For control purposes *D* has been chosen to be control parameter and modified as $D = D + u$, where *u* signifies the deviation in *D*. Using x_2 as the control variable, the set-point error (*e*) is computed as, $e = x_2^{set} - x_2$. The system dynamics was simulated using Gear's ODE solver with integration step-size of .001 dimensionless time units. The time profiles of the FLC controlled process variable (x_2) and the manipulated variable (*u*) are shown in the Figure 5.4.2. It can be seen from the figures that the FLC has satisfactorily stabilized the chaotic dynamics at the USS ($x_{1s} = 1.324$, $x_{2s} = 0.63655$, $x_{3s} = 1.180$).

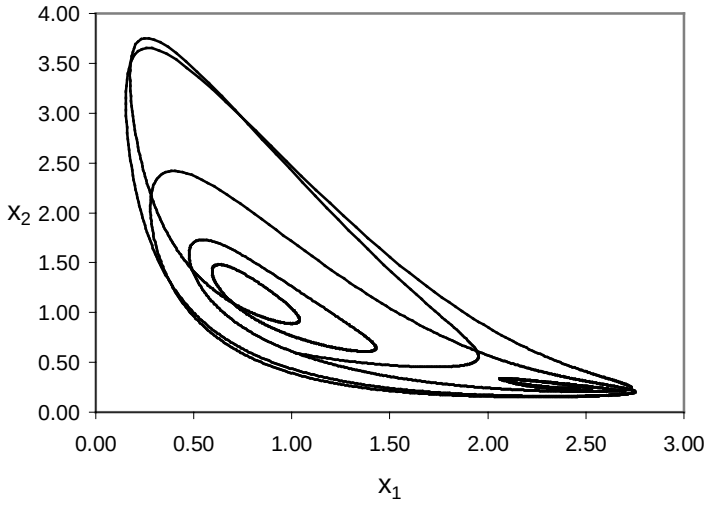

Figure 5.4.1: Phase plane plots showing the chaotic dynamics of the biochemical chaos

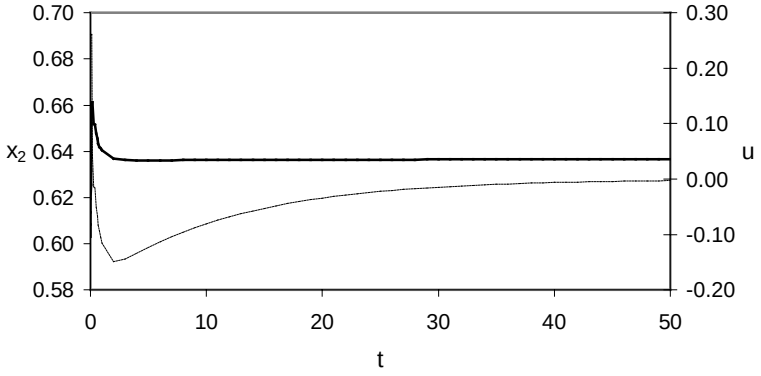

Figure 5.4.2: Plot showing x_2 (—) and u (- - -) **versus time** (t) **for the FLC controlled CSTR system with no load disturbances**

5.4 Comparison of FLC with Conventional PID controller

Comparative analysis of the results of FLC and those corresponding to an optimally-tuned PID controllers were also performed. For comparison purposes, the plots for the non-isothermal CSTR and chemical chaos systems are shown in Figure 5.5.1 and 5.5.2, respectively. The figures clearly indicate that the controller fares better than the PID controller.

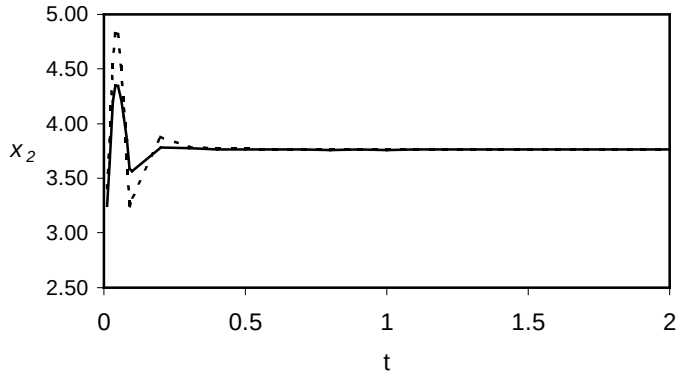

Figure 5.5.1: Plot comparing the optimally tuned PID controller(- - -) and FLC(—) for the chemical chaos (PID constants akc **= 6,** τ_I **= 0.7,** τ_D **= 0.001)**

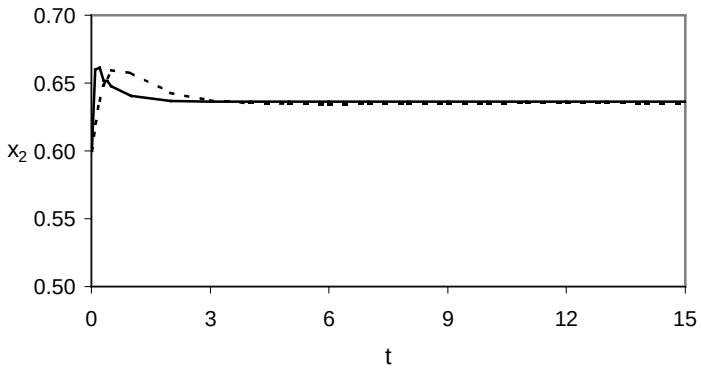

Figure 5.5.2: Plot comparing the optimally tuned PID controller(- - -) and FLC(—) for the chemical chaos (PID constants *akc* = 4, τ_I = 0.7, τ_D = 0.002)

5.5 Conclusions

This study proposes a fuzzy logic based controller for stabilizing a chaotic trajectory exactly at an unstable steady-state. The control objective is nontrivial since an unstable steady-state repels trajectories in its neighborhood. The efficacy of the fuzzy controller has been demonstrated on two chemical reaction systems exhibiting chaotic dynamics. It is also shown that the fuzzy controller works effectively in presence of random and deterministic load disturbances. A comparison with PID controller shows that the FLC outperforms the PID controller.

References

Ott, E., Grebori, C., Yorke, J.A., 1990, Controlling chaos, *Phys. Rev. Lett.*, 64: 1196-1199.

Shinbrot, T., Grebori, C., Ott, E., Yorke, J.A.,1993, Using small perturbations to control chaos, *Nature*, 363: 411-417.

Bielawski, S., Derozier, D. and Glorieux, P., 1994, Controlling unstable periodic orbits by a delayed continuous feedback, *Phys. Rev. E*, 49:R971-974 and references therein.

Pyragas, K.,1992, Continuous control of chaos by self-controlling feedback, *Phys. Lett. A*, 170: 421-427.

Bandyopadhyay, J. K., Tambe, S.S., Jayaraman, V. K., Deshpande, P.B., Kulkarni, B.D., 1997, On control of nonlinear system dynamics at unstable steady state, *The Chemical Engineering Journal*, 67:103-114.

Huddleston T., and Flowers, S., 1998, Keep complex processes under control, *Chemical Engineering*, Sept.: 117.

Zadeh, L.A., 1965, Fuzzy sets, *Informat. Control*, 8:338-353

Mendel, J., 1995, Fuzzy logic systems for engineering: A tutorial, *Proceeding of the IEEE*, 83: 345-377

Zhu, L., Toncich, D., Nagarajah, R., Romanski, K., 1997, A PID fuzzy controller model for machine control applications, *Int. J. Adv. Manufacturing Technology*, 13: 696.

Kahlert, C., Rossler, O. E., Varma, A., 1981, Chaos in a continuous stirred-tank reactor with two consecutive first-order reactions, one exo- one endothermic, in modeling of chemical reaction systems, eds. Ebert, K. H. *et al*., *Springer Series in Chemical Physics*, 18: 355.

Peng, B., Petrov, V., Showalter, K., 1991, Controlling chemical chaos, *J. Phys. Chem*., 95(13): 4957-4959.

Kosko, B.,1997, *Fuzzy Engineering*, Prentice Hall Internal Inc., New York.

Chapter 6

Optimization of Fuzzy Logic Controller Using Genetic Algorithms

6.1 Introduction

In the last decade, fuzzy logic based controllers are increasingly utilized for chemical process control owing to their significant advantages such as : (i) ability to handle processes for which only subjective knowledge is available ('subjective knowledge' represents linguistic information that is usually impossible to quantify using conventional mathematics), (ii) ability to control nonlinear, complex and ill-defined systems and, (iii) capability of incorporating heuristic process knowledge during controller design. A typical FLC comprises four components (Figure 6.1): (i) input fuzzy membership functions (fuzzifier), (ii) rule-base, (iii) inference engine and, (iv) defuzzifier. The input to the fuzzifier may be the setpoint error (difference between process setpoint and the actual process output). This 'crisp' error value is converted by the fuzzifier into an appropriate fuzzy set describing a linguistic variable such as, "small", "medium", "large", etc. Fuzzy sets are quantatively described in terms of membership functions (MFs) that can assume different shapes (e.q. Gaussian, triangular and trapezoidal). The fuzzy rule-base is a collection of IF-THEN rules derived from the heuristic knowledge of a skilled process operator and or the process design engineer. In the fuzzy inference engine, fuzzy logic principles are used to combine fuzzy IF-THEN rules from the rule base into a mapping from fuzzy input sets into fuzzy output sets. Finally, the defuzzifier maps the output from the inference engine into a crisp value for executing the control action using a suitable defuzzification method.

The most troublesome aspect of FLC design is construction of control rules using linguistic terms describing controller input and output variables and tuning of the associated MFs. These difficulties can however be overcome by using a novel artificial intelligence (AI) technique known as genetic algorithms (GAs) (Pham and Karoboga, 1998; Morimoto *et al.*, 1997). GAs are stochastic optimization procedures inspired by the principles of natural evolution (Goldberg, 1989; Deb, 1995) followed by biologically evolving species. They have proved effective when optimization search space is discontinuous, multimodal and highly non-linear. In the present paper, a single input-single output (SISO) FLC has been designed on the basis of only five control rules, wherein controller input and the output are described using five MFs each. The novel

feature of the MFs used in this study is that all five of them could be characterized in terms of multiples of a single parameter.

6.2 FLC Design

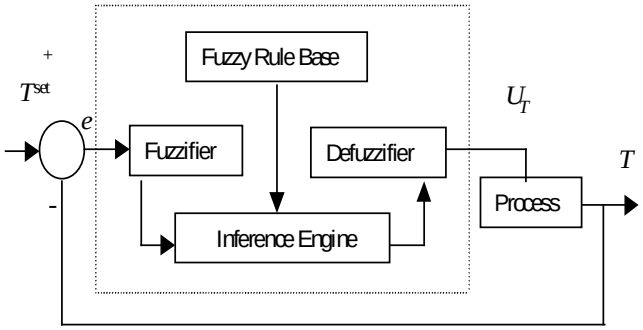

Figure 6.1: Block diagram of fuzzy logic controller

In the FLC design (Figure 6.1) studied here, the setpoint error e ($=T^{set}-T_p$), and the manipulated variable, U_T, are controller input and output, respectively. Both e and U_T are described using five triangular fuzzy sets (Figures. 6.2.1 and 6.2.2). A fuzzy set is characterized by an MF, which takes on values in [0,1] interval. The five linguistic variables used for describing FLC's input (e) and output (U_T) are: negative large (NL), negative small (NS), zero (ZE), positive small (PS) and positive large (PL); while the five triangular fuzzy sets in respect of e $(e\in[-c,+c])$ are represented as A_1, A_2,..., A_5, the fuzzy sets corresponding to U_T are B_1, B_2, ..., B_5 spanning the interval [–d, +d]. It is now possible to define five fuzzy control rules as ; Rule i (i = 1, 2, …, 5) :

IF e is A_i THEN U_T is B_j,

wherein j represents an integer number in the range 1 to 5. For ith rule, the consequent part B_j needs to be appropriately chosen from the set $\{B_j\}$. The task of FLC design thus essentially boils down to : (i) optimizing control rules i.e., selection of appropriate B_j for the five control rules, and (ii) optimizing domains of MFs $\{A_i\}$ and $\{B_j\}$ such that the control objective of setpoint error minimization is satisfactorily fulfilled. As can be seen in the Figures 6.2.1 and 6.2.2 that the five MFs for e and U_T can be defined in

terms of parameters *m* and *n*, respectively. This feature of the MFs has an advantage that it does not require tuning of five MFs separately since all five of them can be represented in terms of multiples of the MF parameters *m* or *n*.

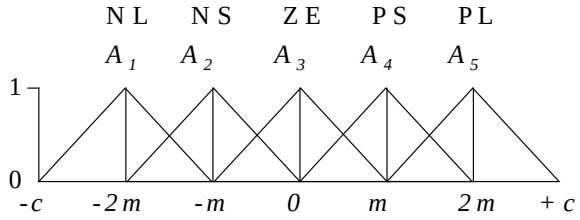

Figure 6. 2.1: Fuzzy sets for setpoint error, *e*

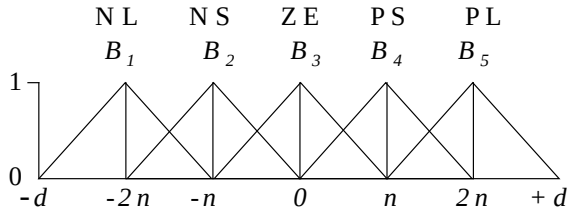

Figure 6. 2.2: Fuzzy sets for manipulated variable, U_T

6.2.1 Optimization of Control Rules and Membership Functions

In order to optimize the control rules and MFs, we define following optimization objective:

$$\text{Minimize} \quad E = \sum_{t=1}^{\tau} T^{set} - T_p \tag{6.1}$$

where E is the objective function; T^{set} and T_p are the desired (set-point) and actual process outputs and τ is the simulation time over which the error is computed. Note that the process output T_p depends on the FLC output U_T, which in turn is a function of the MF parameters *m*, *n* and also of B_j. Thus for a given value of i (i.e. setpoint error is either NL (i =1), NS (i =2), ZERO (i =3), PS (i =4) or PL (i =5), the minimization problem (equation 6.1) boils down to selecting appropriate B_j and tuning of MF parameters *m* and *n*. Since all the five control rules need to be optimized simultaneously, the decision variable vector X becomes seven dimensional $[X=(x_1, x_2, ..., x_7)]$ where $x_1 =$

m, $x_2 = n$ and $x_3, x_4, \ldots, x_7$ describe five integer j values. In the following, the GA-based procedure followed in the optimization of seven-dimensional decision vector X is described alongwith an overview of GAs.

6.3 Genetic Algorithms

The Genetic Algorithms (Holland, 1975, Goldberg 1989) are based on the 'survival-of-the-fittest' mechanism of natural selection and propagation of genetic characteristics, which play dominant roles in the Darwinian evolution of biological organisms. GAs utilize these principles for efficient searching of noisy, discontinuous and nonconvex solution spaces and arriving at an optimal solution. The characteristic features of GAs are : (i) they need only scalar values and not derivatives of the objective function being minimized, (ii) GAs perform a stochastic (random) search and hence they mostly converge to (or in the vicinity of) the global optimum of the objective function, and (iii) the search procedure of GA's is stochastic and hence they can be utilized without invoking ad-hoc assumptions (as required by the most traditionally used gradient-based optimization techniques) such as smoothness, differentiability, and continuity, pertaining to the form of the objective function.

6.3.1 Implementation of Genetic Algorithms

For obtaining a GA-based solution to the minimization problem (equation 6.1), first a population of probable (candidate) solutions is randomly generated. Each solution is coded as a binary string (also termed 'chromosome') that is subdivided into as many segments (substrings) as the number of decision variables. How well the candidate solutions perform at fulfilling the optimization task is ascertained by evaluating their fitness values (scores); the fitness score of a solution is obtained by evaluating a prespecified fitness function ξ. Thereafter, three GA operators, namely, selection, crossover and mutation, are sequentially employed to produce a 'new generation' of probable solutions. The selection operator selects strings possessing above-average fitness values from the current population with a view of forming a mating pool of fitter parent strings. The action of crossover operator produces offspring strings wherein randomly selected parts of two parent strings are mutually exchanged to form two

offspring strings per pair of parent strings. In mutation, a randomly selected element of an offspring string is mutated (changed) from zero to one and vice versa, using a preselected mutation probability value (P_{mut}=0.01). Following mutation, a fresh population of candidate solutions is obtained which is again operated upon using the above-described three GA operators. Owing to the repetitive actions of the GA operators, the resulting solution population improves itself from one generation to the next. The GA converges eventually and the best chromosome i.e., the solution possessing maximum fitness score, represents the solution to the optimization problem.

6.3.2 GA-based Optimization of Membership Functions and Control Rules

As stated above, the decision vector X in the current study is seven dimensional. The GA procedure for optimizing X begins by creating randomly an initial population of N_{str} (=30) strings representing as many candidate solutions to the minimization problem. A solution string contained seven binary segments where first two segments (representing m and n) were 10-bit long, and the remaining five segments were four-bit long. The parameter ranges defined by this binary coding scheme were: $0.001 \le m \le 0.1$, $0.01 \le n \le 2$ and $1 \le (\text{int}(x_3), \text{int}(x_4),..,\text{int}(x_7) \le 5$.

In the present study, it is assumed that the nonlinear process model is known. Thus the FLC can be designed off-line by utilizing the process model for evaluating the control performance of each candidate solution. To be specific, each candidate solution describing a different FLC design was examined by computing its goodness (fitness) towards fulfilling the control objective. Accordingly, FLC's control performance was evaluated based on the ITAE (integral of time multiplied by absolute error) criterion defined as:

$$\text{ITAE} = \sum_{l=1}^{\tau} l\tau (T^{set} - T_p) \tag{6.2}$$

and the fitness ξ_k of the kth candidate solution (k = 1,2,…, N_{str}) was evaluated as given below:

$$\xi_k = (\text{ITAE} + C_c)\text{-}1 \tag{6.3}$$

where C_c is a small-valued constant (= 0.01) added to the ITAE as a precautionary measure to avoid "division by zero" error. The GA convergence criterion employed in the present study is: the fitness score of the best string (solution) in a population undergoes a very small or no change over a large number of successive generations. Upon convergence, the number of binary segments in the chromosome possessing maximum fitness score, were decoded and the values of the decision variables obtained thereby represent the optimal solution (X^{opt}) searched by the GA.

6.4 Case Studies

6.4.1 Non-isothermal CSTR Using GA-optimized FLC

For testing the efficacy of the optimal FLC design procedure described above, we consider a jacketed CSTR wherein an irreversible non-isothermal first-order reaction R $\rightarrow$ S takes place. A coolant flowing through the jacket removes the heat of reaction to maintain the reactor temperature (process output) at the setpoint. The dimensionless CSTR model given below (Uppal *et al.*,1974) consists of dynamic mass and energy balances including terms describing the control action towards regulating the reactor temperature. The model equations are:

$$dC/dt = -C + Da(1-C)\exp(T/[1+(T/\gamma)]) + d_1 \quad (6.4)$$

$$dT/dt = -T + B_o Da(1-C)\exp(T/[1+(T/\gamma)] + \beta(T - T_{co}) + \beta U_T + d_2 \quad (6.5)$$

where C and T are the dimensionless concentration (of species R) and CSTR temperature, respectively; Da refers to the Damkohler number; γ is the activation energy; B_o is the adiabatic temperature rise; β represents heat transfer coefficient; T_{co} is the reference value for coolant temperature; U_T refers to the control input (manipulated variable) and d_1, d_2, respectively denote the load disturbances in C and T. In certain parameter regions (see Table 6.1), the non-isothermal CSTR model exhibits multiplicity and instability of steady states (parameter sets 1 and 2). The system is also known to perform sustained limit cycle (LC) oscillations (Table 6.1, set 3). Owing to these complex features exhibited by the CSTR dynamics, FLC's performance was tested using the parameter sets listed in Table 6.1. The model equations describing CSTR dynamics were

integrated using the fourth order Runga-Kutta method with integration step size of 0.001 dimensionless time units.

Table 6.1 : CSTR parameters and corresponding steady-state solutions (SS)

Set No.	Process parameters	Steady-state (SS) solution		
		C	T	Stability of SS
1	$Da = 0.072,\ \beta = 0.3,\ \gamma = 20.0,$ $B_o = 8.0,\ T_{co} = 0.0,\ d_1 = d_2 = 0$	0.2028 0.3258 0.7986	1.3473 2.1041 5.0140	Stable Unstable Stable
2	Same as case 1	0.1286 0.4996 0.7409	0.746 3.0274 4.5126	Stable Unstable Stable
3	$Da = 0.32,\ \beta = 3.0,\ \gamma \to \infty,\ B_o =$ $11.0,\ T_{co} = 0.0,\ d_1 = d_2 = 0$	0.6671	1.8344	Unstable (LC)

For optimizing the MFs and the control rules, the parameter set (1) was selected; CSTR's steady state (SS) behavior exhibits multi-stationarity for the chosen set. The objective of FLC was to switch between different steady-states in the multi-stationary region. The GA-optimized values of the seven-dimensional decision vector X that could satisfactorily fulfill the stated optimization goal were: $x_1 = m = 0.008$, $x_2 = n = 1.922$, $x_3 = 1$, $x_4 = 2$, $x_5 = 3$, $x_6 = 3$, $x_7 = 4$. The optimal value of $x_3 = 1$ suggests that the first ($i = 1$) FLC rule has been optimized as : IF e is NL THEN U_T is NL; the remaining four optimal control rules can be interpreted analogously from the GA-optimized values of x_4 to x_7. The results of the control action imparted by the GA-optimized FLC are portrayed in Figures 6.3.1-6.3.3. In these figures it is seen that the FLC was successful in : (i) switching the system (servo control) from the lower SS ($T = 1.3473$) to the middle unstable state ($T^{set} = 2.1041$) , (ii) switching the system from the lower stable SS state to upper SS ($T^{set} = 5.0140$) and ($T = 1.3473$) to the middle unstable SS defined in set-2 ($T^{set} = 3.0274$). It is also noticed in the figures that the FLC action (U_T) is smooth.

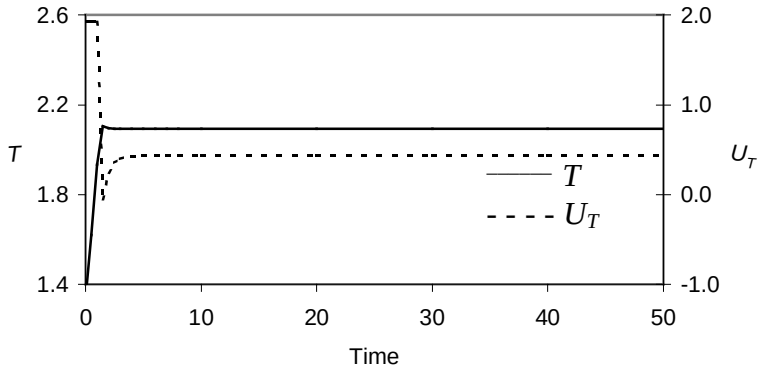

Figure 6.3.1: Set point change from lower stable steady state to middle unstable steady state(parameter set 1)

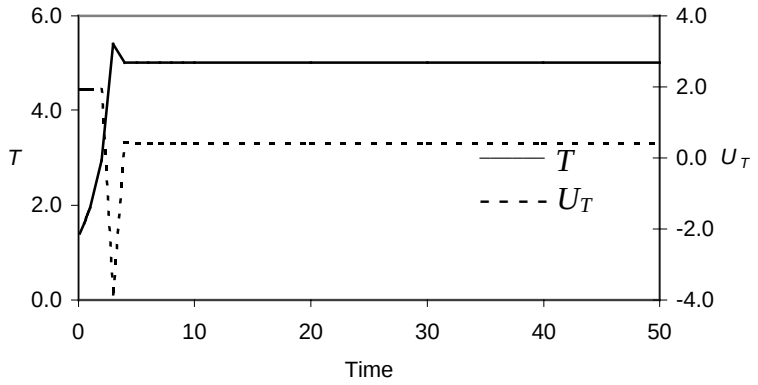

Figure 6.3.2: Set point change from lower stable steady state to middle unstable steady state(parameter set 1)

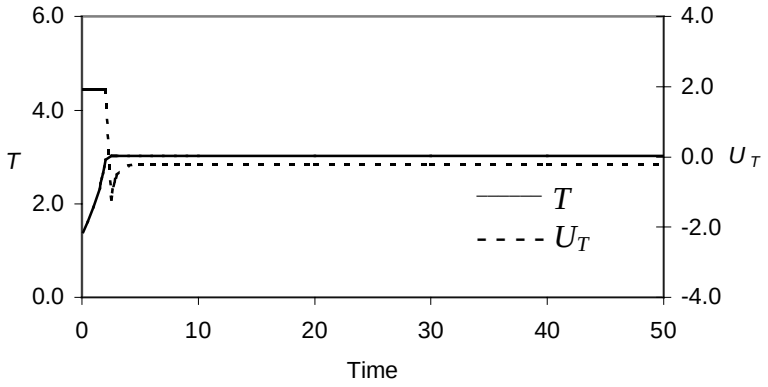

Figure 6.3.3: Set point change from lower stable steady state to middle unstable steady state(parameter set 1)

The open-loop dynamics of the CSTR for the parameter set 3 exhibits sustained oscillatory behavior. Thus optimized FLC's efficacy in stabilizing the oscillatory behavior exactly at the corresponding unstable SS (T^{set} = 1.8344) was examined. The simulation results shown in Figure 6.3.4 indicate that the FLC has fulfilled the stated control objective satisfactorily i.e., the controller could stabilize the open-loop oscillatory trajectory exactly at the unstable SS. Additionally, optimized FLC's performance in executing regulatory control action was studied by subjecting the CSTR separately to deterministic (constant) and stochastic (random) load disturbances. Accordingly, a constant load disturbances of unit magnitude (d_2 =1) was incorporated in the differential equation describing the CSTR temperature (Equation 6.5); in the case of stochastic load disturbance, the d_2 term corresponds to the Gaussian random numbers (added at each integration time step) with mean and standard deviation of 0 and 0.25 respectively. FLC's regulatory performance in the presence of deterministic and stochastic load disturbances for a representative case involving limit cycle trajectory (T^{set} = 1.8344), is portrayed in Figures 6.3.5and 6.3.6 respectively. As can be noted from these figures that

the FLC delivers excellent regulatory action in the presence of either type of load disturbance.

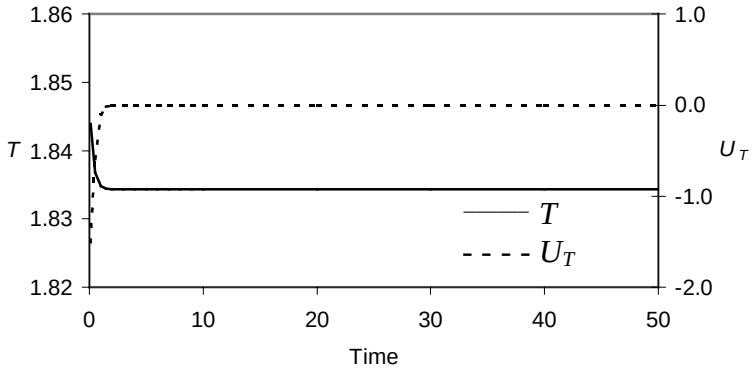

Figure 6.3.4: Stabilization of oscillatory dynamics exactly a the unique unstable steady state (parameter set3)

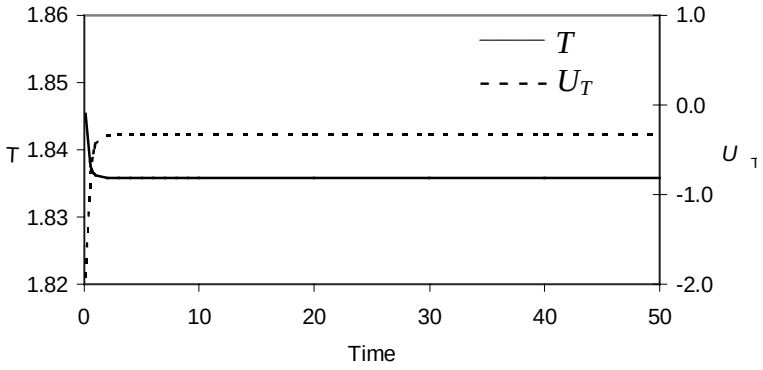

Figure 6.3.5: FLC controlled dynamics in the presence of deterministic load disturbance (parameter set3)

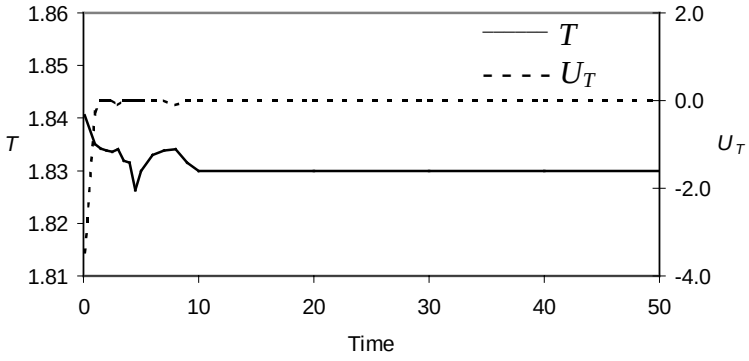

Figure 6.3.6: FLC controlled dynamics in the presence of stochastic load disturbance (parameter set3)

In chemical processes, *Proportional-Integral-Derivative* (PID) type controllers are most widely used. It thus becomes necessary to compare the FLC's control performance vis-à-vis PID control. Such a comparison has been performed for a representative case involving parameter set-2 where the servo control objective was to shift the CSTR operating at the upper steady state (T = 4.5126) to the middle unstable steady state (T^{set} = 3.0274). The comparative plots portrayed in Figure 6.3.7 indicate that FLC fares better than an optimally tuned PID controller (PID parameters: K_c =6.0, τ_I =0.7, τ_D=0.001).

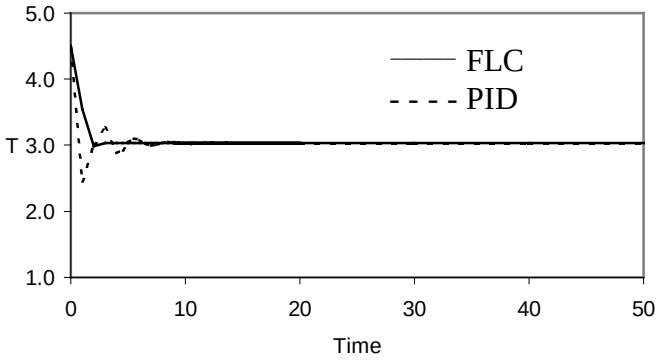

Figure 6.3.7: Comparison of FLC with PID at setpoint 3.0274

6.4.2 pH Control System Using GA-optimized FLC

The pH-control systems have important role in several industrial process such as wastewater treatment, micro-biological and electro-chemical process. Neutralization is problematic because of the inherent nonlinearity of pH, the measured variable. The acidity and alkalinity of a solution is expressed in pH units, defined in terms of the hydrogen ion concentration by the nonlinear expression pH=-log[H+]. Moreover, the pH of a solution is highly sensitive to small perturbations around the equivalent point.

The process under study is the neutralization of aqueous solutions of HCl with sodium hydroxide in a single CSTR. Assuming perfect mixing, reaction at equilibrium, constant volume and constant density, the unsteady-state material balance for pH system can be written as (Kulkarni *et al*, 1991).

$$\frac{dC}{dt} = \frac{[C + c_a C^2 - C^3]P + [C - c_b C^2 - C^3]Q}{(1 + C^2)60(V)} \tag{6.6}$$

The goal of control effort is to control the effluent pH at 7 by manipulating the flow rate of NaOH. The load variables are the flow rate of the waste stream being neutralized and concentration of HCl in that stream. The model differential equation were solved by the fourth order Runga-Kutta method with a specified fixed step size (0.001).

The system dynamics were simulated using the fourth order Runga-Kutta. The optimal parameters in the membership function (m,n) and consequent fuzzy sets ($X_1, X_2, \ldots, X_5$) by GA were found to be 0.152, 2.46, 5, 5, 3, 2 and 2.

An acceptable control algorithm must give good servo and regulatory response and offset-free performance in the present of modeling errors. The controller under investigation satisfies these criteria. To assess the servo capabilities of fuzzy controller change in pH set point from 7 to 8 was introduced (Figure 6.4.1).

To assess the regulatory performance of the controller, a + 4 % step change in the flow rate and – 4 % step change in the HCl concentration of the waste stream was introduced, the responses are shown in Figure 6.4.2 and 6.4.3. The figures shows excellent disturbance rejection. Comparison of FLC with PID (K_c =0.1, τ_I =0.48, τ_D=0.12) is also shown in Figure 6.4.4 for a +4% step change in the flow rate.

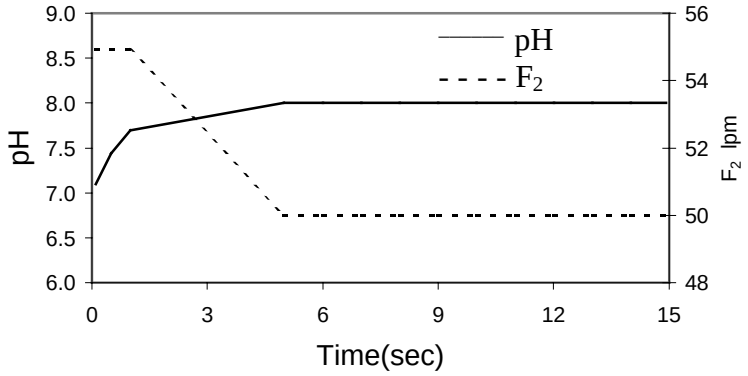

Figure 6.4.1: Setpoint response of FLC from pH 7 to 8

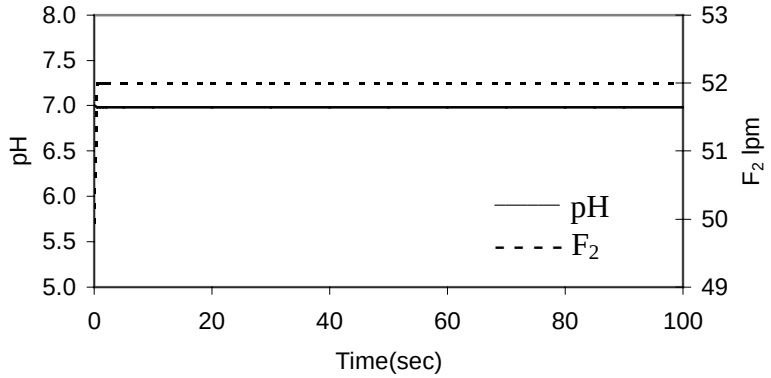

Figure 6.4.2: Response of the FLC to a +4 % step change in waste stream flow

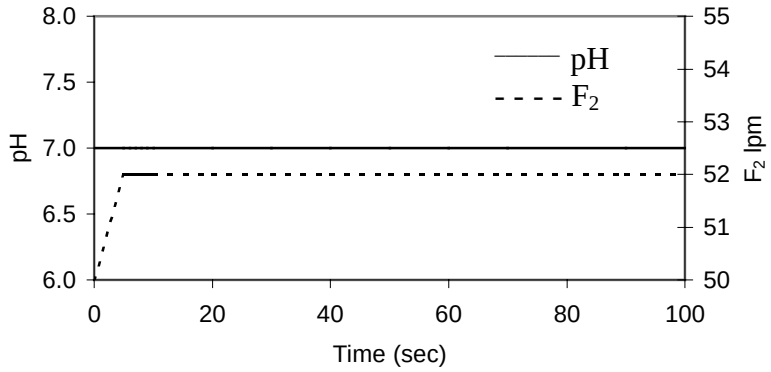

Figure 6.4.3: Response of the FLC to a +4 % step change in HCl concentration

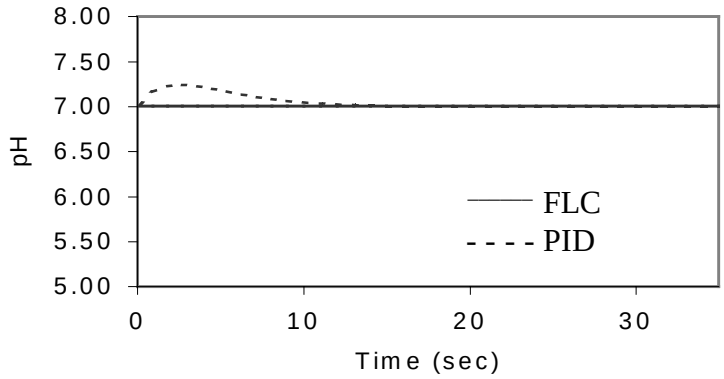

Figure 6.4.4: Responses of the FLC and PID to a +4 % step change in waste stream flow

6.5 Conclusion

This paper presents a GA-based method for optimizing fuzzy logic control rules and the membership functions (fuzzy sets) thereof. The methodology has the advantage of minimizing significantly the laborious and tedious steps involved in the manual tuning of control rules and MFs. The novel feature of optimizing MFs is that all of them could be characterized and optimized in terms of multiples of a single parameter. The efficacy of the proposed optimal FLC design has been successfully demonstrated on the non-isothermal CSTR system for a variety of regulatory and servo control tasks.

Nomenclature :

C = dimensionless concentration of hydrogen ions, $C_H / \sqrt{K_w}$

c_a = dimensionless concentrations of inlet acid (HCl) stream, $C_{Cl1} / \sqrt{K_w}$

c_b = dimensionless concentrations of inlet base (NaOH) stream, $C_{Na2} / \sqrt{K_w}$

C_{Cl1} = concentration of inlet HCl acid stream (design concentration: 0.01 gmol l^{-1})

C_H = concentration of hydrogen ions in the tank (gmol l^{-1})

C_{Na2} = concentration of inlet NaOH stream (design concentration: 0.1 gmol l^{-1})

F_1 = flow rate of inlet acid stream (design flow - 500 l min^{-1})

F_2 = flow rate of inlet base stream (design flow - 50 l min^{-1})

K_w = dissociation constant of water, 10^{-14}

$P = \frac{F_1}{60V}$ $\quad$ $Q = \frac{F_2}{60V}$

V = reactor volume, 20000 l

References

Deb, K., 1995, *Optimization for Engineering Design, Algorithms and Examples*, Prentice-Hall: New Delhi.

Goldberg, D. E., 1989, *Genetic Algorithm in Search Optimization and Machine Learning*, Addison-Wesley, Reading: MA.

Holland, J., 1975, *Adaptation in Natural and Artificial Systems*, University of Michigan Press: Ann Arbor, MI.

Morimoto, T., Suzuki, J., Hashimoto, Y., 1997, Optimization of a fuzzy controller for fruit storage using neural networks and genetic algorithms, *Engg. Appl. Artf. Intl.*, 10: 453-461.

Pham, D.T., Karaboga D., 1998, Cross breeding in genetic optimization and its application to fuzzy logic controller design, *Artf. Intl. in Engg.*, 12:15-20.

Uppal, A., Ray, W. H., Poore, A. B., 1974, On the dynamic behavior of continuous stirred tank reactors, *Chem. Engg. Sci.*, 29(4): 967-985.

Kulkarni B.D., Tambe S.S., Shukla N. V., Deshpande P.B.,1991, Nonlinear pH control, *Chem. Engg. Sci.*, 46(4): 995-1003.

Chapter 7

Adaptive Recursive Least Square Fuzzy Logic Controller

7.1 Introduction

Fuzzy logic controllers (FLCs) have recently gained considerable importance due to their significant advantages such as, ability to control complex ill-defined systems and capability of incorporation of heuristic knowledge into the controller. A typical FLC (Figure 7.1.1) consists of four elements: fuzzifier, rule-base, inference engine, and defuzzifier. The input to the fuzzifier may be the setpoint error (difference between the process setpoint and the actual process output). This 'crisp' error value is converted by the fuzzifer into an appropriate fuzzy set describing a linguistic variable such as, "zero", "small", "large", etc. Fuzzy sets are quantitatively described in terms of membership functions (MFs) that can have different shapes (e.g. Gaussian, triangular and trapezoidal). The fuzzy rule-base is a collection of "IF-THEN" rules derived from the heuristic knowledge of a skilled process operator and/or a process engineer. The inference engine combines IF-THEN rules to produce a fuzzy output. Finally, the defuzzification method maps the fuzzy output from inference engine into the crisp value of the output (manipulated) variable.

The performance of an FLC relies on the choice of the membership functions and the rule-base. The most troublesome aspect of the FLC design is formulation of fuzzy control rules and, construction and tuning of the membership functions. In systems where the process dynamics is nonlinear or when the operation conditions of the system are time-varying, it becomes necessary to tune the membership functions on-line. Adaptive FLCs based on various self-tuning control algorithms are available for this purpose; they retune the parameters (membership functions) automatically in response to the current process characteristics. A number of studies attempting to develop an adaptive FLC, which modifies the control rules and membership functions according to its closed-loop performance are reported (e.g., Moore and Harris, 1992; Pham and Karaboga, 1999). These studies either employ a performance table (amount of modification depending upon the setpoint error), a reference model, or some form of intermediate model of the process. It is in general difficult to develop an optimal performance table since there is no systematic way to produce it for a specific problem (Pham and Karaboga, 1999).

In this study, a simple adaptive FLC based on the recursive least squares (RLS) technique is proposed. The FLS comprises five predefined input membership functions and five IF-THEN proportional rules. The output membership function is tuned by the on-line RLS method, thus making the FLC adaptive. In the past, RLS technique has been used in the off-line mode to optimally select the output MFs of a fuzzy logic system (Mendel and Mouzouris, 1997) and a neuro-fuzzy network system (Chak and Feng, 1995) from the input-output process data. To the best of our knowledge, the application of the RLS for online tuning of output membership functions has so far not been reported in the literature. The RLS method being linear converges very fast and therefore is an attractive alternative for designing accurate fuzzy control systems. An important factor for the RLS implementation is that the FLC designer should provide fairly good choice of the antecedent part in the rule so as to estimate the centers of the consequent part.

In the proposed FLC following five membership functions are used: *negative large* (*NL*), *negative small* (*NS*), *zero* (*ZE*), *positive small* (*PS*), and *positive large* (*PL*). Input to the fuzzifier is the setpoint error as shown in Figure 7.1.2. The membership functions have triangular shape and the optimal value of parameter *a* defines the base of the membership functions. The FLC output is the value of the manipulated variable (*u*); the five rules in the rule base are defined as proportional rules, for instance, "if *error* (*e*) is ZERO (antecedent part) then *manipulated variable* (*u*) is ZERO (consequent part)". The height defuzzification method is used to calculate the crisp control action (*u*); centroid of the consequent membership function in height defuzzification method is updated by the RLS. The proposed FLC scheme is described in Section 7.2. In Section 7.3, a description of the two case studies and the results of control simulations are provided; the conclusions are stated in Section 7.4.

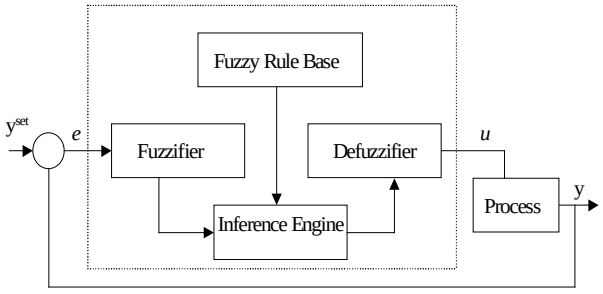

Figure 7.1.1: Block diagram of fuzzy logic controller

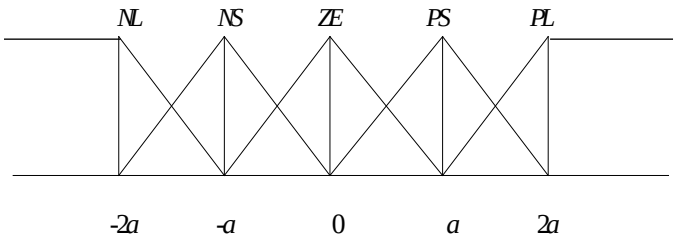

Figure 7.1.2: Membership function corresponding to set point error (*e*)

7.2 Adaptive RLS Fuzzy Logic Controller

A schematic of the fuzzy logic controller is shown in Figure 7.1.1. An input to the FLC, after been processed by the fuzzifier, will activate each rule in the rule base to a (possibly) specific degree. The fuzzy rules R^l, $l = 1,2,\ldots,M$ can be described as ;

Rule l: If e is A_k^l then u is B_k^l

where A_k^l and B_k^l are linguistic variables (*NL*, *NM*, *ZE*, *PS* and *PL*). The inference engine combines the activated rules to produce a fuzzy output which the defuzzification unit converts into the corresponding crisp value, u, of the manipulated variable. For this conversion height defuzzifier is used that for SISO systems can be expressed as follows.

$$u = f(e) = \sum_{l}^{M} \bar{y}^l \, p^l(e) \qquad (7.1)$$

$$p^l(e) = \mu_{A_k^l}(e) / \sum_{l=1}^{M} \mu_{A_k^l}(e) \tag{7.2}$$

where $\mu_{A_k^l}(e)$ is the membership for the input variable (e) and kth input fuzzy set , A_k^l, of the lth rule; $\bar{y}^l$ denotes the center of the kth consequent fuzzy set B_k^l; $p^l(e)$ is the fuzzy basis function (FBF) and M (= 5)is the number of rules in the rule base.

7.2.1 Recursive Least Square Method

While it is easy to produce the antecedent part of a fuzzy control rule, it is difficult to specify the consequent part without an expert knowledge. In order to achieve fast convergence rate while maintaining good approximation capability, a recursive least-squares (RLS) fuzzy logic controller can be designed based on the general formulation (Mendel and Mouzouris, 1997) of an FLS as a linear expansion of nonlinear FBFs. The RLS-based FLS updates only the centers of the consequent fuzzy sets; therefore, overall FLC performance depends on the proper selection of the input fuzzy sets which remain constant during the adaptation procedure. Given the input-output pairs [*e(t), d(t)*], the problem is to design an FLC such that

$$J_{RLS}(t) = \sum_{i=1}^{t} \lambda^{t-i}[d(i) - f(e(i))] \tag{7.3}$$

is minimized, where $\lambda \in (0,1)$ is a forgetting factor. Collecting all $\bar{y}^l$ in an M-dimensional vector $\bar{y}$, and all p^l in an M-dimensional vector $p(e(t))$, equation (7.1) can be written in a vector form as

$$f(e(t) = p(e(t))^T \bar{y} \tag{7.4}$$

Since f is linear in $\bar{y}$, the RLS algorithm can be used to update the centers of the consequent fuzzy sets. The recursions for $\bar{y}$ can be obtained by minimizing $J_{RLS}(t)$. Let $P(t) \equiv p(e(t))$ denote the FBF vector at time instant t, the recursion relations are given by

$$\phi(t) = \tfrac{1}{\lambda}\left[\phi(t-1) - \phi(t-1)P(t)(\lambda + P^T(t)\phi(t-1)P(t))^{-1}P^T(t)\phi(t-1)\right] \tag{7.5}$$

$$K(t) = \phi(t-1)P(t)[\lambda + P^T(t)\phi(t-1)P(t)]^{-1} \tag{7.6}$$

$$\bar{y}(t) = \bar{y}(t-1) + K(t)[d(t) - P^T(t)\bar{y}(t-1)] \tag{7.7}$$

for t = 1, 2,… Initially the matrix ϕ is set to $\phi(0) = \beta I$, where I is an $M \times M$ identity matrix and β is a small positive constant. The initial value of $\bar{y}$ i.e., $\bar{y}(0)$, and the values of the fixed system parameters, can be selected from the linguistic information, such that the supports of the resulting membership function cover the corresponding universe of discourse.

7.3 Case Studies

FLC performance depends on the membership functions and control rules and it is usually difficult to determine these objects efficiently. Figure 7.1.2 shows the triangular shape membership functions that need to be determined and tuned. As can be seen, all the five membership functions of error e can be defined in terms of a single parameter, a. The optimal value of a is determined by a thumb rule and has been taken equal to 10^{-3} times the setpoint. For the proposed FLC, the five linguistic control rules are defined as follows :

(i) Rule 1 (R^1): If e is NL then u is NL ,
(ii) Rule 2 (R^2): If e is NS then u is NS,
(iii)Rule 3 (R^3): If e is ZE then u is ZE,
(iv) Rule 4 (R^4): If e is PS then u is PS,
(v) Rule 5 (R^5): If e is PL then u is PL.

To test the efficacy and robustness of the FLC, a number of scenarios typifying possible control situations are simulated.

7.3.1 Continuous Fermentor

A continuous fermentor typically consists of a stirred tank with provision for a feed and an outlet stream. The constant volume fermentor can be represented by the following nonlinear ordinary differential equations (Henson and Seborg, 1991a).

$$\dot{X} = -DX + \mu X \tag{7.8}$$

$$\dot{S} = D(S_f - S) - \frac{1}{Y_{x/s}}\mu X \tag{7.9}$$

$$\dot{P} = -DP + (\alpha\mu + \beta)X \tag{7.10}$$

$$\mu = \frac{\mu_m[1-(P/P_m]S}{K_m + S + (S^2/K_i)} \tag{7.11}$$

The parameters and variables in the above equations are defined in the nomenclature section along with their nominal values.

Here, a simple regulatory control objective has been chosen, i.e., the control objective is to maintain X (cell concentration) at the specified set-point in the presence of disturbance(s) affecting μ_m and/or $Y_{x/s}$ by manipulating D (dilution rate). The open-loop response for ±10% changes in D, indicate that the fermentor exhibits significant nonlinear behavior. The FLC response for the step changes in the set point: (a) 6.0 to 7.0 g/l and (b) 6 to 5 g/l are shown in Figures 7.2.1 and 7.2.2, respectively. Also, the disturbances rejection capabilities of the FLC for an unmeasured step disturbance of –12.5% in μ_m and a –20 % step disturbance in $Y_{x/s}$ are depicted in Figures 7.2.3 and 7.2.4, respectively. The above control objectives are the same as those used by Hu and Rangaiah (1999) and it is found that results are superior (better setpoint tracking) to the IMC results obtained by them.

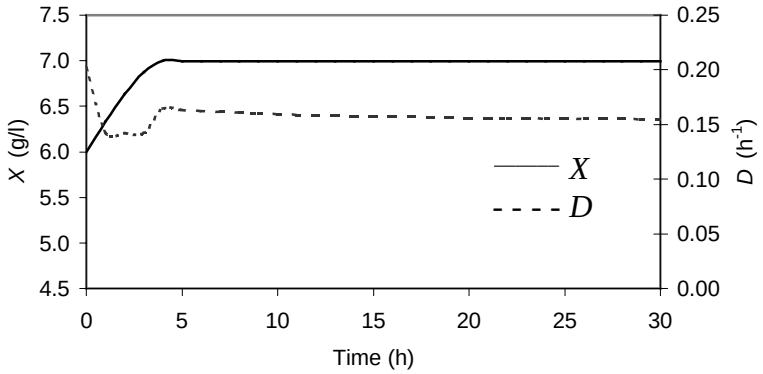

Figure 7.2.1: Response of FLC to change in setpoint 6 to 7

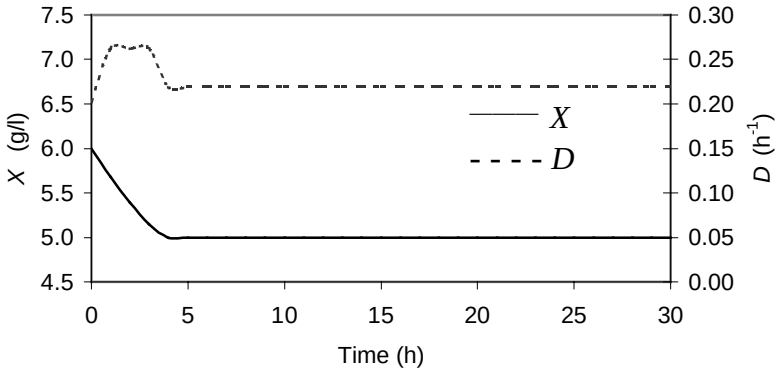

Figure 7.2.2: Response of FLC to change in setpoint 6 to 5

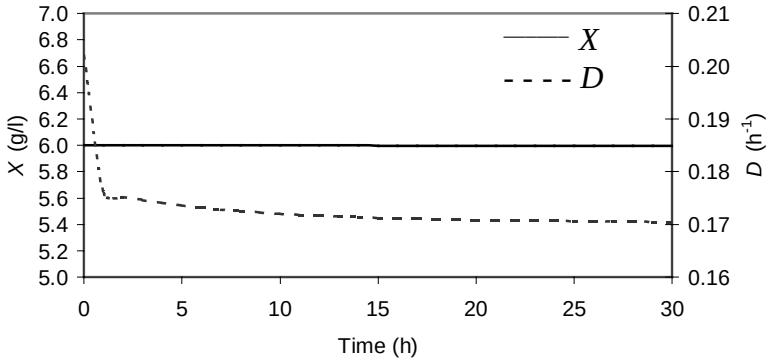

Figure 7.2.3: FLC performance for –12.5 % μ_m disturbances

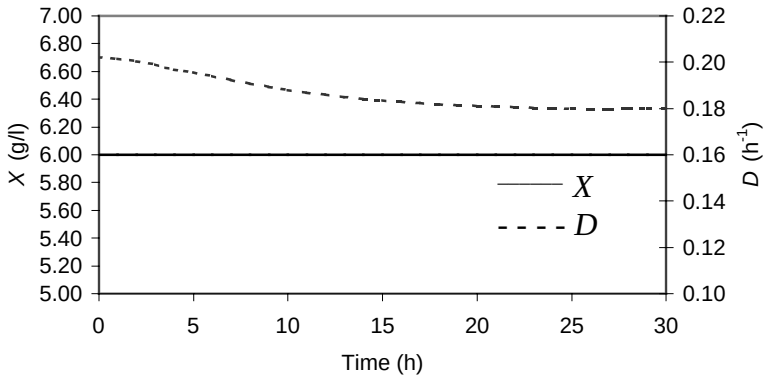

Figure 7.2.4: FLC performance of 15 % $Y_{x/s}$ disturbances

The performance of the FLC and PI (K_c =10.0, τ_I =10.0 h) controllers is also compared for an unmeasured step disturbance of – 12.5% in μ_m and is shown in Figure 7.2.5. It can be seen in the figure that the control action of the fuzzy controller is smoother as compared to that of the PI controller.

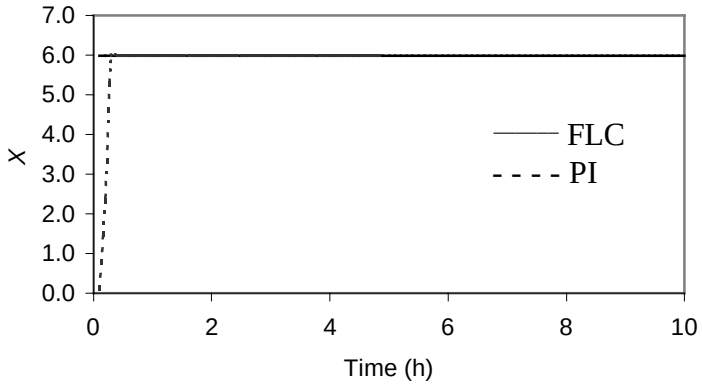

Figure 7.2.5: Comparison of FLC with PI

7.3.2 Non-isothermal CSTR

The model describing the dynamics of an exo-, end-othermic reaction, A à B à C, in a jacketed continuous stirred tank reactor (CSTR), is given as Bandopadhyay *et al.* (1997):

$$dx_1/dt = 1 - x_1 - Da\ x_1 \exp[x_3/(1+\varepsilon_A x_3)] + d_1 \tag{7.12}$$

$$dx_2/dt = -x_2 + Da\ x_1 \exp[x_3/(1+\varepsilon_A x_3)] - Da\ S\ x_2 \exp[\kappa x_3/(1+\varepsilon_A x_3)] + d_2 \tag{7.13}$$

$$dx_3/dt = -x_3 + B\ Da\ x_1 \exp[x_3/(1+\varepsilon_A x_3)] - Da\ B\ \alpha\ S\ x_2 \exp[\kappa x_3/(1+\varepsilon_A x_3)] - \beta(x_3 - x_{3c}) + \beta\ u + d_3 \tag{7.14}$$

Here, x_1 and x_2 represent the dimensionless concentrations of species A and B, respectively; x_3 denotes the dimensionless temperature, and x_{3c} refers to the reactor coolant temperature. The load disturbances in the feed compositions and in the temperature are denoted by d_1, d_2 and d_3, respectively. For control purposes, the manipulated variable (u) has been defined as the deviation from the reference value of x_{3c}. The numerical integration of the CSTR system was performed using Gear's algorithm. For control simulations, the set-point error (e) was evaluated as: $e = x_3^{set} - x_3$, where x_3^{set} refers to the reactor temperature set-point. The steady-state and linear stability analysis of the model equations (12-14) has been performed by Bandopadhyay *et al.* (1997) and the parameter values for which the system shows multi-stationarity, oscillations and even chaos are listed in Table 7.1. In the following, the performance of the FLC corresponding to the different representative control objectives is reported.

Table 7.1 : Characterization of steady states for CSTR system

Set No.	Parameter values	$x_{1,s}$	$x_{2,s}$	$x_{3,s}$	Stability
I	Da=0.06, S=0.0005, ε=0, κ=1, α=0.426, β=7.7, B=55.0	0.8965 0.6595 0.0378	0.1034 0.3404 0.9501	0.6540 2.1523 6.0500	Stable Unstable Unstable
II	Da=0.26, S=0.5, ε=0, κ=1, α=0.426, β=7.7, B=57.55	0.0729	0.1259	3.890	Stable limit cycle
III	Same as Set 2 except β=7.9999	0.0819	0.1391	3.7627	Unstable chaotic

7.3.2.1 Controlling the System at an Unstable Steady State in the Multiplicity Region

The process setpoint as the unstable steady-state (see Table 7.1, set-I) in the multiplicity region (x_3^{set} = 6.05) is chosen. The controller goal is to shift the process operating at an arbitrary point x_3 = 5.75, to the setpoint and maintain it at that state. The plots in Figure 7.3.1 clearly shows that the FLC has fulfilled the control objective satisfactorily.

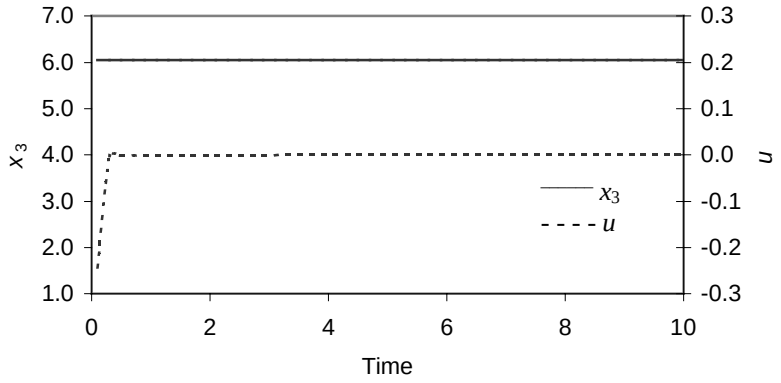

Figure 7.3.1: FLC output for setpoint(x_3 = 6.05) in the multiplicity region

7.3.2.2 Controlling the System at the Unique Unstable Steady State(USS) Responsible for Limit Cycle Oscillations.

For this case, the model parameters corresponding to the parameter set II for which the system exhibits sustained oscillatory behavior (stable limit cycle) were selected. The FLC is required to regulate the trajectory at the setpoint (x_3^{set} = 3.89) with the system starting at that unstable point itself. It can be seen from Figure 7.3.2, the controller has exerted excellent control action in regulating the oscillatory trajectory exactly at the setpoint.

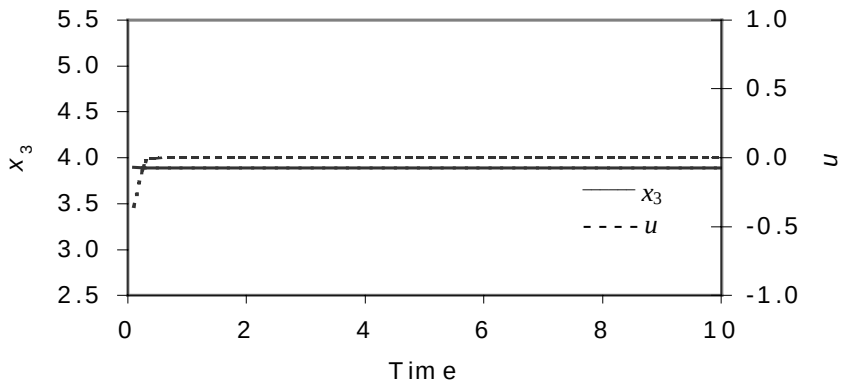

Figure 7.3.2: FLC controlled dynamic behavior for stabilization of oscillatory dynamics (x_3 = 3.89)

7.3.2.3 Controlling the System at the Unique USS Responsible for Chaotic Motion

In this control objective, the FLC is required to stabilize the chaotic trajectory exactly at the corresponding unique USS. For simulating contoller actions, the parameter set III is used with the setpoint, x_3^{set} =3.7627; the system is initially at an arbitrarily chosen point in the state-space. The plot of FLC action (Figure 7.3.3) clearly indicates that the FLC has fulfilled the control objective of stabilizing the chaotic motion at the USS without allowing any offset.

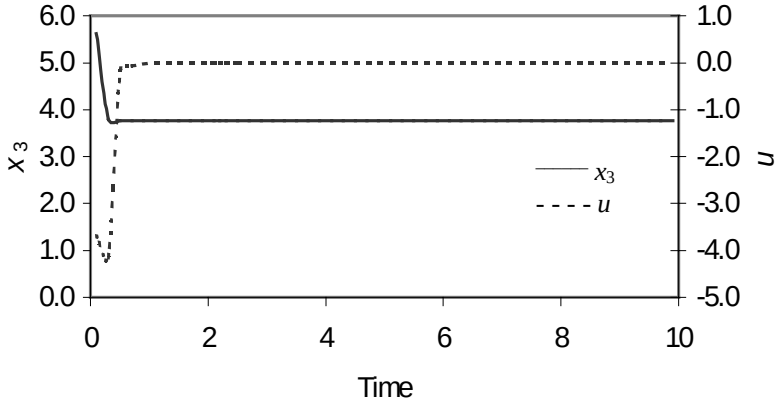

Figure 7.3.3: FLC controlled dynamic behavior for stabilization of chaotic dynamics (x_3 = 3.7627)

7.3.2.4 Controlling the System at USS Responsible for Chaotic Motion in the Presence of Stochastic and Deterministic Load Disturbances.

The ability of the proposed FCL to impart the desired control action in the present of stochastic load disturbances was tested by incorporating random noise at very integration step ($\Delta t=0.001$) in the time evolution for the CSTR temperature equation (7.14). Thus, the load disturbance term d_3 assumes random values (with $d_1 = d_2 = 0$) obeying the Gaussian distribution with mean and standard deviation values of 0 and 0.5, respectively. The time profiles of the controlled CSTR temperature, x_3, and the controller output (u) in the presence of the random disturbances are shown in Figure 7.3.4. Additionally, the FLC results when a constant (deterministic) disturbance of unit magnitude ($d_3 = 1$) is added to equation (7.14) are depicted in Figure 7.3.5. As can be noted from these graphs, the FLC delivers excellent action in the presence of either type of load disturbances.

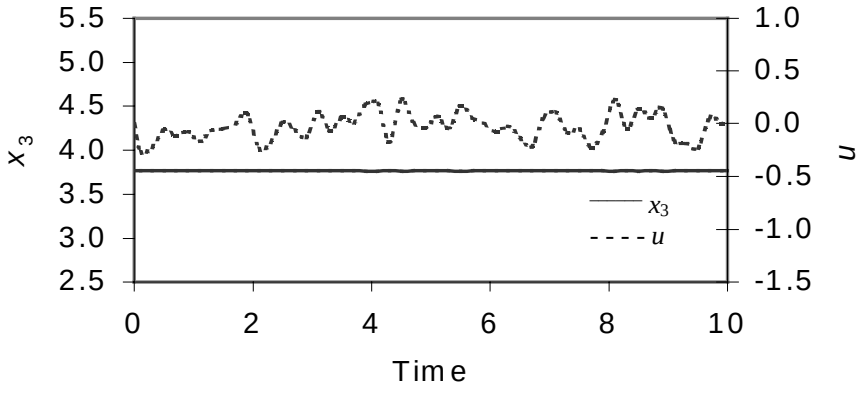

Figure 7.3.4: FLC time profile in the presence of disturbance obeying Gaussian distribution of mean zero and standard deviation 0.5

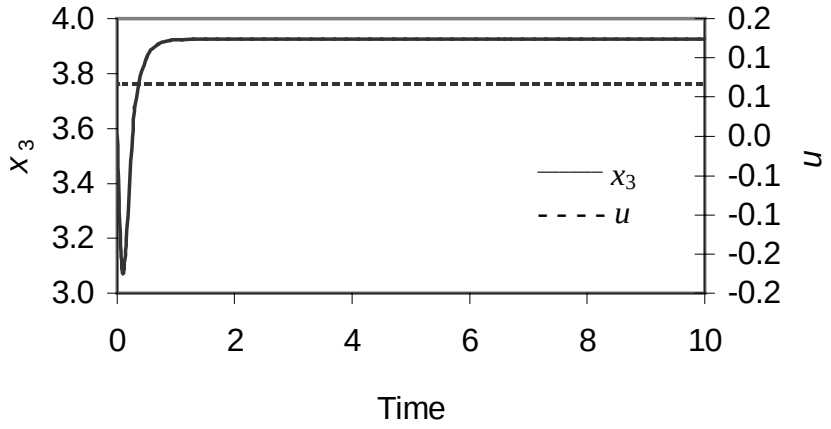

Figure 7.3.5: FLC time profile in the presence of fixed (deterministic load disturbance of unit magnitude).

7.3.2.5 Comparison of FLC and PID Actions

The FLC action is compared (Figure 7.3.6) with PID (K_c = 6.0, τ_I = 0.7, τ_D = 0.001) for the case of random load disturbance obeying Gaussian distribution with mean and standard deviation values of 0 and 0.5. Here the controller objective was to stabilize the chaotic trajectory exactly at the corresponding unique USS (x_3^{set} = 3.7627). The time profiles corresponding to the FLC and PID actions clearly show the superiority of FLC over PID.

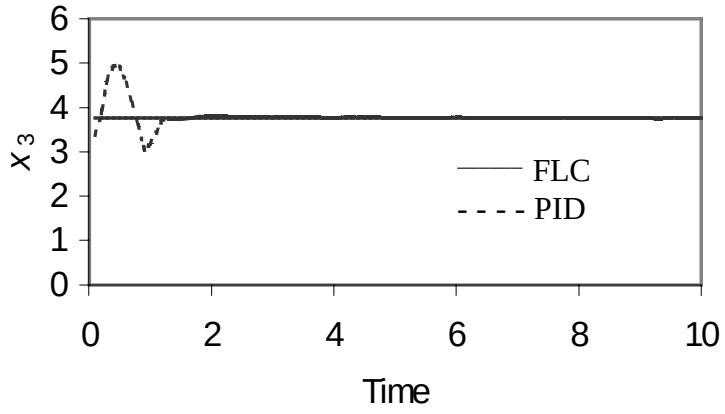

Figure 7.3.6: Comparison of FLC with PID at set point x_3 =3.76

7.4 Conclusions

The study presents a simple method for the self-tuning of a fuzzy-logic controller by RLS technique. The strategy eliminates the laborious design steps of a manually tuned FLC, such as the tuning of the fuzzy membership functions and control rules. Moreover, no reference or intermediate model is necessary for implementing the FLC.

Nomenclature

D - dilution rate - $0.202\ h^{-1}$

K_i - substrate inhibition constant - $22\ gl^{-1}$

K_m - substrate saturation constant - $1.2\ gl^{-1}$

P - process or product concentration - $19.14\ gl^{-1}$

S - substrate concentration in the outlet stream – $5.0\ gl^{-1}$

S_f - substrate concentration in the feed - $20.0\ gl^{-1}$

X - cell concentration - $6.0\ gl^{-1}$

$Y_{x/s}$ - cell mass yield - $0.4\ g/g$

α - kinetic parameter in fermentor -$2.2\ g/g$

β - kinetic parameter in fermentor -$0.2\ h^{-1}$

μ_m - maximum growth rate - $0.48\ h^{-1}$

References

Moore, C.G., Harris, C.J., 1992, Indirect adaptive fuzzy control, *Int. J. Control*, 56(2): 441-468.

Pham, D.T., Karaboga, D., 1999, Self-tuning fuzzy controller design using genetic optimization and neural network modeling, *Artificial Intelligence in Engineering*, 13: 119-130.

Mendel, J. M., Mouzouris, G.C., 1997, Designing fuzzy logic systems, *IEEE Transactions on Circuit and Systems- II: Analog and Digital Signal Processing*, 44(11): 885-894.

Chak, C. K., Feng, G., 1995, A new fuzzy neural network system, *Journal of Intelligent and Fuzzy Systems*, 3:131-144.

Henson M.A., Seborg, D.E., 1991a, An internal model control strategy for nonlinear systems, *A.I.Ch.E. Journal*, 37:1065-1081.

Hu, Q., Rangaiah, G.P., 1999, Adaptive internal model control of nonlinear processes, *Chemical Engineering Science*, 54:1205-1220.

Bandyopadhyay, J.K., Tambe, S.S., Jayaraman, V.K., Deshpande, P.B., Kulkarni, B.D., 1997, On control of non-linear system dynamics at unstable steady state, *Chemical Engineering Journal*, 67:103-114.

Chapter 8

Nonlinear Control Using Neurofuzzy Network

8.1 Introduction

The control of polymer reactors is a difficult and complex problem for several reasons. Firstly, these reactors often exhibit highly interactive nonlinear dynamic behavior resulting in multiplicity of steady-states, instability, parametric sensitivity, oscillations and even chaos in some parameter regions. Recently, several control algorithms based on the predictions of an input-output process model have been developed for the control of polymer processes. Often, a single polymerization reactor is used to produce polymers of different grades (varying molecular weights, compositions, etc.). Hence, one major control objective is minimization of the grade transition time, which reduces the off-spec production. However, the interactive nonlinear dynamic behavior of polymer reactors becomes more apparent during the grade transitions than at a steady-state operation. Hence, a nonlinear model-based control is expected to yield a better performance when compared with a linear model-based controller for grade transition control. Secondly, a "first principles" model of a polymerization process may contain a large number of kinetic and transport parameters, which may be difficult to estimate. It is therefore convenient to use a model structure whose parameters can be identified exclusively from the input-output process data.

There exists a considerable amount of literature on the model-based control of polymerization reactors. Most of these techniques are based on linear models and therefore are not able to control effectively and precisely the nonlinear polymer processes over a wide operating range. For this reason, recently a number of studies have extended the model based control technique to nonlinear processes. Cutler and Ramaker (1979) initiated dynamic matrix control algorithm, and then a few experimental studies with various chemical systems were reported in literature. Maner and Doyle (1997) used nonlinear MPC scheme based on Volterra model to control polymerization reactor where the control action was determined by solving nonlinear programming problem. Recently Ozkan *et al*.(2001) applied NMP to batch polymerization problem, where system dynamics was represented by NARMAX was obtained and control action by DMC technique.

A wide variety of nonlinear input-output models have been proposed for use in the control of nonlinear processes. In this work, a B-spline neurofuzzy network (BSNN) based model is proposed. The principal advantage of neuro-fuzzy systems is that they combine adaptive learning, parallel processing and generalization capabilities of ANNs with the high-level human-like thinking and reasoning of fuzzy systems.

Accordingly, this study presents results of the control of number-average molecular weight (NAMW) using a B-spline neurofuzzy network by manipulating the inlet initiator flow rate of an isothermal free-radical polymerization process of methyl methacrylate using azobisisobutyronitrile (AIBN) as an initiator and toluene as a solvent in a CSTR.

8.2 Neurofuzzy Network Structure

8.2.1 B-spline Neural Network

The most important feature of the B-spline algorithm is the smooth network output which is due to the shape of the basis function. It has been proved that the B-spline network can approximate a continuous function at any level of arbitrary accuracy (Brown and Harris 1994). B-spline theory can be found in (Brown and Harris, 1994, Schumaker, 1981).

Assuming the n-input vector is $\mathbf{x} = [x_1, x_2, ..., x_n]$ and that defined on each input axis is a ith univariate B-spline basis function of order m, $B_i^{k_i}(x_i)$, $k_i = 1, 2, ..., m_i$, $i = 1, 2, ..., n$. Univariate B-spline basis functions of order m = 0, 1, 2, 3 are shown in Figure 8.1. Here the orders of B-splines are omitted for brevity.

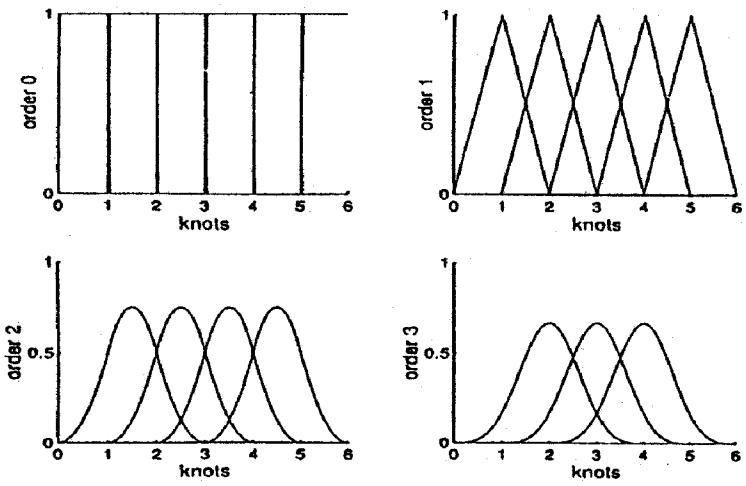

Figure 8.1: B-splines of order m = 0, 1, 2, 3

The kth multidimensional B-spline basis functions $N_k(\mathbf{x})$, are formed by the tensor product of n univariate basis functions $B_i^{ki}(x_i)$, and given by.

$$N_k(\mathbf{x}) = \prod_{i=1}^{n} B_i^{ki}(x_i) \tag{8.1}$$

where the total number of $N_k(\mathbf{x})$ is $p = m_1 m_2 \ldots . m_n$, that is $k = 1,2,\ldots,p$.

A multivariate function $y(\mathbf{x})$ is then approximated by the linear combination of the multivariate B-spline basis functions as:

$$y(\mathbf{x}) = \sum_{k=1}^{p} N_k(\mathbf{x}) w_k = \sum_{k=1}^{p} \prod_{i=1}^{n} B_i^{ki}(x_i) w_k \tag{8.2}$$

where w_k is the kth weight on the kth B-spline basis function.

The above equation can also be represented as B-spline neural network and is shown in Figure 8.2.

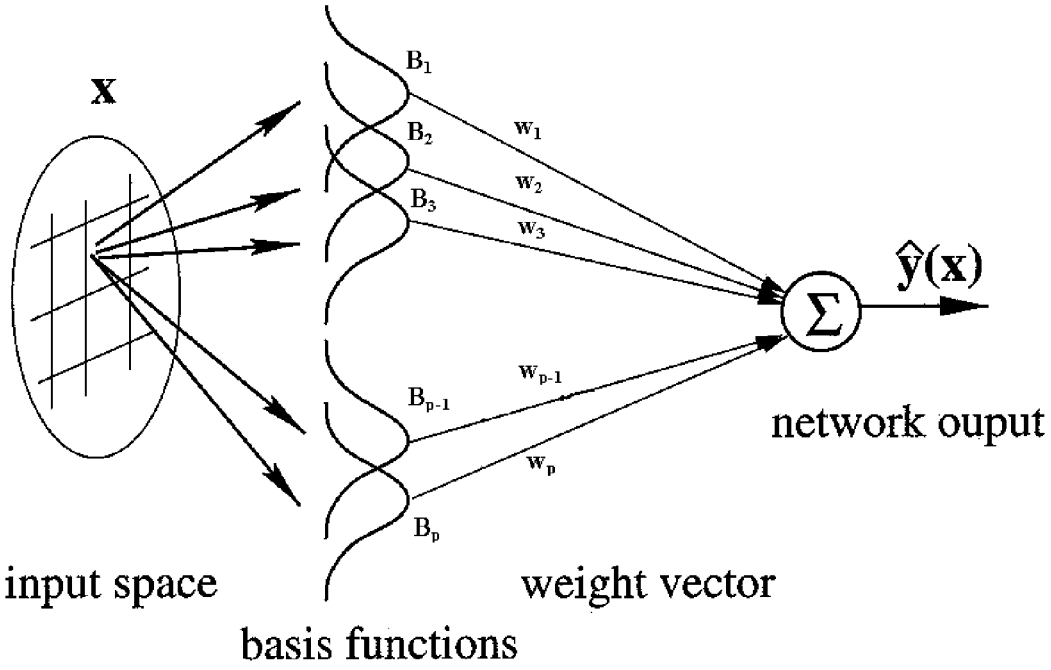

Figure 8.2: The B-spline neural network

8.2.2 Neurofuzzy Modelling

The general form of a discrete-time, multi-input, single-output (MISO) can be represented as

$$y(t) = f(x_1(t), x_2(t), ..., x_n(t)) \tag{8.3}$$

$$y = f(y(t-1)+...+y(t-n_y)+u(t-1)+...+u(t-d-m_u)) \tag{8.4}$$

where $f(\cdot)$ is an unknown nonlinear function, $u(t)$ and $y(t)$ are the system's input and output, respectively, and n_y, m_u and d are assumed a priori and represent the orders and times delays of the model.

For system identification purpose, $y_k(\mathbf{x})$ in fuzzy rule is set to a linear combination of the components of the input vectors.

$$y_k(\mathbf{x}) = a_1^k x_1 + a_2^k x_2 + ...+ a_n^k x_n \tag{8.5}$$

The output of the fuzzy system by B-spline basis functions after simplification can be written as

$$y = \sum_{k=1}^{p} \prod_{i=1}^{n} B_i^{k_i}(x_i) y_k(x) = \sum_{k=1}^{p} N_k(\mathbf{x}) y_k(\mathbf{x}) \tag{8.6}$$

By substituting $y_k(\mathbf{x})$ into (8.6) with (8.5), the consequent part of the fuzzy rule bases becomes

$$y = \sum_{k=1}^{p} N_k(\mathbf{x})(a_1^k x_1 + a_2^k x_2 + ... + a_n^k x_n) \tag{8.7}$$

$$y = a_1(\mathbf{x}) x_1(t) + ... + a_1(\mathbf{x}) x_2(t) + a_1(\mathbf{x}) x_3(t) + ... + a_n(\mathbf{x}) x_n(t) \tag{8.8}$$

$$y = a_1(\mathbf{x}) y(t-1) + ... + a_{n_y}(\mathbf{x}) y(t-n_y) + a_{n_y+1}(\mathbf{x}) u(t-1) + ... + a_n(\mathbf{x}) u(t-d-m_u) \tag{8.9}$$

where

$$a_i(\mathbf{x}) = \sum_{k=1}^{p} N_k(\mathbf{x}) a_i^k, \qquad i = 1,2,...,n, \tag{8.10}$$

The neurofuzzy network is represented in Figure 8.3. The above equation (8.9) is a linear combination of the multi-dimensional B-spline functions, and can be approximated by a B-spline neural network shown in Figure 8.3. Actually, equation (8.9) can be viewed as an operating point dependent ARMA model, where autoregressive parameters $a_i(\mathbf{x})$ are nonlinear functions of the operating point $\mathbf{x}$ representing the past values of the systems input-output states.

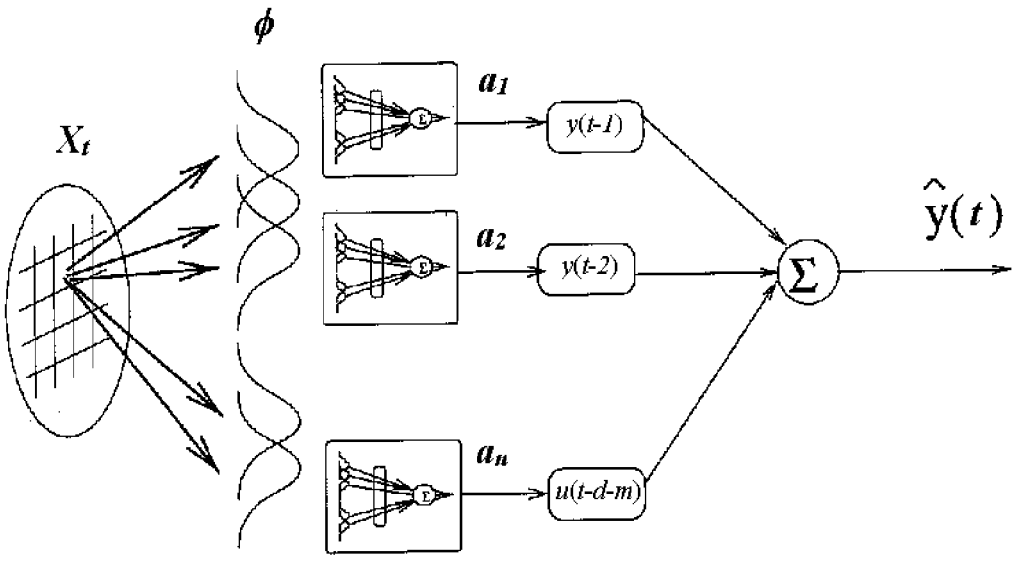

Figure 8.3: Neurofuzzy modeling network

By representing each autoregressive parameter of (8.9) as a neurofuzzy network in the form of Figure 8.3; the whole equation (8.9) can be represented as a neural network structure shown in Figure 8.3, where

$$\phi = [N_1(\mathbf{x}) \quad N_2(\mathbf{x}) \quad \ldots \quad N_p(\mathbf{x})]^T \tag{8.11}$$

$$\theta_{a_i} = [a_i^1 \quad a_i^2 \ \ldots \ a_i^p]^T, \quad i = 1,2,\ldots,n. \tag{8.12}$$

The first layer is composed of n neurofuzzy subnetworks of the form of Figure 8.2; each output corresponds to an autoregressive parameter $a_i(\mathbf{x})$. All the subnetworks share the same B-spline functions $\phi\ (t-1)$ as inputs.

This network structure is referred to as a neurofuzzy network. It is well structured two-layered feedforward network. Its connections are very simple and it is very easy to train by traditional learning algorithms used in feedforward neural networks.

This completes the description of the neurofuzzy network model for system identification.

8.2.3 Training of the Neurofuzzy B-spline Network

The modelling network shown in Figure 8.3 can be viewed as a two-layered neural network. The first layer is composed of standard neurofuzzy (B-spline) subnetworks (Figure 8.2) and second layer is simply the regression calculation of (8.9). The free parameters are the weights of the B-spline subnetworks in the first layer, and the 'weights' of the second layer are viewed as fixed in every iteration of the back-propagation training. The network can be trained by many traditional learning algorithms for feedforward neural networks. In the rest of this section we present a method of training the networks by the normalized least mean squares (NLMS) algorithm.

At time t the input vector $\mathbf{x}(t)$ is presented to the neural network of Figure 8.3. In the forward pass the network calculates the output by (8.9) denoted by $\bar{y}(\mathrm{t})$. Let ε

$$\varepsilon = y(\mathrm{t}) - \bar{y}(\mathrm{t}) \tag{8.13}$$

be the error between the system and the network outputs. Because no free parameters in the second layer are to be trained, the error ε is propagated back through the second layer to the output of the first layer. Therefore, the errors in a_i, normalized by $\mathbf{x}(t)^T\mathbf{x}(t)$, are given by

$$\varepsilon_{a_i} = \frac{x_i(t)\varepsilon}{\mathbf{x}(t)^T \mathbf{x}(t)}, \quad i = 1,2,\ldots,n \tag{8.14}$$

Then the errors ε_{a_i} are used to update the weights of the network's first layer. The NLMS algorithm for the network is therefore

$$\theta(t) = \theta(t-1) - \eta \frac{\phi(t-1)x_i(t)\varepsilon}{c + \phi(t-1)^T \phi(t-1)\mathbf{x}(t)^T \mathbf{x}(t)} \qquad i = 1,2,\ldots,n \tag{8.15}$$

with $\theta_{a_i}(0)$ given, where η is the learning rate and $c > 0$ is arbitrary small number which has been added to avoid division by zero.

8.3 Nonlinear Model Predictive Control (NMPC) Algorithm

The basic philosophy of NMPC is to use a model of the system to predict future process outputs and thereby determine a suitable control move to be made in the future. For example, the equation presented below represents the present output as a function of the two lagged values of the output and the current and one lagged value of the manipulated variable. In this study, the neurofuzzy network has been used to develop a dynamic process model predicting one step ahead value of the control variable and the model predicted value is used in the framework of Newton-Raphson method to determine the control action. The block diagram of B-spline NMPC is shown in Figure 8.4. In B-spline neuro-fuzzy network, autoregressive parameters $a_i(\mathbf{x})$ are nonlinear functions of the operating point **x,** which are the past values of the systems input-output states.

$$y_m(t+1) = a_1(t+1)y(t) + a_2(t+1)y(t-1) + a_3(t+1)u(t) + a_4(t+1)u(t-1) \tag{8.16}$$

$$f_e = y_p(t+1) - y_{set}(t+1) \tag{8.17}$$

$$y_p(t+1) = y_m(t+1) + d(t) \tag{8.18}$$

$$d(t) = c(y_p(t) - y_m(t)) \tag{8.19}$$

$$y_p(t+1) = y_m(t+1) + c(y_p(t) - y_m(t)) \tag{8.20}$$

By Newton-Raphson method the manipulated variable for future control action is given by

$$f_e' = \frac{df_e}{du} = a_3 \tag{8.21}$$

$$u(k+1) = u(k) - \frac{f_e}{f_e'} \tag{8.22}$$

Thus in the control algorithm the manipulated variable is computed as

$$u(t+1) = u(t) - \frac{f_e}{a_3(t+1)} \tag{8.23}$$

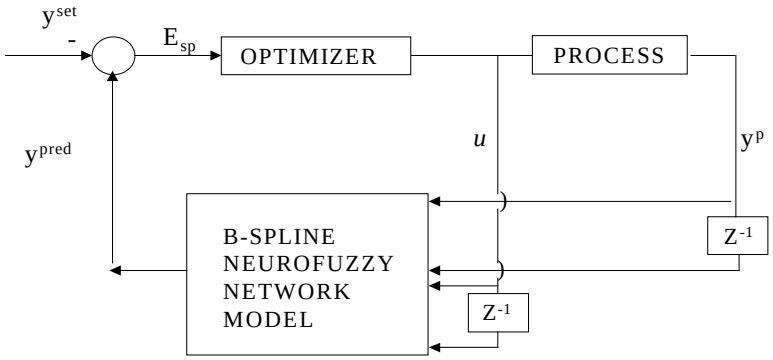

Figure 8.4: The block diagram of B-spline model predictive control.

8.4 Isothermal Polymerization Reactor Case Study

Consider an isothermal free-radical polymerization of methyl methacrylate using azobisisobutyronitrile (AIBN) as initiator and toluene as solvent. In the study, the number-average molecular weight (NAMW) is controlled by manipulating the inlet initiator flow rate (F_I). Thus the manipulated variable and controlled variable are

$$u = F_I, \quad y = \text{NAMW} \tag{8.24}$$

The following isothermal model was obtained by setting the reactor temperature at its steady-state model value of 335 K (Maner and Doyle-III,1997).

$$\frac{dC_m}{dt} = -\left(k_p + k_{f_m}\right)C_m P_o + \frac{F\left(C_{m_f} - C_m\right)}{V} \tag{8.25}$$

$$\frac{dC_I}{dt} = -k_I C_I + \frac{F_I C_{I_f} - FC_I}{V} \tag{8.26}$$

$$\frac{dD_o}{dt} = \left(0.5k_{T_c} + k_{T_d}\right)P_o{}^2 + k_{f_m} C_m P_o - \frac{FD_o}{V} \tag{8.27}$$

$$\frac{dD_I}{dt} = M_m\left(k_p + k_{f_m}\right)C_m P_o - \frac{FD_1}{V} \tag{8.28}$$

$$y = \frac{D_1}{D_o} \tag{8.29}$$

where $$P_o = \left[\frac{2fk_I C_I}{k_{T_d} + k_{T_c}}\right]^{0.5}$$

Table 8.1: Steady-state operating conditions for the SISO case study

C_m	5.506774 kmol/ m^3
C_I	0.132906 kmol/ m^3
D_o	0.0019752 kmol/ m^3
D_1	49.38182 kg/ m^3
u_o	0.016783 m^3/h
y_o	25000.5 kg/kmol

8.4.1 Identification of System

The B-spline neurofuzzy network (BSNN) has been utilized for identifying the system representing the dynamics of polymerization. For convenience, the process input-output data of the system was collected using the phenomenological model. Specifically, the manipulated variable is varied randomly using a pseudo-random sequence and its effect on the controlled variable is monitored. This input-output data were partitioned into two sets, i.e. training and test sets. While the former is used to train the neuro-fuzzy network, the latter is used to evaluate the generalization ability of the network. Note that the phenomenological model is used only for generating process data. The NMPC described here is based on the neuro-fuzzy model which is exclusively data-driven. The number of input-output data generated by simulating an open-loop system of the isothermal polymerization reactor was 800 using a sample time of $T_s = 0.03$ h and random steps with a switching probability of $P_s = 0.05$, with the values at each transition drawn from a uniform distribution in the range $u = [0.0046, 0.028966]\ m^3/\text{h}$. The

number of lags on the input and output were specified to be $n_u = 2$ and $n_y = 2$, respectively. In the neurofuzzy network, B-spline basis function of order 2 was used. Figure 8.4 shows that the prediction, closely follow the actual trajectory for these parameter values.

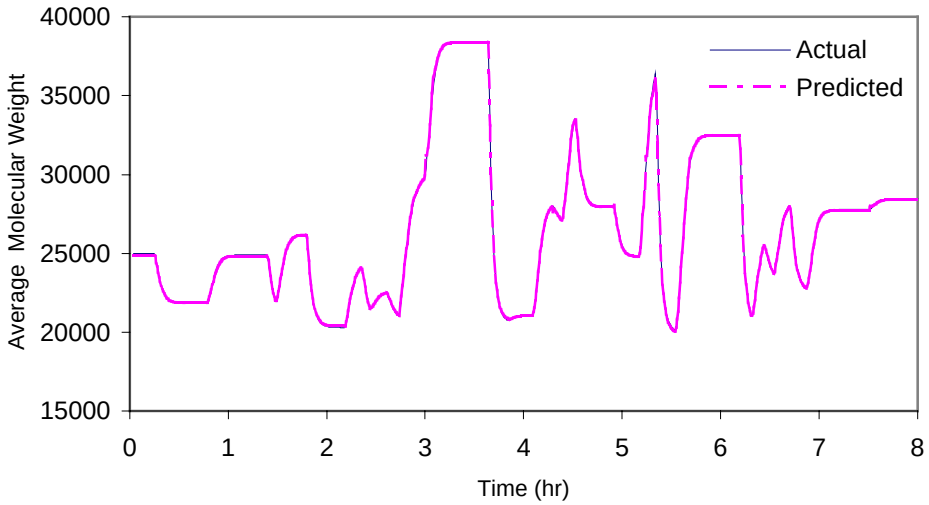

Figure 8.5: Comparison of actual and predicted by BSNN.

8.4.2 Control Results

8.4.2.1 Setpoint Tracking

For closed-loop simulations, it was assumed that there was a performance specification of $\pm$ 1,000 kg/kmol around the setpoint for which the product is considered acceptable. Hence for a setpoint change simulating a grade change, it is desirable to quickly enter and remain within the new product specification bounds.

Firstly, NMPC was employed for a setpoint change from 25,000 kg/kmol to 38,000 kg/kmol. The closed–loop responses by the Nonlinear MPC are shown in Figure Figure 8.6.1. It is seen that the number-average molecular weight enters into the new product specification bounds after 30 minutes.

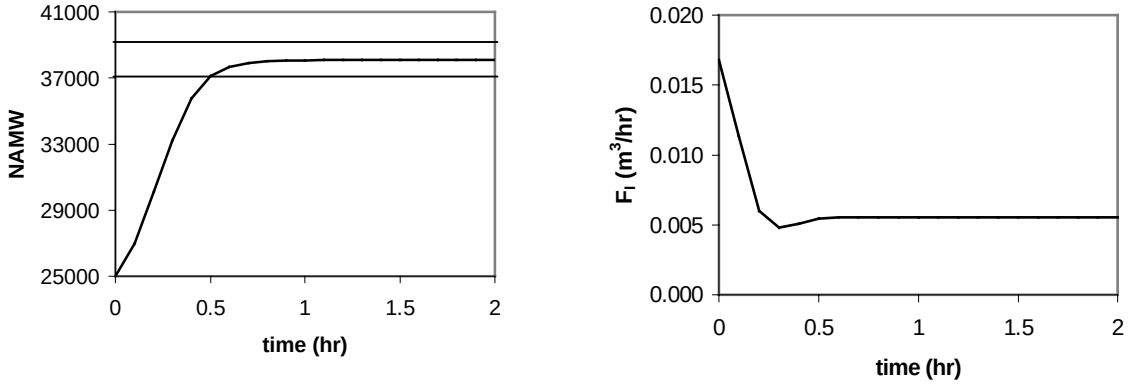

Figure 8.6.1: Closed-loop simulation for a step setpoint change from 25000 kg/kmol to 38000 kg/kmol in number-average molecular weight

The closed-loop responses for a new setpoint of 20000 kg/kmol are shown in Figure 8.6.2. The BSNN based NMPC brings the process into the new operating region after 18.0 min.

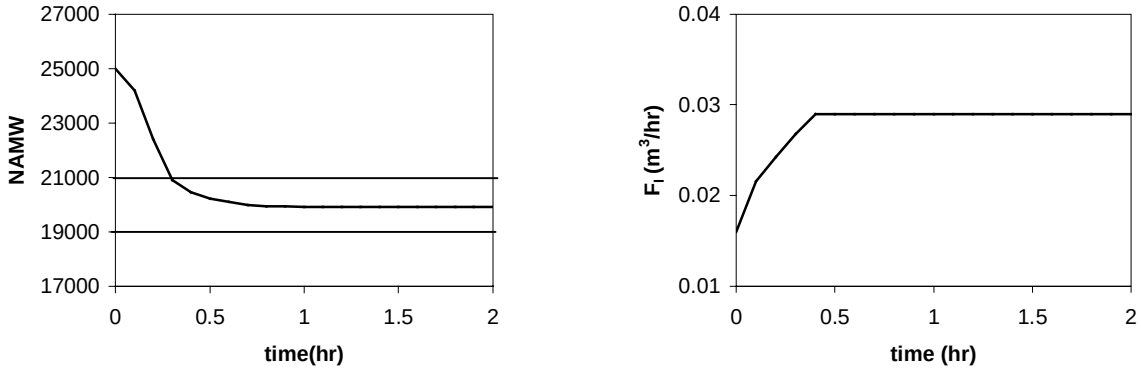

Figure 8.6.2: Closed-loop simulation for a step setpoint change from 25000 kg/kmol to 20000 kg/kmol in number-average molecular weight

8.4.2.2 Disturbances Rejection

An important measure of control system's performance is the ability to reject unmeasured disturbances. In response to an unmeasured disturbance, it is desired that the process re-enters the product specification bounds quickly.

In Figure 8.6.3, the responses of the Nonlinear MPC for a change in monomer feed concentration from $C_{m_f} = 6.00$ to $C_{m_f} = 5.00$ kmol/m^3 is shown

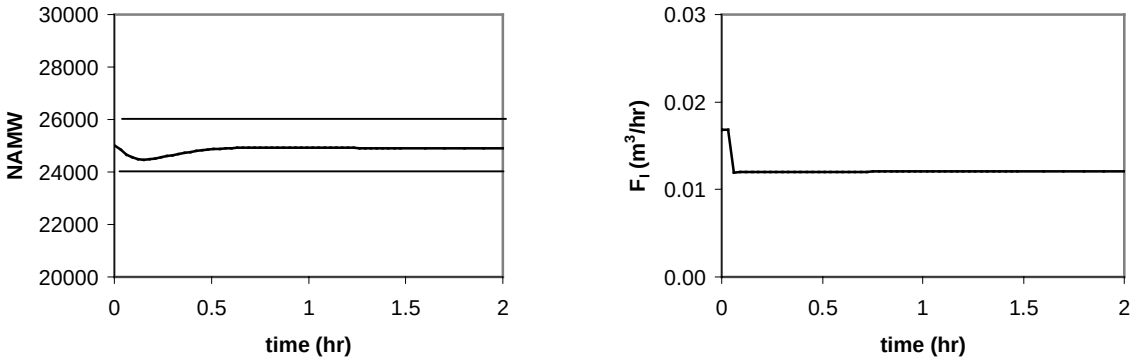

Figure 8.6.3: Closed-loop simulation for an unmeasured step disturbance in monomer feed composition from its nominal value of $C_{m_f} = 6.00$ kmol/m^3 to $C_{m_f} = 5.00$ kmol/ m^3

8.4.2.3 Comparison

Maner and Doyle-III (1970) studied a nonlinear model-predictive control scheme based on the autoregressive-plus Volterra model and compared its performance with PI control and linear MPC. The results of these controllers (i.e. time taken to reach product specification bounds for different controller), alongwith B-spline neurofuzzy model are listed in Table 1. The tabulated results show that the BSNN based NMPC outperformed the other controller in one case.

Table 8.2: Time to reach the product specification bounds for different controller

Controller \ Product Specification (NAMW)	38,000 kg/kmol	20,000 kg/kmol	25,000 kg/kmol
Linear MPC	19.8 min	54.0 min	37.8 min
PI	19.8 min	54.0 min	37.8 min
NMPC(Voltera)	21.6 min	16.2 min	25.2 min
NMPC(BSNN)	30.0 min	18.0 min	0 min

8.5 Conclusions

This chapter presents a nonlinear model based control algorithm and results of its application to isothermal free-radical polymerization of methyl methacrylate. Here the process model is developed using B-spline neuro-fuzzy network. Process identification and control by B-spline neurofuzzy network is shown to perform well. In terms of closed loop performance, an improvement over the earlier reported result was demonstrated for single variable case involving disturbance rejection.

Nomenclature

C_I - monomer concentration of initiator, kmol/ m^3

C_{I_f} - molar concentration of the initiator in the intiator inlet stream- 8.00 kmol/m^3

C_m - monomer concentration of monomer, kmol/m^3

C_{m_f} - molar concentration of the monomer in the monomer inlet stream - 6.00 kmol/m^3

D_1 - mass concentration of the dead polymer chains, kg/m^3

D_o - molar concentration of the dead polymer chains, kmol/ m^3

f - initiator efficiency – 0.58

F - volumetric flow rate – 1.00 m^3/h

F_I - initiator volumetric flow rate – m^3/h

k_{T_c} - kinetic rate constant for termination by coupling – 1.31281×10^{10} m^3/(kmol.h)

k_{T_d} - kinetic rate constant for termination by disproportionation-

$1.0930\times10^{11}m^3$/(kmol.h)

k_I - kinetic rate constant for initiation - 1.0225×10^{1} 1/h

k_p - kinetic rate constant for propagation - 2.4952×10^{6} m^3/(kmol.h)

k_{f_m} - kinetic rate constant for chain transfer to monomer - $2.4522\times10^{3}m^3$/(kmol.h)

M_m - molecular weight -100.12 kg/kmol

u_o - nominal value of inputs, m^3/h

V - reactor volume – 10.0 m^3

y_o - nominal value of output, kg/kmol

References

Wu, Z. Q., Harris, C.J., 1997, A neurofuzzy network structure for modeling and state estimation of unknown nonlinear systems, *Internal Journal of System Science*, 28(4): 335-345.

Maner, B.R. and Doyle III, F.J., 1997, Simulated polymerization reactor control using autoregressive plus Volterra-based MPC, *AIChE, J.*, 43:1763-1784.

Lennox, B., Motague, G.A., Frith, A.M., Chris Gent, Bevan, V., 2001, Industrial application of neural networks – an investigation', *Journal of Process Control*, 11: 497-507.

Yuce, S. Hasaltun, A., Erdogan, Alpbaz, M., 1999, Temperature control of a batch polymerization reactor, *Trans. I. ChemE*,. 77, Part A (5):413-420.

Ozkan, G., Ozen, S., Erdogan, S., Hapoglu, H., Alpbaz, M., 2001, Nonlinear control of polymerization reactor, *Computers and Chemical Engineering*, 25:757-763.

Cutler, C. R. Ramaker, B. L., 1979, Dynamic matrix control - a computer control algorithm, *AIChE National Meeting*, Houston, TX.

Henson, M. A., 1998, Nonlinear model predictive control: current status and future directions, *Computers and Chemical Engineering*, 23:187-202

Brown, M., Harris, C.J., 1994, *Neurofuzzy Adaptive Modeling and Control*, Prentice Hall, Hemel Hempstead.

Schumaker, L.L, 1987, *Spline Functions: Basic Theory*, J. Wiley, NY.

Chapter 9

Summary and Future Prospects of Research

9.1 Summary

Chemical systems exhibit nonlinear and often time-varying behavior. Successful process monitoring and control schemes require good knowledge of process in the form of an adequate mathematical model. A number of mechanistic and/or empirical mathematical models describing various chemical processes have been proposed in the past decades. The main disadvantage of the mechanistic models is their complexity, especially when kinetic, thermodynamic and physical mechanism are not completely determined. Methods based on artificial intelligence have offered new, effective tools for system modeling.

The optimization problems in chemical engineering have been tackled using various NLP and MINLP techniques. However these techniques involve gradient based sequential search and often converge into arbitrary local optima instead of global optima. Genetic Algorithms have been proposed as a robust stochastic optimization tool wherein the random nature of stochastic optimization significantly reduces the likelihood of being trapped into local optima. In addition, no derivatives are needed for the optimization and this reduces or even eliminates the problem of non-convergence.

AI techniques are generic in nature and possess tremendous potential for applications in Chemical Engineering. In this thesis, genetic algorithms have been applied to optimize the batch, continuous and reactive distillation columns. Fuzzy logic and hybrid techniques have been explored for the control of chemical processes.

In chapter 2, Genetic Algorithms (GA) are applied to batch distillation columns to determine the optimal reflux policy for two industrially relevant binary mixtures i.e. acetone-water and para/ortho nitrochlorobenene. The objective function is thus to obtain the position of cut subject to minimization of total vapor load. Improved results are obtained by calculating reflux ratio for infinitesimal cut within the cut.

Chapter 3 reports feasibility of utilizing the GA technique for simple and azeotropic distillation. The two binary systems considered are ethanol-water and methanol-water. One azeotropic system of benzene-ethanol-water is also considered. For a specified degree of separation, the optimal values of: (i) number of stages, (ii) reflux ratio (entrainer quantity in the case of azeotropic distillation), and (iii) feed location(s) are determined for minimization of total cost of column as objective function.

Manufacture of ethylene glycol and MTBE by reactive distillation have been selected for optimization by Genetic algorithms in Chapter 4. For a specified degree of production and separation by reactive distillation , the optimal values of number of trays, boil up fraction, liquid hold up and feed flow rate on trays are determined. The utility of GA technique for optimization of catalytic distillation system is also demonstrated in the example of MTBE production from ethylene. In this case of catalytic distillation column, reflux ratio, column pressure and bottom flow rate are optimized.

In chapter 5, a fuzzy logic based control strategy has been introduced for controlling chaotic dynamics. The effectiveness of the proposed strategy is demonstrated on nonisothermal CSTR and biochemical reaction exhibiting a chaotic behavior.

Chapter 6 describes designing the FLC by optimizing control rules and membership functions by genetic algorithms. Efficacy of the genetic algorithms designed FLC has been demonstrated for the servo and regulatory control of a non-isothermal continuous stirred tank reactor (CSTR) and nonlinear pH control.

Recursive least square(RLS) algorithm is combined with FLC in Chapter 7. RLS algorithm tunes the output membership function online deals resulting in adaptive fuzzy logic controller. Effectiveness of the proposed FLC has been demonstrated by considering the control of two non-linear chemical systems namely : (i) continuous fermentation process, and (ii) non-isothermal continuous stirred tank reactor (CSTR). In literature, we have not cited use of RLS algorithm online in FLC.

B-spline neurofuzzy network, a hybrid AI technique is applied to a nonlinear model-predictive control scheme in chapter 8. It is applied to isothermal free-radical polymerization of methyl methacrylate using azobisisobutyronitrile (AIBN) as initiator and toluene as solvent in CSTR. The model identification and control action are determined by the B-spline neurofuzzy model. To the best of our knowledge, this is the first application of B-spline neural network in model based controller in chemical engineering.

9.2 Future Prospects of Research

Recently stochastic optimization techniques have been used for phase equilibrium and stability problems. Phase equilibrium calculations require global minimization of free energy, and phase stability analysis too often involves global minimization of tangent plane distance function. Optimization of azeotropic distillation column in conjunction with phase equilibrium and stability algorithm by stochastic optimization technique like GA needs to be explored.

The proposed nonlinear model based control (NMPC) strategy using B-spline neural network is useful and future studies should focus on novel process applications for large-scale systems. A wide variety of problem formulations have been proposed for NMPC in literature. B-spline neural network can also be investigated for other types of problems.

Appendix

Appendix A: Modeling and Simulation

A.1 Details of the Batch Distillation Model

The short-cut method for design of batch distillation proposed by Diwekar *et al.* (1987) is used for simulation. It is based on the assumption that the batch distillation column can be considered as continuous distillation column with changing feed at any instant. Since continuous distillation theory is well-developed and tested, the short cut method (Fenske-Underwood-Gilliland method (FUG)) for continuous distillation is modified for batch distillation. The other assumptions of the short-cut method include constant molal overflow and negligible plate holdup. Some relevant details of the short-cut method (Diwekar *et al.*,1987) are as under:

The Hengestebeck-Geddes' equation for the *k*th reference component :

$$x_d^{(i)} = \left(\frac{\alpha_i}{\alpha_k}\right)^{C_1} \frac{x_d^{(k)}}{x_b^{(k)}} x_b^{(i)} \qquad i = 2, 3, \ldots, nc \ (nc\text{- number of component}) \qquad \text{(A1)}$$

where x_b, x_d and α are still composition, distillate composition and relative volatility.

The Fenske's equation for minimum number of plates (N_m):

$$N_m = \frac{ln\left[\frac{x_d^{(lk)}}{x_d^{(hk)}} \frac{x_b^{(hk)}}{x_b^{(lk)}}\right]}{ln(\alpha_{lk})} \qquad \text{(A2)}$$

where *lk* - light key component and *hk*- heavy key component.

$$C_1 = N_m \qquad \text{(A3)}$$

The Underwood equations for minimum reflux (R_m) :

$$\sum_{i=1}^{nc} \frac{\alpha_i x_b^{(i)}}{\alpha_i - \phi} = 0 \qquad \text{(A4)}$$

$$R_m + 1 = \sum_{i=1}^{nc} \frac{\alpha_i x_d^{(i)}}{\alpha_i - \phi} \qquad \text{(A5)}$$

where ϕ is Underwood equation constant.

Eduljee's correlation:

$$A = (1 - 1.333B)^{1.7648} \qquad \text{(A6)}$$

in which $$A = \frac{R_k - R_m}{R_k + 1}, \qquad B = \frac{N - N_m}{N + 1} \tag{A7}$$

and $$\sum_{i=1}^{nc} x_d^{(i)} = 1 \tag{A8}$$

In order to match the R_m predicted by the Underwood's equations (where the compositions $x_d^{(i)}$'s are used to calculate R_m) with the R_m obtained by the Gilliland's correlation (which uses N, R and N_{min} or C_1), the following additional condition is provided:

$$G(1) = \frac{R_{m_{underwood}}}{R} - \frac{R_{m_{gilliland}}}{R} \tag{A9}$$

For specific $x_b^{(1)}$ at each state, it is necessary to estimate $x_d^{(i)}$, $i = 1,\ldots,n$ and $x_b^{(i)}$, $i = 2,\ldots,n$. The differential material balance can be converted into a difference material balance equation using prior values of $x_b^{(i)}$'s and $x_d^{(i)}$'s and can be written as

$$x_{b_{new}}^{(i)} = x_{b_{old}}^{(i)} + \Delta x_b^{(k)} \frac{(x_d^{(i)} - x_b^{(i)})_{\text{old}}}{(x_d^{(k)} - x_b^{(k)})_{old}} \qquad i = 1,2,\ldots,nc \tag{A10}$$

To obtain initial values of $x_d^{(k)}$'s, the procedure given below is used.

The Hengestebeck-Geddes' equation along with equation (A10) when substituted in equation (A8) results in

$$\sum_{i=1}^{nc} \left(\frac{\alpha_i}{\alpha_k} \right)^{C_1} x_b^{(i)} \frac{x_d^{(k)}}{x_b^{(k)}} = 1 \tag{A11}$$

So, the key distillate composition $x_d^{(k)}$ can be obtained as:

$$x_d^{(k)} = \frac{1}{\sum_{i=1}^{nc} \left(\frac{\alpha_i}{\alpha_k} \right)^{C_1} \frac{x_b^{(i)}}{x_b^{(k)}}} \tag{A12}$$

Substituting equation (A12) in equation (A1) and then using equation (A9), one can obtain the value of C_1 and hence $x_d^{(k)}$. The Newton-Raphson procedure is used for obtaining the solution with some assumed value of C_1.

A.2 Napthali-Sandholm (NS) Model for Continuous Simple Distillation

The case of N stages separating C components is considered where first stage refers to the reboiler and the Nth stage is condenser. The NS model accounts for, material balance, equilibrium, summation and heat balances (MESH) on each stage thus forming a set of $N(2C+1)$ algebraic equations in as many unknowns. The total liquid and vapor flows entering the ith ($i = 1,2,...,N$) stage are expressed as L_i and V_i, respectively, while the individual flow of the jth ($j = 1,2,....,C$) component is expressed as l_{ij} and v_{ij} respectively. It is now possible to write the MESH equations as given below.

- Component material balance:

$$M_{ij} = \left(1+\frac{S_i}{V_i}\right)\times v_{ij} + \left(1+\frac{s_i}{L_i}\right)\times l_{ij} - f_{ij} - l_{i+1,j} - v_{i-1,j} \;;\; i = 2,\ldots, N\text{-}1 \;;\; j = 1, 2,\ldots,C \quad \text{(A13)}$$

- Material balance equations for the reboiler and condenser:

$$M_{1j} = \left(1+\frac{S_1}{V_1}\right)\times v_{1j} + \left(1+\frac{s_1}{L_1}\right)\times l_{1j} - f_{1j} - l_{2j} \quad \text{(A14)}$$

$$M_{Nj} = \left(1+\frac{S_N}{V_N}\right)\times v_{Nj} + \left(1+\frac{s_N}{L_N}\right)\times l_{Nj} - f_{Nj} - v_{N-1,j} \quad \text{(A15)}$$

where, M_{ij} represents the discrepancy function expressed in terms of moles/hr; S_i and s_i are the vapor and liquid side-streams, and f_{ij} refers to the feed flow.

- Equilibrium relationship:

$$Q_{ij} = \frac{\eta_i \times m_{ij} \times V_i \times l_{ij}}{L_i} + \frac{(1+\eta_i)\times v_{i-1,j} \times V_i}{V_{i-1}} - V_{ij} \quad \text{(A16)}$$

where Q_{ij} refers to the discrepancy function (moles/hr); η_i is the Murphree stage efficiency, and m_{ij} represents the equilibrium constant for component j on ith stage. In equation (A16), the UNIQUAC method enters into calculations via the equilibrium constant m_{ij}.

- Energy balance equation:

$$E_i = \left(1+\frac{S_i}{V_i}\right)\times H_i + \left(1+\frac{s_i}{L_i}\right)\times h_i - h_{fi} - H_{i-1} - h_{i+1} \;;\; i = 2,\ldots, N\text{-}1 \qquad \text{(A17)}$$

- Energy balance equations for reboiler and condenser:

$$E_1 = \left(1+\frac{S_1}{V_1}\right)\times H_1 + \left(1+\frac{s_1}{L_1}\right)\times h_1 - h_{f1} - h_2 \qquad \text{(A18)}$$

$$E_N = \left(1+\frac{S_N}{V_N}\right)\times H_N + \left(1+\frac{s_N}{L_N}\right)\times h_N - h_{fN} - H_{N-1} \qquad \text{(A19)}$$

where E_i refers to the discrepancy function (kcal/hr). In equation (A17), the enthalpy values H_i and h_i are for the vapor and liquid, respectively. Equations (A17-A19) were solved simultaneously using the Newton-Raphson method for obtaining stage temperature and component liquid and vapor flow rates for which a linear pressure and temperature profile has been assumed. The pressure on the *i*th stage (p_i) is given by

$$p_i = P_1 - i\times\Delta p \qquad \text{(A20)}$$

where, P_1 is the bottom pressure and Δp refers to the pressure drop across the stage. The initial guess value of temperature at each stage is given by:

$$T_i = T_1 + \frac{(i-1)\times(T_N - T_1)}{(N-1)} \qquad \text{(A21)}$$

where T_N and T_1 are temperatures of the condenser and reboiler, respectively assuming values of the boiling points of MVC and LVC .

A.3 Simulation Model for Continuous Azeotropic Distillation

Behavior of azeotropic distillation was simulated using simplified Napthali-Sandholm model (Magnussen *et al.*, 1979) coupled with the phase separation calculations for the condenser. The assumptions for the model are: ideal vapor phase, constant column pressure and molar overflow, and ideal stages. In the model, independent variables are temperature and component liquid flow at each stage; under the stated assumptions the NS model gets simplified and only the total stage mass balance and the component balances coupled with the equilibrium equations need to be solved. Here, the material

balance on each stage for a *C*-component system is represented by a set of [*C*+1] algebraic equations. For solving the case of phase splitting, the overall component flow ($l_{i,j}$), and the total flow, L_i, are used. The component balance equations applicable for the *j*th component on the *i*th stage are:

$$l_{i,j} + l_{i,j}\,\varphi_{i,j} - \varphi_{i-1,j}\,l_{i-1,j} - l_{i+1,j} - f_{i,j} = 0\,;\; i = 2,\ldots, N\text{-}1\;\;;\;\; j = 1, 2,\ldots, C \qquad \text{(A22)}$$

The material balance equations for the reboiler and *N*th stage are:

$$l_{1,j} + l_{1,j}\varphi_{1,j} - l_{2,j} - f_{1,j} = 0 \qquad \text{(A23)}$$

$$l_{N,j} + l_{N,j}\varphi_{N,j} - \varphi_{N-1,j}\,l_{N-1,j} - f_{N,j} = 0 \qquad \text{(A24)}$$

where, l_{ij} represents the moles of *j*th component in the liquid stream leaving the *i*th stage ; $f_{i,j}$ refers to the moles of *j*th component fed to the *i*th stage and $\varphi_{i,j}$ is a stripping factor defined as:

$$\varphi_{i,j} = \frac{V_i\,\gamma_{i,j}\,P_{i,j}}{P_o\,L_i} \qquad \text{(A25)}$$

where L_i is the total liquid flow from the *i*th stage; V_i refers to the total vapor flow from the *i*th stage; $\gamma_{i,j}$ describes the activity coefficient of the *j*th species in the *i*th stage; $P_{i,j}$ represents the vapor pressure of *j*th pure component corresponding to the temperature of *i*th stage, and P_o denotes the system pressure.

- The total material balance on *i*th stage is given as:

$$L_i - l_{i,j} - \ldots\ldots - l_{i,C} = 0\,; \qquad i = 1, 2,\ldots, N\,; \qquad j = 1, 2,\ldots, C \qquad \text{(A26)}$$

Vapors leaving the *N*th stage usually form two immiscible phases after condensation. Accordingly, following equations apply for the condenser:

- Component balance equations:

$$l^{I}_{N+1,j} + l^{II}_{N+1,j} = \upsilon_{N,j} \quad \text{for } j = 1 \text{ to } C \qquad \text{(A27)}$$

where $l^{I}_{N+1,j}$ represents the moles of *j*th component in the entrainer-rich phase which is refluxed to the column and $l^{II}_{N+1,i}$ represents moles of *j*th component in the water rich phase.

- Phase equilibria equations:

$$\left(\frac{l^{I}_{N+1,i}}{\sum_{j=1}^{C} l^{I}_{N+1,j}}\right)\gamma^{I}_{N+1,j} = \left(\frac{l^{II}_{N+1,j}}{\sum_{j=1}^{C} l^{II}_{N+1,j}}\right)\gamma^{II}_{N+1,j} \qquad \text{(A28)}$$

where $\gamma^{I}_{N+1,j}$ and $\gamma^{II}_{N+1,j}$ represent the activity coefficients of jth species in the decanter corresponding to the composition of phases I and II, respectively.

In the GA optimization simulations, equations (A22-26) were solved by the Gauss elimination method using a prespecified value for the reflux composition. The computed values of $\upsilon_{N,j}$ were then used to solve equations (A27-28) and to obtain values of reflux ($l^{I}_{N+1,j}$). The calculations for the main column are then repeated till the assumed and optimized reflux values match closely.

A.4 Column Model for Reactive Distillation

The assumptions made modeling the reactive distillation column are: the vapor and liquid phases are in equilibrium on each tray; no reaction occurs in the vapor phase; the liquid phase is always homogenous; the enthalpy of the liquid streams is negligible; the enthalpy of the liquid phase is constant; and both condenser and reboiler are total.

Component material balance equations:

$$F_{i1} - L_1 x_{i1}(1-\beta) - L_2 x_{i2} - V_1 K_{i,1} x_{i,1} + \sum_{j=1}^{R} v_{ij}\varepsilon_1 = 0 \qquad i = 1,\ldots,C \qquad \text{(A29)}$$

$$F_{ik} + V_{k-1}K_{i,k-1}x_{i,k-1} + L_{k+1}x_{i,k+1} - L_k x_{i,k} - V_k K_{i,k} x_{i,k} + \sum_{j=1}^{R} v_{ij}\varepsilon_{jk} = 0 \qquad \text{(A30)}$$

$$k = 2,\ldots,N,\ i = 1,\ldots,C \qquad \varepsilon_{jk} = W_k r_{jk}$$

$$\sum_{i=1}^{C} x_{ik} - 1 = 0 \qquad \text{(A31)}$$

$$\sum_{i=1}^{C} K_{ik} x_{ik} - 1 = 0 \qquad \text{for ideal case} \qquad \text{(A32)}$$

$$\sum_{i=1}^{C}\left(\frac{Ps_{ik}\alpha_{ik}}{P}\right)x_{ik} - 1 = 0 \quad \text{for non-ideal case} \qquad \text{(A33)}$$

$$\lambda V_{k-1} - \lambda V_k - \sum \Delta H_j r_{jk} = 0 \tag{A34}$$

$$B_i = (1-\beta)\, L_1 x_{i1} \tag{A35}$$

$$x d_i D + B_i = P_i \tag{A36}$$

$$D = V_N - L_{N+1} \tag{A37}$$

$$\beta = V_o / L_1 \tag{A38}$$

V_k is the vapor flow rate off tray k, α_{ik} is the activity coefficient for component i on tray k, x_{ik} is the mole fraction of component i on liquid phase off tray k, L_k is the liquid flow rate off tray k, ν_{ij} is stoichiometric coefficient of component i in the reaction j is the extent of reaction r_{ij} on tray, B_i is the flow rate of component off the bottom of the column and P_i is the production rate of component i. P_c represent the pressure within the column and Ps is the saturation pressure. The temperature on each tray is computed by Eq. A32/A33 by Newton-Raphson method.

The application of this method based on the algorithm proposed by Bastos (1987), considering the chemical reaction may be distributed over several column trays. For this process the material balance equation become

$$\Delta M_{i1} = F_{i1} - L_1 x_{i1}(1-\beta) - L_2 x_{i2} - V_1 K_{i1} x_{i1} + \sum_{j=1}^{R} \nu_{ij} r_{j1} \qquad i = 1,\ldots,C \tag{A39}$$

$$\Delta M_{ik} = F_{ik} + V_{k-1} K_{i,k-1} x_{i,k-1} - L_{k+1} x_{i,k+1} - L_k x_{i,k} - V_k K_{i,k} x_{i,k} + \sum_{j=1}^{R} \nu_{ij} r_{jk} \tag{A40}$$

$k = 2,\ldots, N \quad i = 1,\ldots,C$

$$x^{n+1} = x^n + \Delta x^n \tag{A41}$$

where

$$\Delta x = -\left[\frac{\partial \Delta M}{\partial x}\right]^{-1} \Delta M \tag{A42}$$

and $\left[\frac{\partial \Delta M}{\partial x}\right]^{-1}$ is the Jacobian matrix of the system of equations. Since negative values for composition can obtained with Newton-Raphson method, a relaxation factor, η, is defined such that composition are always positive

$$x^{n+1} = x^n + \Delta x^n \eta \tag{A43}$$

where η takes values between 0 and 1.

Reference

Diwekar, U. M., Malik, R. K., Madhavan, K. P., 1987, Optimal reflux rate policy determination for multicomponent batch distillation columns, *Comput. Chem. Eng.*, 11:629-637.

Napthali, L.M. and Sandholm, D. P., 1971, Multicomponent separation calculations by linearization, *AIChE. J.*, 17: 1148.

Magnussen, T., Michelsen, M. L. and Fredenslund, Aa, 1979, Azeotropic distillation using UNIFAC, *I. Chem. E. Symp. Ser.*, 56: 4.2,1.

Cardoso, M.F., Salcedo, R.L., Azevedo, S.F., Barbosa, D., 2000, Optimization of reactive distillation processes with simulated annealing, *Chem. Eng. Sci.*, 55, 5059-5078.

Bastos, J., 1987, *Modeling extractive distillation processes*, Ph.D. thesis, Universidade do Porto (in Portuguese).

Appendix B: Thermodynamic Models and Data

B.1 Thermodynamic Models

Vapor-liquid equilibrium (VLE) data for multicomponent system is necessary for simulating distillation column. The VLE for the *n* component system is given by the following relationship

$$y_i = \frac{x_i \gamma_i \, p_i}{P} \qquad i = 1,....,n \tag{B1}$$

where p_i is vapor pressure, P total pressure.

Liquid non-ideality in terms of the activity coefficients γ_i can be calculated using the UNIFAC, UNIQUAC or Wilson thermodynamic model and the Antoine vapor pressure equation. Pure component vapor pressure were computed by the Antoine Equation:

Antoine equation : $$\log(p_i) = A + \frac{(B_i)}{[(T + C_i]} \tag{B2}$$

where the temperature T is in Kelvin and the pressure is in Pa.

B.1.1 Wilson's Equation :

The liquid activity coefficients in the VLE relationship were computed using the Wilson model.

$$\ln \gamma_i = 1 - \ln\left(\sum_j \Lambda_{ij} x_j\right) - \sum_j \frac{\Lambda_{ij} x_j}{\sum_k \Lambda_{jk} x_k} \qquad i = 1,....,n \tag{B3}$$

$$\Lambda_{ij} = \frac{v_i}{v_i} \exp[-\frac{\lambda_{jk} - \lambda_{kk}}{RT}] \quad \text{and} \quad \Lambda_{ij} = 1.0 \tag{B4}$$

$(\lambda_{jk} - \lambda_{kk})$ can be obtained from binary data.

$$\ln \Lambda_{ij} = a_{ij} + \frac{b_{ij}}{T} \tag{B5}$$

B.1.2 UNIQUAC Model :

In the UNIQUAC model, the expression for the activity coefficients contains two parts: the combinatorial part, essentially due to differences in size and shape of the molecules, and a residual contribution, essentially due to energetic interactions. This is expressed as

$$\ln\gamma_i = \underset{\text{combinatorial}}{\ln\gamma_i^C} + \underset{\text{residual}}{\ln\gamma_i^R} \qquad \text{(B6)}$$

The combinatorial contribution is given by

$$\ln\gamma_i^C = \ln\frac{\phi_i}{x_i} + \frac{z}{2}q_i\ln\frac{\theta_i}{x_i} + l_i - \frac{\phi_i}{x_i}\sum^j x_j l_j \qquad \text{(B7)}$$

$$l_i = \frac{z}{2}(r_i - q_i) - (r_i - 1) \qquad z = 10 \qquad \text{(B8)}$$

$$\theta_i = \frac{q_i x_i}{\sum_j q_j x_j} \qquad \phi_i = \frac{r_i x_i}{\sum_j r_j x_j} \qquad \text{(B9)}$$

volume fraction surface fraction

$$\ln\gamma_i^R = q_i[1 - \ln(\sum^j \theta_j\tau_{ji}) - \sum^j \theta_j\tau_{ij})/\sum^k \theta_k\tau_{kj}) \qquad \text{(B10)}$$

$$\tau_{jk} = \exp[-\frac{u_{jk} - u_{kk}}{RT}] \qquad \text{(B11)}$$

In the distillation calculations of Chapter 3, the temperature dependent parameter is linearized as follows :

$$\tau_{jk} = A_{jk}^{(O)} + A_{jk}^{(I)}.T \qquad \text{(B12)}$$

The parameters can be obtained from binary data. For each possible binary pair in the solution, two parameters are needed.

B.2 Thermodynamic Data

Table B.1: Antoine coefficients of the component

Component	A	B	C	Molar volume (ml mol^{-1})
Ethanol	23.5807	-3673.81	-46.875	
Water	23.2256	-3835.18	-45.343	
Benzene	20.7936	-2788.51	-52.360	-
Methanol	23.49989	-3634.01	-33.434	
Ethylene oxide	21.3066	-2428.2	-35.388	-
water	23.2256	-3835.18	-45.343	-
Ethylene glycol	25.1431	-6022.18	-28.25	-
Diethylene glycol	34.4262	-16224.92	190.015	-
Isobutene	21.64556	-2125.74886	-33.160	93.33
Methanol	23.49989	-3643.31362	-33.434	44.44
MTBE	20.71616	-2571.58460	-48.406	118.8

Table B.2: UNIQUAC unary parameters

Component	r	q
Ethanol	2.1055	1.972
Water	0.92	1.4
Benzene	3.1878	2.4
Methanol	1.4311	1.432

Table B.3: UNIQUAC binary parameters for benzene-ethanol-water system

Binary interaction parameters $A_{jk}^{(O)}$			
	Benzene	Ethanol	Water
Benzene	1.0	-.105916748	-0.12740
Ethanol	1.710002099	1.0	1.1153
Water	0.012231	0.30048	1.0
Binary interaction parameters $A_{jk}^{(I)}$			
Benzene	0	0.00098361	0.00057616
Ethanol	-0.001098918	0	-0.0001
Water	0.00097984	0.00084	0

Table B.4: UNIQUAC binary parameters for the methanol-water system

Binary interaction parameters $A_{jk}^{(O)}$		
	Methanol	Water
Methanol	0	2.5168
Water	0.081308	1
Binary interaction parameters $A_{jk}^{(I)}$		
Methanol	0	-0.002392
Water	0.0010154	0

Table B.5: Wilson coefficient(cal mol^{-1}) for ethylene oxide-water-ethylene glycol-diethylene glycol system(Cardoso *et al.*,, 2000)

Component	Ethylene oxide	Water	Ethylene glycol	Diethylene glycol
EO	-	124.965	-79.471	220.233
W	1905.77	-	1266.0109	-180.210
EG	635.823	-1265.7398	-	856.192
DEG	157.874	923.33	-112.337	-
Molar volume(ml mol^{-1})	49.09	18.07	55.92	94.78

Table B.6: Vapor-liquid Equilibrium constant, K at 1 atm. for ethylene oxide water-ethylene glycol-diethylene glycol system(Cardoso *et al.*,, 2000)

Component	K (dimensionless)
Ethylene oxide	71.9exp{5.720[(T-469)/ (T-35.90)]}
Water	221.2exp{6.310[(T-647)/ (T-52.90)]}
Ethylene glycol	77.0exp{9.940[(T-645)/ (T-71.40)]}
Diethylene glycol	47.0exp{10.42[(T-681)/ (T-80.60)]}

T – temperature (K)

Table B.7: UNIQUAC binary parameters, u_{ij} (cal mol^{-1}) for MTBE-methanol-Isobutene (Rehfinger & Hoffman, 1990)

i	j	u_{ij} (cal mol^{-1})
Methanol	Isobutene	-70.3003
Isobutene	Methanol	1403.50
Methanol	MTBE	-174.94
MTBE	Methanol	931.43
Isobutene	MTBE	103.73
MTBE	Isobutene	-48.931

References

Rehfinger, A., Hoffman. U., 1990, Kinetics of methyl tertiary butyl ether liquid phase synthesis catalyzed by ion exchange resin-I, Intrinsic rate expression in liquid phase activities, *Chem. Eng. Sci*., 45(6):1605-1617.

Gmehling J. and Onken U., 1977, *Vapor-liquid equilibrium data collection, aqueous-organic systems*. DECHEMA Chem. Data Series, DECHEMA, Frankfurt/Main, Germany.

Cardoso, M.F., Salcedo, R.L., Azevedo, S.F., Barbosa, D., 2000, Optimization of reactive distillation processes with simulated annealing, *Chem. Eng. Sci.*, 55, 5059-5078.

Fredenslund A., Gmehling J., Rasmussen P.,1977, *Vapor-liquid equilibria using UNIFAC*, Elsevier Scientific Publishing Co., Amsterdam.

Appendix C: Reaction data

C.1 Ethylene oxide-water-ethylene glycol-diethylene glycol system

Table C.1: Reaction kinetics and heat of reaction of the reaction between ethylene oxide-water

Reaction	Rate (mol m^{-3} s^{-1})	r H (J mol^{-1})
R1	$3.15\times10^{15}\exp(-9547/T)x_1x_2$	-80.0×10^{3}
R2	$6.30\times10^{15}\exp(-9547/T)x_1x_3$	-13.10×10^{3}

Reaction (R1) - Production of ethylene glycol from ethylene oxide and water.
Reaction (R2) - Production of diethylene glycol from ethylene glycol and ethylene oxide.

C.2 MTBE-methanol-isobutene system

The rate expression given by Rehifinger and Hoffman (1990)

$$r = qk_r\left[\frac{\alpha_{IB}}{\alpha_{MeOH}} - \frac{\alpha_{MTBE}}{K_a\alpha^{2}_{MeOH}}\right] \qquad \text{(C1)}$$

where r represents the reaction rate per unit catalyst mass, q is the amount of acid groups on the resin per unit mass (4.9 equiv./kg). α is the activity of a component. The reaction rate constant, k_r and thermodynamic equilibrium constant, K_a are reported

$$k_r = 3.67x10^{12}\exp(-11110/T) \qquad \text{(C2)}$$

$$K_a = 1.65x10^{-4}\exp(-4224.34/T) \qquad \text{(C3)}$$

References

Rehfinger, A., Hoffman. U., 1990, Kinetics of methyl tertiary butyl ether liquid phase synthesis catalyzed by ion exchange resin-I, Intrinsic rate expression in liquid phase activities, *Chem. Eng. Sci.*, 45(6):1605-1617.

Cardoso, M.F., Salcedo, R.L., Azevedo, S.F., Barbosa, D., 2000, Optimization of reactive distillation processes with simulated annealing, *Chem. Eng. Sci.*, 55, 5059-5078.

Appendix D: Computation of Distillation Column Cost

D.1 Total Annual Cost for Continuous Distillation Column

The objective function (C_T) for both i.e., continuous simple and continuous azeotropic distillations represents the total annual cost ($). This cost comprises two additive components:

$$\begin{Bmatrix} Total\ \ Cost, \\ C_T \end{Bmatrix} = \begin{Bmatrix} Energy \\ Cost, C_1 \end{Bmatrix} + \left\{ (\text{depreciation} + \text{interest} + \text{maintenance}) \text{x} \begin{pmatrix} Fixed \\ Cost, C_2 \end{pmatrix} \right\} \quad \text{(D1)}$$

where energy cost, C_1, which is directly proportional to the heating load is calculated according to

$$C_1 = \frac{Q_r \times C_s \times N_D \times 24}{\lambda_{steam}} \quad \text{(D2)}$$

where Q_r is the reboiler duty (kcal/hr); λ_{steam} (=500 kcal/hr) is the latent heat of steam vaporization; C_s refers to the steam cost (=0.0186 $/kg) and N_D denotes the number of yearly working days (=330).

The fixed cost, C_2 ($/yr), consists of packing (C_{pack}) and column (C_{col}) costs where C_{pack} is computed as:

$$C_{pack} = A_c \times N \times HETP \times C^o_{pack} \quad \text{(D3)}$$

Here, A_c representing the column area is calculated from the total vapor load on the basis of vapor velocity corresponding to the top temperature and capacity factor (C_f) of the packing (C_f = 1.5); C^o_{pack} denotes packing cost per unit volume (=2325.58 $/m^3) and the *HETP* value for the packing is taken to be 0.6 m. The second cost component of C_2 i.e., C_{col}, is calculated on the basis of internals from the following correlation.

$$C_{col} = 3.14 \times 1.4 \times d_c \times N_{st} \times HETP \times W_s \times \rho_s \times C_{steel} \quad \text{(D4)}$$

In this expression, d_c, W_s, ρ_s and C_{steel} respectively refer to the column diameter,

column thickness (= 0.006 m), density (=8000 kg/m^3) of the column material (steel) and its cost ($/kg). Assuming depreciation, interest, and maintenance costs of 18%, 15% and 2%, respectively, the total annual cost to be minimized is evaluated as:

$$C_T = C_1 + 0.35\, C_2 \tag{D5}$$

In the operation of an azeotropic distillation column, a small quantity of entrainer is lost through the vent condenser and bottom product. Thus the cost of entrainer loss approximately amounting to 3% of the total entrainer quantity, must be additionally considered while evaluating C_T ;

$$C_T = C_1 + 0.35\, C_2 + C_3 \tag{D6}$$

where C_3 (=0.23$/kg) refers to the cost of entrainer, i.e. benzene

D.2 Total Annual Cost for Continuous Reactive Distillation Column

The objective function for total annual cost comprises of raw material(c_i), steam(c_H), cooling water (c_w) and annualized installed costs of the column shell(C_{cs}), trays(C_{ci}), reboiler(C_r), and condenser(C_c) and Q_B, Q_c correspond to reboiler and condenser duties. (Cardoso *et al*., 2000).

$$OB_J = \min\left\{ \sum_{i=1}^{c} c_i \sum_{k=1}^{N} F_{ik} + c_H Q_B + c_w Q_c + (C_{cs} + C_{ci} + C_r + C_c) \right\} \tag{D11}$$

$$D^4 = C_D \beta^2 L^2_1 \tag{D12}$$

$$Q_B = \beta \lambda L_1 \tag{D13}$$

$$Q_C = \lambda L_N \tag{D14}$$

$$H = H_o + \sum_{k=1}^{N} H_k \tag{D15}$$

$$H_k = H_{\min} + 1.27\frac{W_k}{D^2} \tag{D16}$$

$$OB_J = \min\left\{c_o \sum_{i=1}^{c} c_i \sum_{k=1}^{N} F_{ik} + c_R Q_B + c_c Q_c + c_T D^{1.55} \times \sum_{k=1}^{N}(0.61+1.27\frac{W_k}{D^2}) + c_{SH} D(H_o + \sum_{k=1}^{N}(0.61+1.27\frac{W_k}{D^2})\right\} \tag{D17}$$

where the H_o is a fixed extra column height corresponding to the free space below the bottom tray and above the top tray. The height H_k are evaluated by adding the minimum tray spacing, $H_{\min}$ to the height of liquid in tray k corresponding to volume W_k (liquid holdup, m^3). And c_i, c_o, c_R, c_c, c_T and c_{SH} corresponds to cost parameters(Appendix E).

Appendix E: Cost Data

Ethylene oxide cost	43.70×10^{-3} US$mol^{-1}
c_{SH}	222 US$mol^{-1}
c_T	15.70 US$yr^{-1}
c_R	146.80×10^{-3} US$W^{-1}yr^{-1}
c_c	24.50×10^{-3} US$W^{-1}yr^{-1}
c_o	10000 US$yr^{-1}
Isobutylene cost	16.7×10^{-3} US$mol^{-1}
Methanol cost	8.17×10^{-3} US$mol^{-1}